8-2016

Characterization of an Ethylene Receptor in *Synechocystis* sp. PCC 6803

Randy Francis Lacey
University of Tennessee, Knoxville, rlacey1@vols.utk.edu

To the Graduate Council:

I am submitting herewith a dissertation written by Randy Francis Lacey entitled "Characterization of an Ethylene Receptor in *Synechocystis* sp. PCC 6803." I have examined the final electronic copy of this dissertation for form and content and recommend that it be accepted in partial fulfillment of the requirements for the degree of Doctor of Philosophy, with a major in Biochemistry and Cellular and Molecular Biology.

Brad Binder, Major Professor

We have read this dissertation and recommend its acceptance:

Barry Bruce, Gladys Alexandre, Albrecht Von Arnim, Alison Buchan

Accepted for the Council:

Carolyn R. Hodges

Vice Provost and Dean of the Graduate School

(Original signatures are on file with official student records.)

Characterization of an Ethylene Receptor in *Synechocystis* sp. PCC 6803

A Dissertation Presented for the
Doctor of Philosophy
Degree
The University of Tennessee, Knoxville

Randy Francis Lacey
August 2016

Acknowledgements

First, I would like to thank Dr. Binder for training and guiding me throughout graduate school. You've helped me to grow and develop into a scientist that is able to think independently, and for that I will always be grateful. Also, I appreciate the patience. Thanks to past and present lab members and other graduate students in the department who may not have contributed directly to this research but have offered thoughtful and stimulating discussion. I would also like to thank my committee members for providing help and guidance throughout the years. Finally, thank you to Hannah for always being there for me after long days. You're the best person I've ever known, and I couldn't have done this without you.

Abstract

In plants, ethylene functions as a hormone regulating many growth and developmental processes. Ethylene receptors in plants resemble bacterial two-component signaling systems. Because of this, ethylene receptors are thought to have been acquired by gene transfer from the cyanobacterial endosymbiont that lead to the development of the chloroplast. However, prior to this work, functional ethylene receptors were thought to only be found in green plants. Here, I show that the cyanobacterium *Synechocystis* sp. PCC 6803 (*Synechocystis*) contains a functional ethylene receptor, SynEtr1. SynEtr1 contains a predicted ethylene binding domain, a photosensory cyanobacteriochrome (CBCR) domain, and a histidine kinase domain. We find SynEtr1 to display high affinity ethylene binding, and residues conserved in plant ethylene receptors are required for ethylene binding in SynEtr1. As a photoreceptor, SynEtr1 was previously reported to mediate phototaxis in *Synechocystis*. We show that ethylene regulates phototaxis via SynEtr1 by altering extracellular components of *Synechocystis* including type IV pili and extracellular polymeric substances (EPS). Both type IV pili and EPS are involved in many physiological processes, suggesting that the function of ethylene is not physiologically limited to phototaxis. We find that ethylene and SynEtr1 also affect cell sedimentation and biofilm formation. Thus, SynEtr1 functions as a bifunctional receptor mediating responses to both ethylene and light. This is the first known characterization of an ethylene receptor in a non-plant organism. Additionally, by scanning sequenced genomes, we discovered that putative ethylene receptors exist in many different species of both cyanobacteria and non-photosynthetic bacteria, indicating that ethylene may have a wide-spread function throughout prokaryotes.

Table of Contents

List of Tables

List of Figures

List of Abbreviations

EBD – Ethylene Binding Domain

EBP – Ethylene Binding Protein

AtETR1 – Arabidopsis Thaliana Ethylene Receptor 1

SynEtr1 – Synechocystis Ethylene Receptor 1

CBCR – Cyanobacteriochrome

GAF – cGMP Specific Phosphodiesterases, Adenyl Cyclases, and FhlA

PAS – Per, Arnt, Sim

PAC – PAS C-terminal

Cph2 – Cyanobacterial Phytochrome 2

EPS – Extracellular Polymeric Substances

Chapter 1

Background and Literature Review

Ethylene as a Plant Hormone

Ethylene is the simplest alkene and exists as a gas under standard conditions (Yang and Hoffmann, 1984). Though simple in structure the role of ethylene as a plant hormone is very complex. As one of the first plant hormones to be discovered, many different physiological functions of ethylene have been uncovered. While famous for its role in fruit ripening, ethylene has been shown to mediate many different responses in plants ranging from regulation of seed germination to abscission and organ senescence (Abeles et al., 1992; Bleecker and Kende, 2000; Schaller and Kieber, 2002; Stepanova and Alonso, 2009; Schaller, 2012; Cho and Yoo, 2014). In mediating these different processes, it has been estimated that ethylene is responsible for agricultural losses in the billions of dollars annually (Theologis, 1992). Because of this, a significant amount of work has been done in understanding the biochemical mechanisms that mediate ethylene perception and signaling in plants.

The majority of what is known about ethylene signaling comes from studies done in *Arabidopsis thaliana*. In *Arabidopsis*, ethylene is perceived by a family of five receptors located in the endoplasmic reticulum membrane (Figure 1.1) (Chen et al., 2002; O'Malley et al., 2005; Grefen et al., 2007; Lacey and Binder, 2014). The receptors constitutively signal in air, with binding of ethylene causing a loss of signal output (Hua and Meyerowitz, 1998). Thus, ethylene functions as an inverse agonist. Structurally, the ethylene receptors are characterized by a N-terminal transmembrane ethylene binding domain (EBD)

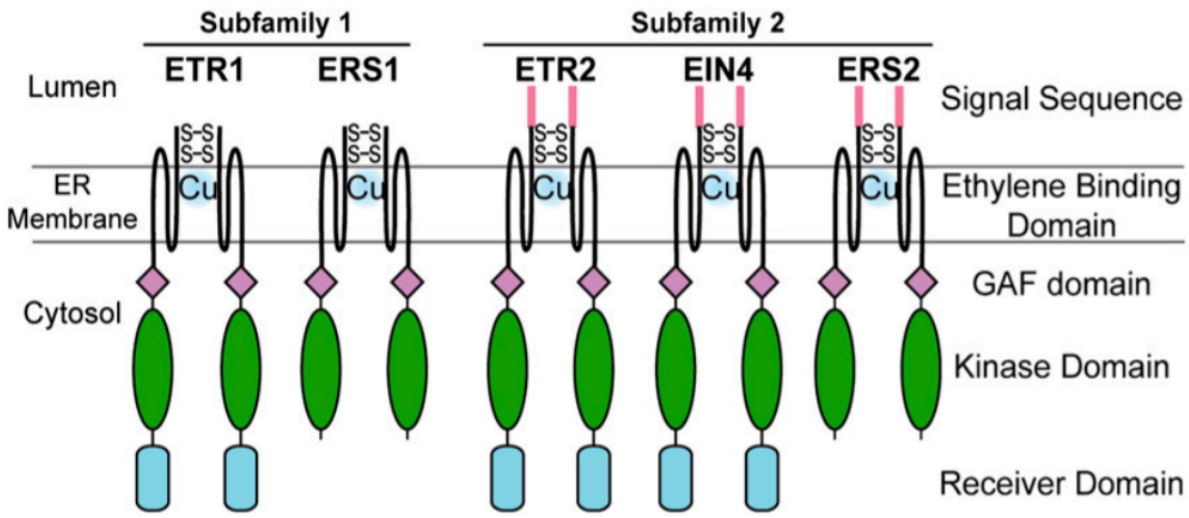

Figure 1.1 – The *Arabidopsis* Ethylene Receptors (From Lacey and Binder, 2014)

The *Arabidopsis* ethylene receptors are located in the ER membrane and can be divided into two subfamilies based on the sequence of the ethylene binding domain. The receptors contain an N-terminal transmembrane ethylene binding domain, a soluble GAF domain, and a kinase domain. Three of the receptors contain an additional receiver domain. The architecture of these receptors resembles that of bacterial two-component systems.

followed by soluble GAF domain and kinase domains. Three of the five *Arabidopsis* receptors contain receiver domains at the C-terminus (West and Stock, 2001; Schaller and Kieber, 2002; Binder et al., 2012). The receptors in *Arabidopsis* can be further divided into two subfamilies, subfamilies I and II, based on sequence comparisons of their EBDs (Wang et al., 2006) . Both subfamilies contain three transmembrane alpha helices, however subfamily II contains an N-terminal extension that possibly creates a fourth alpha helix. Structural data does not exist for the EBD, however significant mutational analysis of the Arabidopsis receptor AtETR1 has led to a model for how the receptor binds and transduces the ethylene signal. Seven conserved residues in the AtETR1 EBD have been shown to be required for ethylene binding, with mutation of any of these residues leading to an ethylene insensitive, constitutively active receptor (Hall et al., 1999; Rodriguez et al., 1999; Wang et al., 2006). Additionally, it is known that copper(I) is a required cofactor for ethylene binding (Rodriguez et al., 1999; McDaniel and Binder, 2012). It has been suggested that two of seven residues, C65 and H69, are involved in coordinating the copper ion (Rodriguez et al., 1999).

The general architecture of these receptors resembles that of bacterial two-component signal transduction systems (Figure 1.2A) (Chang et al., 1993; Chang and Meyerowitz, 1995; Schaller et al., 2011). Commonly, two-component systems involve the perception of a signal by a sensor domain with a subsequent conformational change that leads to autophosphorylation of a histidine residue on the kinase domain (Stock et al., 2000; Mason and Schaller, 2005; Mitrophanov and Groisman, 2008). Phosphorelay then occurs between the kinase domain and the response

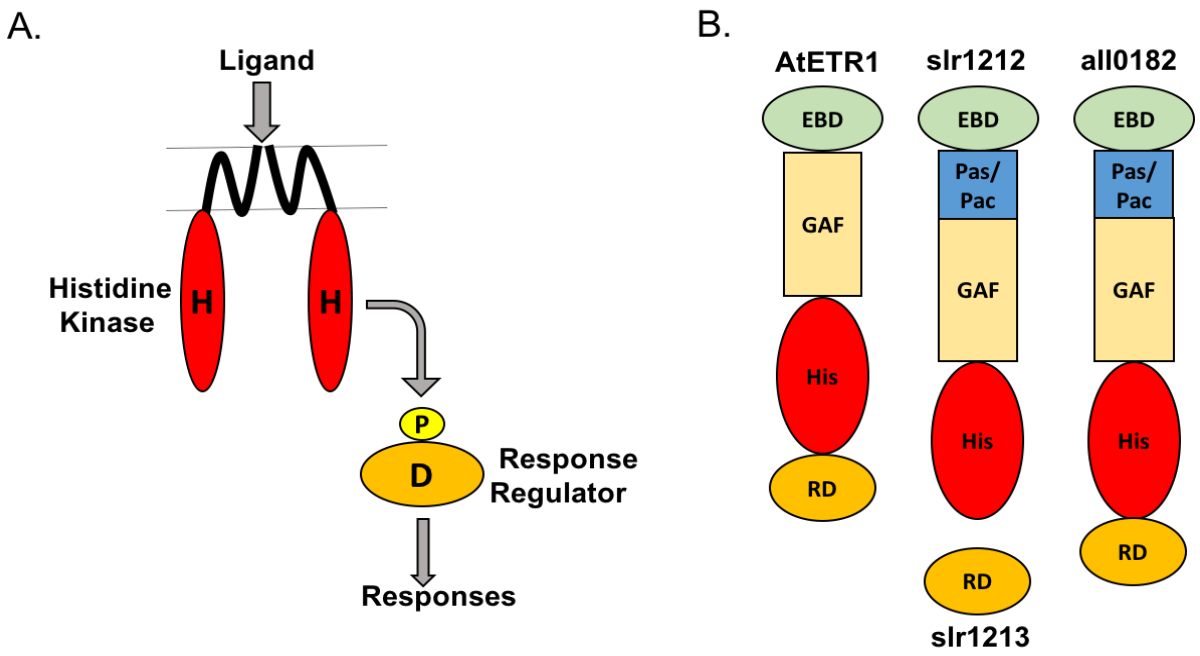

Figure 1.2: Two-Component Signaling and Domain Architecture Comparison of Plant and Cyanobacterial Ethylene Receptors (Adapted from Mason and Schaller, 2005(A) and Mount and Chang, 2002 (B))

(A) General depiction of two-component signaling. In this case, a ligand interacts the membrane bound ligand binding domain stimulating activity of the histidine kinase domain. The histidine kinase domain autophosphorylates and transfers a phosphate to an aspartate on the receiver domain of a response regulator. The response regulator is then able to illicit cellular responses. (B) Comparison of the predicted domain architecture of AtETR1 and the protein products of slr1212 and all0182. Each contain a predicted transmembrane ethylene binding domain (EBD), a GAF domain, and a histidine kinase domain (His). Slr1212 and all0182 contain Pas and Pac domains. All three have receiver domains that however, the receiver domain of slr1212, slr1213, is encoded as a separate gene.

regulator with a phosphorylated response regulator able to elicit a cellular response (Gao et al., 2007). Whether or not ethylene receptors in plants function as true two-component signaling systems remains unclear. In *Arabidopsis*, subfamily I receptors contain the necessary residues for histidine kinase activity, while subfamily II receptors do not (Kendrick and Chang, 2008; Ju and Chang, 2015). In vitro analysis shows that AtETR1 displays histidine kinase activity, however genetic analysis suggests that functional kinase activity is not needed for ethylene signaling (Wang et al., 2003; Moussatche and Klee, 2004). Additionally, the other Arabidopsis receptors show serine/threonine kinase *in vitro*, but the role of this in ethylene signaling is unknown (Moussatche and Klee, 2004). Collectively, the architecture of the ethylene receptors indicate that they may have previously functioned as standard two-component receptors, however our current knowledge suggests they have evolved alternative mechanisms for signaling.

Discovery of Non-Plant Ethylene Binding Domains

As described above, ethylene has a very well-characterized function as a hormone and signaling molecule throughout higher plants. Despite this ubiquity, the evolutionary origins of ethylene as a signaling molecule have remained less clear. To explore this, cyanobacterial genomes were first examined. Cyanobacteria are photosynthetic prokaryotes that are thought to have given rise to the chloroplast via an endosymbiotic event ~1.5BYA (Sanderson et al., 2004; Yoon et al., 2004). As the cyanobacterial endosymbiont became reduced in function, many of its genes were either lost or transferred to the nuclear genome. It is thought that bacterial two-component like systems such as the phytochromes and ethylene receptors were

acquired during this gene transfer from the plastid (Kehoe and Grossman, 1996; Timmis et al., 2004; Schaller et al., 2011; Kooß and Lamparter, 2016). Several phytochrome-like photoreceptors have been identified and characterized in cyanobacteria (Rockwell et al., 2013), however no known functional cyanobacterial ethylene receptors have been discovered. The first step in determining if ethylene receptors exist in cyanobacteria is identifying genes that encode possible ethylene binding proteins (EBPs). The EBD of the *Arabidopsis* receptors is highly conserved with known residues required for ethylene binding (Wang et al., 2006). Thus, the EBD of AtETR1 provides an ideal sequence for discovering EBDs in previously unexamined organisms.

The first putative cyanobacterial EBP was reported in 1999 in the model cyanobacterium *Synechocystis sp.* PCC 6803 (*Synechocystis*). The gene locus *slr1212* was identified based on sequence similarity to AtETR1 (Rodriguez et al., 1999). It was reported that wildtype (WT) *Synechocystis* is able to specifically bind ethylene and disruption of *slr1212* eliminates ethylene binding. This indicated that *slr1212* either directly encoded an EBP, or encoded a protein somehow involved in ethylene perception. A later study in 2002 uncovered two putative EBPs in *Anabaena* sp. PCC7120, *all1280* and *all2095* (Mount and Chang, 2002). The proteins encoded by *slr1212*, *all1280*, and *all2095* are all predicted to contain the seven conserved residues required for ethylene binding in the *Arabidopsis* receptors (Wang et al., 2006). Additionally, they were all predicted to arrange in a two-component like architecture, however whether these proteins functioned as ethylene receptors was unknown. (Figure 1.2B)

The rapid increase in available genome sequences in the early 2000s offered the opportunity for the discovery of new EBDs in many different organisms. In 2006, Wang et al.

sought to determine the ethylene binding capacity of representative organisms across all kingdoms of life (Wang et al., 2006). All land plants tested were capable of ethylene binding. Additionally, many different cyanobacteria bound ethylene, including both *Synechocystis* and *Anabaena*, as well as one species of green algae. No ethylene binding was detected in any of the non-photosynthetic organism tested. To further expand this study, organisms with either complete or partially complete genome sequences were scanned for the presence of EBDs similar to the *Arabidopsis* receptors and *slr1212*. Sequences corresponding to possible EBDs were discovered in 13 different organisms. Interestingly, several of these sequences came from non-photosynthetic bacteria indicating that non-plant EBDs may not be limited to cyanobacteria.

More recently, a functional ethylene receptor was characterized in the charophyte species of green algae, *Spirogyra pratensis (Spirogyra)* (Ju et al., 2015). Because green algae are the most ancient photosynthetic eukaryotes, they can provide insight into the origins of ethylene signaling in green plants. Several charophyte species have been shown to bind ethylene or contain putative ethylene binding proteins (Wang et al., 2006; Gallie, 2015), indicating that this group of algae may have been the progenitors to higher plants. In *Spirogyra*, ethylene functions to stimulate cell elongation through the ethylene receptor SpETR1. Additionally, it was shown that *Spirogyra* not only contains a functional ethylene receptor, but it also contains several of the downstream components of ethylene signaling found in higher plants. Downstream ethylene signaling components of *Spirogyra* were able to rescue WT phenotypes in the corresponding mutants in *Arabidopsis*. While possibly containing ethylene receptors, no sequenced cyanobacteria are predicted to encode the downstream ethylene

signaling components characterized in *Arabidopsis* (Ju and Chang, 2015). Therefore, it is likely that the ethylene signaling pathway seen in higher plants evolved after the endosymbiotic event that gave rise to the chloroplast. The presence of possible EBPs in cyanobacteria indicate that the ability to sense and respond to ethylene likely evolved prior to this event. The overall goal of this dissertation is to understand if and how cyanobacteria specifically respond to ethylene via an ethylene receptor, thus providing insights into the origins of ethylene as a signaling molecule.

Synechocystis Physiology

Synechocystis is a spherical, unicellular, freshwater, organism and in 1996 it was the first cyanobacterium to have its genome sequenced (Kaneko et al., 1996). It is naturally transformable and readily integrates DNA into its genome by homologous recombination (Kozlovskaya et al., 1982; Williams, 1988). As mentioned above, the *Synechocystis* gene locus *slr1212* is predicted to encode an EBP. It has been shown experimentally that disruption of *slr1212* eliminates the ability of this organism to bind ethylene (Rodriguez et al., 1999). *Slr1212* is the only gene predicted to encode an ethylene binding protein in *Synechocystis*. For these reasons, *Synechocystis* provides an optimal system for studying the possible role of ethylene signaling in prokaryotes, and is thus, the focus of this dissertation. Because of the unknown nature of the function of ethylene in *Synechocystis*, I have explored many different aspects of *Synechocystis* physiology in seeking out an ethylene response phenotype. Here, I will highlight and provide relevant background on several areas of *Synechocystis* physiology: motility, biofilm formation, and spontaneous cell sedimentation.

Motility

As photosynthetic organisms, many cyanobacteria move through their environment to optimal light conditions. This light directed movement is known as phototaxis (Ng et al., 2003; Bhaya, 2004). Movement toward light is referred to as positive phototaxis and movement away from light is negative phototaxis. Phototaxis has been observed in many different species of cyanobacteria with motility often described as either gliding or twitching. Gliding motility is typically seen in filamentous cyanobacteria such as *Oscillatoria* (Hoiczyk, 2000), whereas twitching motility is observed in unicellular species such as *Synechocystis* (Bhaya et al., 2001). Regardless of whether gliding or twitching, phototaxis is dependent upon the ability of the cells to both sense their light environment and move to where light is optimal. The relay of extracellular light cues to intracellular machinery allow *Synechocystis* and other cyanobacteria to effectively navigate their environment.

Several photoreceptors in *Synechocystis* have been identified and shown to mediate phototaxis (Yoshihara et al., 2000; Fiedler et al., 2005; Moon et al., 2012). Many of these photoreceptors are either phytochromes or phytochrome-like proteins known as cyanochromes or cyanobacteriochromes (CBCRs). These phototaxis photoreceptors have been shown to respond to wavelengths of light ranging from ultraviolet (UV) up to far-red (Fiedler et al., 2005; Ikeuchi and Ishizuka, 2008; Rockwell et al., 2013). Additionally, the phototaxis photoreceptors vary in the mechanisms by which they relay light signals. The first characterized phototaxis photoreceptor in *Synechocystis* was TaxD1 (also referred to as PixJ) (Ng et al., 2003; Narikawa et al., 2013). TaxD1 is a CBCR that is blue/green photoreversible and is involved in regulating positive phototaxis. Disruption of the *taxD1* locus causes *Synechocystis* to be

negatively phototactic under conditions that would normally stimulate positive phototaxis. TaxD1 is thought to function similarly to two-component methyl-accepting chemotaxis proteins characterized in *Escherichia coli (E. coli)*. Another well characterized photoreceptor linked to phototaxis in *Synechocystis* is Cph2 (Wilde et al., 2002; Moon et al., 2011; Savakis et al., 2012). Unlike TaxD1, Cph2 contains two photoreceptor domains including a red/far-red photoreversible phytochrome domain and a blue/green photoreversible CBCR domain. Cph2 inhibits movement toward blue light by stimulating production of the second messenger c-di-GMP. Interestingly, this protein also stimulates breakdown of c-di-GMP upon red light activation. The differences in light perception and signal transduction by TaxD1 and Cph2 highlight the complexity of photoperception in phototaxis. The protein encoded by *slr1212* is also a known photoreceptor involved in phototaxis (Narikawa et al., 2011; Song et al., 2011). This will be discussed in detail below in "SynEtr1 overview". While these and several other photoreceptors have been characterized and implicated in phototaxis, the direct link of signal transduction from light perception to movement remains less clear.

Following perception of the light stimulus, if necessary, the cells respond by moving either toward or away from the light source. In *Synechocystis*, this movement is dependent on attachment to a surface and modification of that surface. Surface attachment is mediated by large appendages that protrude from the cell known as type IV pili (Figure 1.3) (Bhaya et al., 2000; Schuergers and Wilde, 2015). Type IV pili function in phototaxis by extending out from the cell, attaching to a surface and retracting, thus propelling the cell toward or away from a light source. Electron microscopy images have shown *Synechocystis* to have two main morphotypes of pili, thick and thin (Bhaya et al., 2000; Yoshihara et al., 2001). Thick pili are

required for motility and are thus considered to be true type IV pili. The function of thin pili is unknown.

Type IV pili are composed of several different proteins (Figure 1.3). The different protein components can be separated by function including structure, biogenesis, and motor proteins. PilA1 is the main structural component of type IV pili (Bhaya et al., 1999). Disruption of *pilA1* creates non-motile *Synechocystis* that lacks thick pili (Bhaya et al., 2000). The gene locus *pilA2* also appears to encode for a pilin subunit, however disruption of this gene locus has no apparent effect on motility or type IV pili abundance (Bhaya et al., 2000). There are two known motor proteins, PilB1 and PilT1, involved in extension and retraction respectively (Okamoto and Ohmori, 2002; Jakovljevic et al., 2008; Schuergers et al., 2015). Both PilB1 and PilT1 are ATPases that stimulate extension and retraction by either energizing assembly or disassembly of the pilus. Disruption of the gene locus encoding either protein leads to non-motile cells. Interestingly, although the cells are spherical in nature with no apparent polarity, PilB1 has been shown to localize at the front edge of moving *Synechocystis* cells (Schuergers et al., 2015). Several other proteins including PilC, PilQ, and PilD are involved in biogenesis of type IV pili (Bhaya et al., 2000). PilC is an inner membrane protein that likely serves as the base platform of the pili as well as an interacting partner for PilT1 and PilB1. PilQ is located on the outer membrane and forms the pore with which the pilus protrudes into the extracellular environment (Schuergers and Wilde, 2015). PilD is a peptidase that processes prePilA1 into mature PilA1. Disruption of *pilC* and *pilD* both eliminate motility in *Synechocystis* (Bhaya et al., 2000; Yoshihara et al., 2001; Yoshihara and Ikeuchi, 2004).

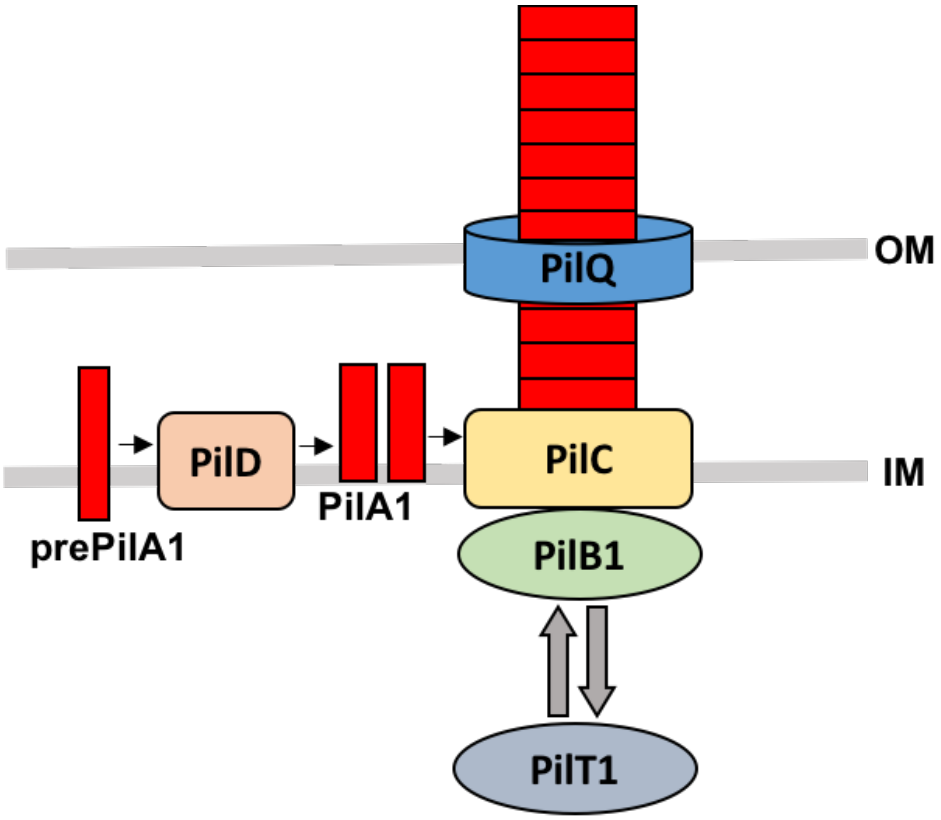

Figure 1.3: Type IV Pili Architecture (Adapted from Wilde and Mullineaux, 2015)

Predicted architecture of cyanobacterial type IV pili. prePilA1 is processed by PilD to its final functional PilA1 form. PilA1 forms large polymers that extend from the cell. PilC is in the inner membrane (IM) and serves as the base for the pilus. PilQ is thought to function as a pore in the outer membrane (OM) for the which the PilA1 polymers can exit. PilB1 and PilT1 are both motor proteins that function in extension and retraction of the pilus.

More recently it has been shown that not only do *Synechocystis* cells attach to a surface, but they also modify the surface on which they are moving (Ursell et al., 2013). Modification of the surface comes in the form of extracellular polymeric substances (EPS), that typically consist of polysaccharides (Burriesci and Bhaya, 2008; Wilde and Mullineaux, 2015). EPS are secreted and left behind as the cells move along surfaces creating a modified surface. The modified surface enhances the rate of movement of cells that are following behind. Essentially, *Synechocystis* cells can move faster when they are moving on a surface modified by other *Synechocystis* cells. EPS secretion systems that are essential for motility have been identified and characterized in other cyanobacteria, however these systems are not present in *Synechocystis* (Khayatan et al., 2015). Thus, the exact nature of how this system is functioning is unclear.

Collectively we are left with an image of a *Synechocystis* cell or group of cells that are able to sense their light environment via a set of photoreceptors which signal the direction in which the cells should move. The force of movement is generated by type IV pili complexes that drag the cells along a surface. Additionally, movement as a group is promoted by the secretion of polysaccharides from leading cells that allow lagging cells to more efficiently follow along. Despite these details, many questions remain regarding the signal transduction pathways that allow communication from photoreceptors to the motility machinery.

Biofilm Formation and Sedimentation

Biofilm formation is an essential process for the survival and proliferation of many different microorganisms (Costerton et al., 1995). In basic terms, biofilms can be described as large populations of cells that come together and adhere to surfaces in response to external stimuli. Often the stimuli are stressful with biofilm formation functioning as a way to mitigate the stress. Similar to the surface based motility described above, biofilm formation often involves both type IV pili and EPS secretion (Neu and Marshall, 1990; Gomez-Suarez et al., 2002; Shi and Sun, 2002). In *Pseudomonas aeruginosa*, type IV pili are not required for initial surface attachment, however they are required for the formation of multi-layered biofilms suggesting that they mediate cell- to-cell interactions during biofilm formation (O'Toole and Kolter, 1998). EPS are thought to also contribute to the formation of stable surface adhered colonies, while also functioning to creating a protective barrier around the surface attached group of cells. EPS provide protection in the form of a barrier from stresses ranging from heavy metals to UV radiation (Ehling-Schulz et al., 1997). EPS production has also been shown to affect the buoyancy of cells which in turn affects rates of spontaneous cell sedimentation (Lowe et al., 2007; Jittawuttipoka et al., 2013). Interestingly, it has been observed that certain sugars associated with EPS can also have a negative effect on biofilm formation (Rendueles et al., 2013), indicating a complicated interplay of signals that dictate both the type and amount of EPS produced.

As a model cyanobacteria, several studies have explored the nature of biofilm formation and cell sedimentation in *Synechocystis*. Little work has explored the role of *Synechocystis* type IV pili in these processes, although due to the role these cell appendages play in surface

adherence and motility it is likely that they are involved in biofilm formation. EPS production and secretion in *Synechocystis* has been explored and implicated in both surface adherence and cell buoyancy (Fisher et al., 2013; Jittawuttipoka et al., 2013). Fisher et al. (2013) identified two genes, *slr0977* and *slr0982*, with sequence homology to *E. coli* genes involved in surface adherence or biofilm formation. Disruption of these genes caused alterations in EPS production and altered biofilm formation. In a similar study, Jittawuttipoka et al. (2013) identified genes with sequence homology to known genes that are involved in EPS production in non-photosynthetic bacteria. Individual disruption of these genes not-surprisingly caused alterations in EPS production, while also altering the rate of spontaneous cell sedimentation. The cells settled faster than WT, thus increasing the rate at which the cells reach a surface upon which they can attach. While not directly monitoring biofilm formation, the authors suggested this enhanced sedimentation rate also enhanced biofilm formation, indicating that these genes may be associated with anti-biofilm EPS production.

Both type IV pili and EPS production likely play a major role in mediating biofilm formation in *Synechocystis*. The functional overlap of the major components of biofilm formation and phototaxis suggest an overlap of signals that may regulate each process.

SynEtr1 Overview

The overall focus of this dissertation is to analyze and determine if the protein product of *Synechocystis slr1212*, SynEtr1 (also known as UirS and NixA) (Song et al., 2011; Narikawa et al., 2013), functions as an ethylene receptor. SynEtr1 has a domain architecture that resembles

a two-component signaling system with its response regulator slr1213 (also known as UirR and NixB) encoded just downstream of *slr1212*. Another putative response regulator, slr1214 (also known as LsiR and NixC), is encoded downstream of *slr1213* (Figure 1.4A). SynEtr1 is characterized by an N-terminal transmembrane ethylene binding domain followed by a series of soluble PAS and PAC domains, a GAF domain, and a histidine kinase domain (Figure 1.4B) (Kwon et al., 2010). The PAS, PAC, and GAF domains make up the CBCR domain. Upon starting work on this project little was known about the function of SynEtr1 in *Synechocystis*. It was known that *slr1212* encoded a protein that was somehow involved in ethylene binding in *Synechocystis*, however a direct link had not been made (Rodriguez et al., 1999). Additionally, it was known that the GAF domain of SynEtr1 binds a chromophore and is photochemically categorized as a CBCR (Ulijasz et al., 2009). Since that time two papers have been published that implicated a role for SynEtr1 in phototaxis, however results from these studies were somewhat conflicting and neither addressed whether SynEtr1 functioned as an ethylene receptor (Song et al., 2011; Narikawa et al., 2013). Here, I will highlight what is currently known about the function of SynEtr1 biochemically and physiologically.

SynEtr1 Photochemistry

As mentioned above, *Synechocystis* possesses a wide variety of photoreceptors that mediate phototaxis and other light sensitive physiological responses (Bhaya, 2004; Fiedler et al., 2005; Hirose et al., 2013; Wiltbank and Kehoe, 2016). SynEtr1 falls into the class of phytochrome-like photoreceptors known as CBCRs (Ulijasz et al., 2009). CBCRs are thought to be unique to cyanobacteria and are one of the more abundant forms of photoreceptors found

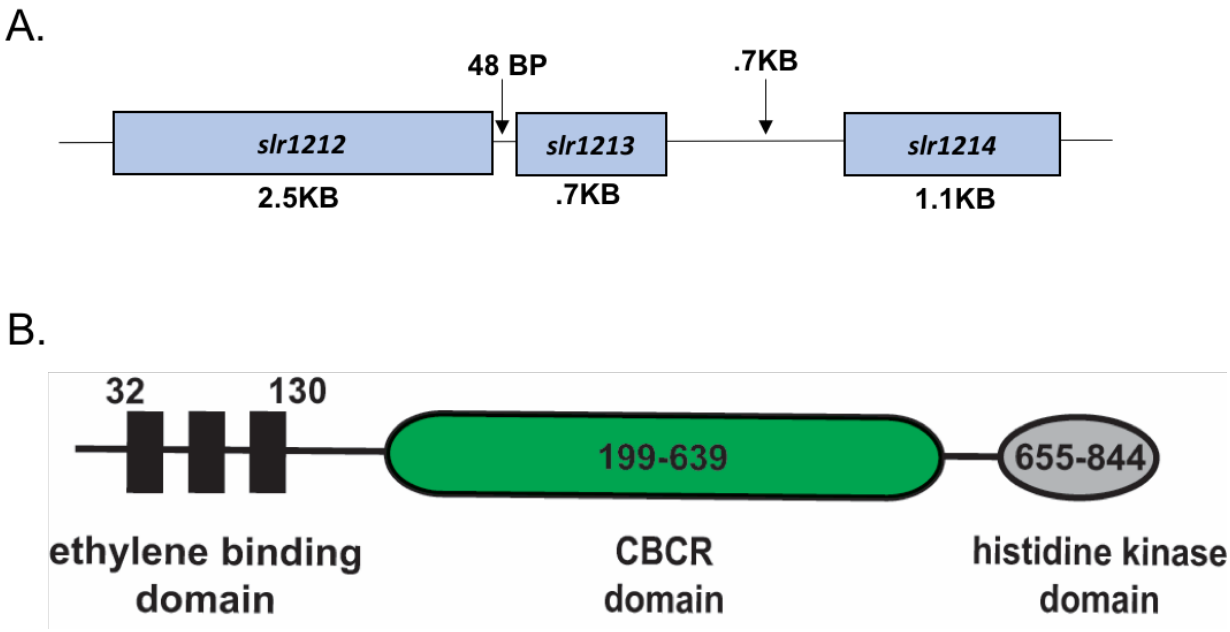

Figure 1.4: *Slr1212*, *slr1213*, and *slr1214* Genetic Arrangement and SynEtr1 Domain Architecture

(A) Arrangement of genes known to be require for SynEtr1 function. *Slr1212*, which encodes SynEtr1, and *slr1213*, which encodes a response regulator, are in very close proximity in the genome. *Slr1214* is approximately 700 base pairs downstream of *slr1213*. *Slr1214* encodes a predicted response regulator that is required for SynEtr1 function. (B) Domain architecture of SynEtr1. Numbers indicate the amino acid residues that constitute each domain. The three black bars represent the three predicted alpha helices of the ethylene binding domain. The CBCR domain (Green) is composed of 2 Pas and Pac domains and a GAF domain. The histidine kinase domain is thought to function in phosphorelay in two-component signaling.

in these organisms (Lamparter, 2004; Ikeuchi and Ishizuka, 2008; Wiltbank and Kehoe, 2016). CBCRs and phytochromes both require GAF domains to bind bilin chromophores (Ulijasz et al., 2009; Enomoto et al., 2015). CBCRs require only the GAF domain with a bound bilin for photoperception, whereas in phytochromes require the presence of PAS, GAF, and PHY domains for photoconversion (Essen et al., 2008; Rockwell et al., 2013). Additionally, the type of bilin bound differs with CBCRs utilizing phycocyanobilin (PCB) and phycoviolobilin (PVB) (Rockwell et al., 2011). Interestingly, as a whole CBCRs, display a broad spectral range spanning from UV to far-red (Enomoto et al., 2015).

The photoreversibility or spectral capacity of SynEtr1 has been examined several times with conflicting reports (Ulijasz et al., 2009; Song et al., 2011; Narikawa et al., 2013). In each case, the GAF domain of SynEtr1 was expressed in PCB producing *E. coli* followed by purification of the protein and light absorption analysis. Initially it was reported that SynEtr1 functioned as a photoreversible blue/green photoreceptor (Ulijasz et al., 2009). Subsequent studies reported that it was UV/green photoreversible and violet/green photoreversible (Song et al., 2011; Narikawa et al., 2013). Thus, what wavelengths SynEtr1 detects is an open question. It is possible that basic experimental differences contributed to the range of observed wavelength dependencies, yet it is also possible that SynEtr1 is actually responding to each of these wavelengths of light. A very recent study reconstituted SynEtr1 and its downstream signaling components in *E. coli* and showed that UV light was able to stimulate signal output of SynEtr1 *in vivo*, suggesting that UV directly activates SynEtr1 (Ramakrishnan and Tabor, 2016). Whether or not violet and blue light elicit a similar response *in vivo* has yet to be examined.

SynEtr1 Role in Phototaxis

While the photochemistry of SynEtr1 has been explored somewhat in depth, less is known about the physiological output of this protein. In addition to the work I am presenting here, two published studies have clearly implicated SynEtr1 as regulator of phototaxis; however, like the photochemistry described above, discrepancies exist regarding an exact role. It should be noted that several lab sub-strains of *Synechocystis* exist that often lead to conflicting physiological observations (Table 1.1) (Trautmann et al., 2012). The various strains include glucose tolerant, non-motile, negatively motile and positively motile strains with varying degrees of positive motility (Table 1.1). Sequencing analysis has attempted to make this picture clearer by determining the origins of these different strains (Kanesaki et al., 2012; Trautmann et al., 2012). Unfortunately, published studies are often unclear as to what strain is being used or fail to make mention of this at all, simply referring to their strain as WT.

In the two published studies regarding the role of SynEtr1 in phototaxis, three different *Synechocystis* strains were used (Table 1.2). Song et al. utilized a motile strain obtained from the Pasteur Institute (Song et al., 2011). In this study, SynEtr1 was initial observed to function as a UV/green photoreceptor. It was hypothesized that SynEtr1 functions as a stress response protein stimulating negative phototaxis in the presence of UV light. To test this, *slr1212* was deleted and replaced with a kanamycin resistance gene. WT and *slr1212* deficient *Synechocystis* were exposed to directional UV, and it was discovered that high levels of UV light elicited a negative phototactic response in WT cells. By contrast *slr1212* deficient cells phototaxed toward the UV light source. This indicated that SynEtr1 was likely playing a role in UV avoidance. Narikawa et al. utilized two separate substrains of *Synechocystis* to examine the role

Table 1.1: *Synechocystis* Sub-strains and Relevant Physiological Traits

	Motility in Standard Conditions	Glucose Tolerance
PCC 6803	Positive Phototaxis	No
PCC-P	Positive Phototaxis	No
PCC-N	Negative Phototaxis	No
PCC-M	Positive Phototaxis	No
GT-Kasuza	Non-motile	Yes
GT-S	Non-motile	Yes
GT-I	Non-motile	Yes

List of known *Synechocystis* sub-strains as described in Trautmann et al. (2012). PCC 6803 is the original strain deposited in the Pasteur Culture Collection in 1968. Standard conditions indicate conditions that would elicit positive phototaxis

Table 1.2: Reported Effects of Phototaxis Caused by Eliminating *slr1212* and Related Genes

	WT	***Slr1212***		***Slr1213***		***Slr1214***	
		deletion	**disruption**	**deletion**	**disruption**	**deletion**	**disruption**
PCC 6803 UV Light	Negative Phototaxis	Positive Phototaxis	N/A	Positive Phototaxis	N/A	Positive Phototaxis	
PCC-P White Light	Positive Phototaxis	N/A	Negative Phototaxis	N/A	Enhanced Positive Phototaxis	N/A	Enhanced Positive Phototaxis
PCC-N White Light	Negative Phototaxis	N/A	Enhanced Negative Phototaxis	N/A	Positive Phototaxis	N/A	Positive Phototaxis

Published phototactic responses caused by disrupting (Narikawa et al., 2011) or deleting (Song et al., 2011) *slr1212*, *slr1213*, and *slr1214*. The specific *Synechocystis* substrain and light source is indicated on the left. The genetic condition is indicated on the top. Each box is what was observed using the strain and light source with each genetic condition.

of SynEtr1 in phototaxis: PCC-P and PCC-N (Narikawa et al., 2011). PCC-P displays positive phototaxis under white light conditions, whereas PCC-N is negatively phototactic under white light conditions (Yoshihara et al., 2001; Kanesaki et al., 2012). To eliminate the function of SynEtr1 in this study, the researchers generated an *slr1212* disruption with a kanamycin resistance gene (Narikawa et al., 2011). Thus, in addition to the strain differences, the nature of the genetic manipulations of *slr1212* were also inconsistent. Narikawa et al. characterized SynEtr1 as a violet/green photoreversible photoreceptor, however they performed phototaxis assays in the presence of directional white light. In these conditions WT PCC-P moved toward the light source and PCC-N moved away. Disruption of slr1212 caused PCC-P to display significant negative phototaxis and caused the observed negative phototaxis in PCC-N to increase. Together these two studies clearly show that SynEtr1 is involved in regulating phototaxis, however the exact role remains unclear.

SynEtr1 Two-Component Signaling

SynEtr1 contains a predicted histidine kinase domain suggesting it functions as a two-component signaling system (Figure 1.4B). The kinase domain contains an H-box region that is typically involved in autophosphorylation (Kim and Forst, 2001; Song et al., 2011). It does, however, lack the conserved histidine involved in autophosphorylation of the histidine kinase domain, while containing a conserved histidine at an alternate site. Just downstream of *slr1212*, *slr1213* encodes the putative response regulator. Slr1213 (also referred to as UirR and NixB) has an N-terminal receiver domain and a C-terminal DNA binding domain. While close in genetic proximity, *slr1212* and *slr1213* are not predicted to be under the same transcriptional control

(Kopf et al., 2014). Approximately 700 base pairs upstream of *slr1213* is another response regulator *slr1214* (Figure 1.4A). Slr1214 (also referred to as LsiR and NixC) is a predicted AraC response regulator (Narikawa et al., 2011; Song et al., 2011). Both Song et al. and Narikawa et al. addressed the role of slr1213 and slr1214 in phototaxis, again producing conflicting results (Table 1.2).

Song et al. separately deleted *slr1213* and *slr1214* and in both cases the cells responded similarly to the SynEtr1 deletion by moving toward high intensity UV light (Table 1.2) (Song et al., 2011). They also found that mutant slr1213 and slr1214 lacking conserved aspartate residues predicted to function as the phospho-acceptor sites were unable to rescue WT UV avoidance. This suggests that phosphorelay to these proteins is essential to their function. This study also explored the function of the DNA binding domain of slr1213 and found that it controlled transcription of *slr1214*. Interestingly, it was found that constitutive expression of WT slr1214 was able to rescue UV avoidance in both *slr1212* and *slr1213* deletions lines. From this the authors concluded that under UV light SynEtr1 signals to slr1213 which activates *slr1214* transcription leading to downstream physiological responses.

Narikawa et al. generated separate gene disruptions of both *slr1213* and *slr1214*. In response to directional white light, they observed *Synechocystis* lacking either slr1213 or slr1214 to move in the exact opposite direction of what was seen with SynEtr1 deficient *Synechocystis* (Table 1.2). They did not explore the function of specific residues on slr1213 or slr1214. Additionally, neither Song et al. nor Narikawa et al. were able to directly observe histidine autophosphorylation of SynEtr1 or phosphotransfer to slr1213 or slr1214. Again, both

studies suggest that slr1213 and slr1214 play a role in signal output of SynEtr1, however the inconsistencies leave many questions unanswered.

In developing a UV sensor in *E. co*li, a very recent paper by Ramakrishnan and Tabor (2016), further explored the transcriptional target of slr1213 and managed to answer the question of phosphotransfer from SynEtr1 (Ramakrishnan and Tabor, 2016). In this study, as mentioned above, the authors expressed both *slr1212* and *slr1213* in *E. coli* and exposed the cells to UV light. Based on the results of Song et al., the authors placed GFP expression under transcriptional control of the predicted *slr1214* promotor, which is thought to be activated by slr1213. In this system an increase in GFP expression would indicate that signaling of SynEtr1 is functional in *E. coli* under UV light. Interestingly, it was observed that slr1213 binds to the promotor of the non-coding RNA (ncRNA) *csiR1* that is located in the intergenic region of *slr1213* and *slr1214*. Various ncRNAs have been shown to function as regulators on a transcriptional and posttranscriptional level in *Synechocystis* (Georg et al., 2009; Hernandez-Prieto et al., 2012). *CsiR1* transcription has been reported to be down-regulated in conditions of high inorganic carbon (Wang et al., 2004; Kopf et al., 2014; Klahn et al., 2015). GFP fluorescence was observed in UV light when GFP expression was under control of only the *csiR1* promotor as opposed to the entire intergenic region. This suggests that slr1213 controls *csiR1* expression and *slr1214* expression in the presence of UV light via the *csiR1* promotor. Additionally, transcriptome analysis shows that *csiR1* and *slr1214* are co-transcribed under certain conditions, such as low inorganic carbon (Wang et al., 2004; Mitschke et al., 2011; Klahn et al., 2015). The authors also explored whether SynEtr1 directly phosphorylates slr1213 (Ramakrishnan and Tabor, 2016). It was reported that slr1213 phosphorylation increased in UV

exposed *E. coli* expressing both *slr1212* and *slr1213*, while no change was seen in UV exposed *E. coli* expressing only *slr1213* (Ramakrishnan and Tabor, 2016). This directly showed that phosphotransfer from SynEtr1 to slr1213 occurs in an in vivo system, a result that had previously evaded researchers (Narikawa et al., 2011; Song et al., 2011).

The studies described here suggest that SynEtr1 is a photoreceptor that is able to respond to wavelengths of light ranging from UV to blue and is photoreversible in green light. It functions as a two-component receptor and has a physiological output that affects phototaxis. It directly phosphorylates its response regulator slr1213 and has another putative response regulator, slr1214. Slr1213 likely transcriptionally activates both the ncRNA *csiR1* and *slr1214*. Slr1214 is likely involved in downstream output of the signal, however it's direct involvement and function is unknown. Interestingly, yeast two-hybrid studies have shown that slr1214 directly interacts with SynEtr1 (Sato et al., 2007). As a ncRNA, it is possible the *csiR1* is functioning as a transcriptional or posttranscriptional regulator. Possible regulatory targets of *csiR1*, if any, are unknown. A model representing what is currently known about the function of SynEtr1 two-component signaling can be seen in Figure 1.5.

While the role of SynEtr1 as a photoreceptor has been explored, a question remains: does SynEtr1 function as an ethylene receptor? The overall goal of this dissertation is to answer that question and to further characterize the function of SynEtr1. In doing so, we will explore the biochemical and physiological function of ethylene in *Synechocystis*. This will help complete the picture of the function of SynEtr1 as well as provide insight into the evolutionary origins of ethylene as a signaling molecule.

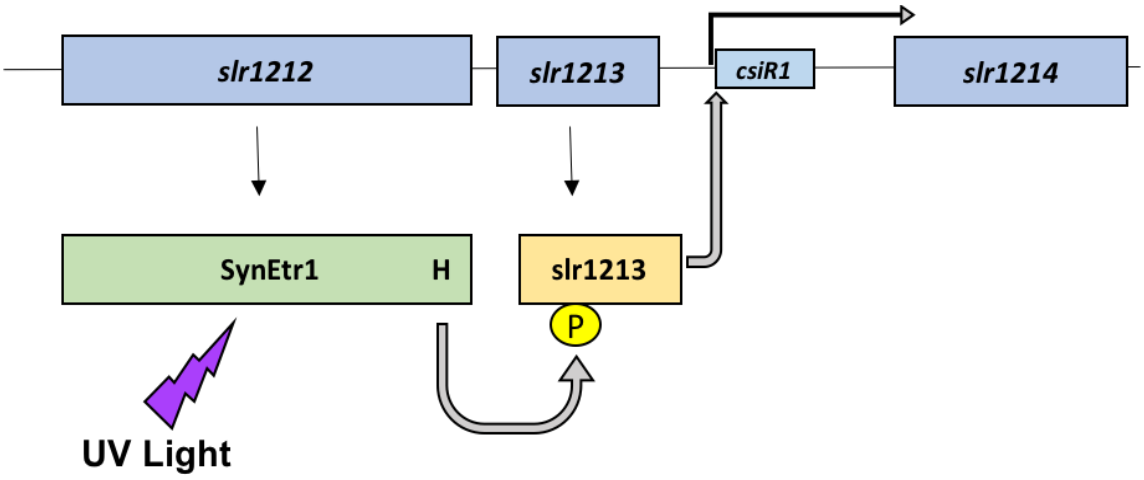

Figure 1.5: Basic Model of Known SynEtr1 Two-Component Signaling

All known components of SynEtr1 two-component signaling. The blue boxes are the genes involved with arrows indicating the proteins they encode. UV-light has been shown to stimulating phosphate transfer from SynEtr1 to slr1213. Activated slr1213 then binds to the promoter of *csiR1*, a non-coding RNA, and is thought to transcriptionally activate it and *slr1214*.

Chapter 2

Materials and Methods

Strains and Growth Conditions

Three organisms were used throughout this work: *E. coli*, *Pichia pastoris (Pichia)*, and *Synechocystis*. *E. coli* strains used included DH5 alpha and S-17, for cloning and conjugal transfer respectively. *E. coli* growth always took place at 37˚C in either liquid LB media or LB agar plates with appropriate antibiotics. For *Pichia*, the strain used was GS115. Pichia was grown at 30˚C in YPD media in either liquid or on agar plates. Growth and maintenance of *Synechocystis* cultures took place on 1% (w/v) agar BG-11 agar plates at room temperature at a fluence range of 10-30 uM/m^2/s. BG-11 was modified to have a reduced amount of $CuSO_4$ (100 nM final concentration) due to the presence of the copper repressible pPetJ promoter controlling gene expression on the pUR plasmid described below. Motile *Synechocystis* was obtained from the Pasteur Institute. We found that over time, cultures kept in liquid media would have reduced motility. Additionally, we found that the age of the cells (ie. generation number on plate) affected motility as well. WT *Synechocystis* revived from frozen stocks displayed enhanced motility compared to *Synechocystis* maintained on agar plates for long periods of time (Figure 2.1). Thus, we attempted to standardize for age of the cells when performing any physiological assays. We also found that *Synechocystis* grew at a much faster rate on fresh (less than one week old) BG-11 plates that were not refrigerated, so all plates were prepared fresh.

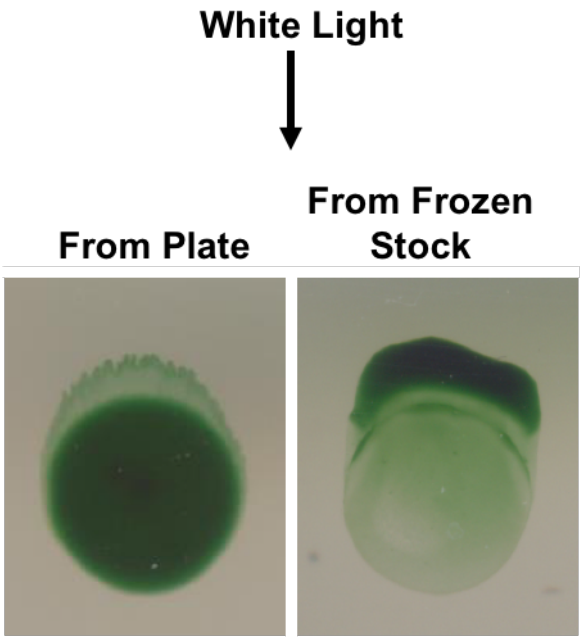

Figure 2.1: Motility Comparison of Cells Maintained on Plates Vs Frozen Stock

Comparison of motility in a culture that has been maintained on 1% (w/v) agar BG-11 plates for many generations vs. a culture that has recently been revived from a frozen DMSO stock. Both assays were performed in 30µMs/m^2/s of white light from an LED source for four days in air.

Cloning and Transformations

Exogenous expression of genes was performed in both *Synechocystis* and *Pichia pastoris*. In all cases the construct to be expressed was initially subcloned into the PGEM vector and transformed into DH5 alpha *E. coli*. All primers for each construct can be found in Appendix A. Primers were designed in DNASTAR with melting temperatures as close as possible for each pair. Additionally, primers were modified with appropriate restriction sites depending on the ultimate destination for the construct being cloned. PCR was used to amplify the constructs with annealing temperatures and extension times optimized for each construct. Standard Taq polymerase was used for amplification of the construct with subsequent ligation into the PGEM vector using TA overhangs. The ligation products were then transformed into competent DH5 alpha *E. coli* and plated on LB-ampicillin plates. Successful ligation and transformation was confirmed by colony PCR with appropriate primers. Successful transformants were then selected and grown overnight in 5 mL of liquid LB. Plasmids were then isolated using the Promega mini-prep kit.

For gene expression in *Pichia*, constructs were digested out of the PGEM vector with appropriate restriction enzymes and ligated into the pPICZA *Pichia* expression vector and subsequently transformed into DH5 alpha *E. coli* and plated on low salt LB plates with Zeocin. All *Pichia* expressed constructs contain an C-terminal GST tag. For expression of point mutants in *Pichia*, site-directed mutagenesis was performed on the construct in the initial PGEM vector. Using DNASTAR, primers were designed to overlap the base pairs to be mutated with the reverse complements being the forward and reverse primers. High fidelity Ex-Taq was use to amplify the entire plasmid by PCR. Following PCR, Dpn1 digestion was performed to remove the

initial WT template. The Dpn1 treated PCR product was then transformed into DH5 alpha *E. coli*. Colonies were grown and the vectors were isolated by mini prep. Successful mutation of the sites of interest were confirmed by sequencing using the UTK Genomics Core sequencing facility. Following confirmation of point mutants, the constructs were then cloned into the pPICZA as described above. Transformation of the WT and point mutant vectors into *Pichia* was performed as described in the pPICZA, B, C manual from Invitrogen.

Both gene disruptions and gene deletions of *slr1212* were used. The *slr1212* gene disruption construct was previously generated (Rodriguez et al., 1999). This construct contains *slr1212* with a kanamycin resistance gene inserted in the region of the gene encoding the ethylene binding binding domain. This construct was transformed into WT *Synechocystis* by natural transformation. 10 ug of the *slr1212* disruption plasmid was incubated with WT *Synechocystis* that had been removed from a BG-11 plate to a density of OD_{730} = .6 - .8 for 5 hours in diffuse light at a fluence rate of 30uM/m^2/s. The mixture was then plated on a nitrocellulose disc on a 1% (w/v) agar BG-11 agar plate. The disc was incubated for 24 hours in diffuse light at 30uM/m^2/s. The disc was then transferred to another BG-11 plate containing 25 ug/mL kanamycin for 48 hours. Finally, the disc was transferred to a BG-11 plate containing 50 ug/mL kanamycin until individual colonies appeared. Successful transformants were confirmed by colony PCR. Gene deletions were generated for both *slr1212* and *slr1214*. Gene deletions were generated by PCR fusion (Wang et al., 2002). Primers used for gene deletions can be found in Appendix A. In both cases the genes were replaced with a kanamycin cassette obtained from the lab of Dr. Barry Bruce. Transformation of the deletion constructs was

performed as described above for the *slr1212* gene disruption construct with successful transformation confirmed by colony PCR.

For exogenous gene expression in *Synechocystis*, constructs were digested out of PGEM with appropriate restriction enzymes and ligated in the pUR *Synechocystis* expression vector obtained from Dr. Annegrette Wilde (Wiegard et al., 2013). The pUR vector has an origin of replication for *Synechocystis*, which allows it to self replicate once transformed in *Synechocystis*. Additionally, gene expression is under the pPetJ promotor, which is copper repressible. For expression of point mutants prior to cloning into the pUR, site-directed mutagenesis was performed as described above on constructs in PGEM. Final pUR plasmids were transformed into either *slr1212* disruption *Synechocystis* (SynEtr1ΔTM2) backgrounds or *slr1212* deletion *Synechocystis* (ΔSynEtr1) by conjugal transfer. For green fluorescent protein (GFP) expression, GFP-pUR was transformed into WT *Synechocystis*. For conjugation pUR plasmids were first transformed into S-17 *E. coli* for biparental conjugation. For biparental mating, 3 mL of the transformed S-17 *E. coli* were grown overnight in LB at 37˚C. The cells were then harvested and washed twice with 2 mLs of fresh LB and they were finally resuspended in 200 µLs BG-11. 5 mLs of *slr1212* disrupted or deleted *Synechocystis* were also harvested and resuspended in 1 mL BG-11. The cyanobacterial cells were then combined with the S-17 *E. coli* cells. This mixture was harvested and resuspended in 200 µLs BG-11. This mixture was then plated on sterile nitrocellulose filter papers on BG-11 + 5% (v/v) LB agar plates. These plates were incubated in low light at 30˚C for 24 hours. The filter paper was then transferred to 1% (w/v) agar BG-11 plates containing 25 ug/mL kanamycin for 48 hours. The filter paper was then

transferred to BG-11 plates with 50 ug/mL kanamycin until colonies were visible. Colonies were selected and streaked on fresh BG-11 plates and transformants were confirmed by colony PCR.

Protein Expression in *Pichia* and Ethylene Binding Assays

Ethylene binding assays were performed on whole cell *Pichia* with the protein of interest expressed. Protein expression in *Pichia* was performed as described in the Invitrogen *Pichia* manual. 5 uM CuSO4 was added to the BMMY expression media. Following 48-hour expression, the cells were harvested at 8,000 RPMs for 10 mins at room temp. Three grams of cells were then spread on Whatman glass microfiber discs. The discs were then folded over, and transferred to glass jars for the ethylene binding assays. Ligand competition ethylene binding assays were preformed as previously described (Schaller and Bleecker, 1995). A general flowchart for the ligand competition assay can be seen in Figure 2.2.

SDS-PAGE and Western Blots

To verify expression of proteins in *Pichia,* western blotting was performed on isolated *Pichia* membranes. Membrane isolation and protein labeling with anti-GST antibodies is described in Rodriguez et al, 1999 (Rodriguez et al., 1999). Secondary labeling of the GST antibodies with HRP conjugated secondary antibodies were used for visualization via addition of HRP. Imaging was done using the Chemidoc XRS+ system from Biorad.

Additionally, western blotting was used to examine levels of PilA1 protein in both isolated pili from *Synechocystis* and from whole cell extracts of *Synechocystis*. PilA1 antibodies

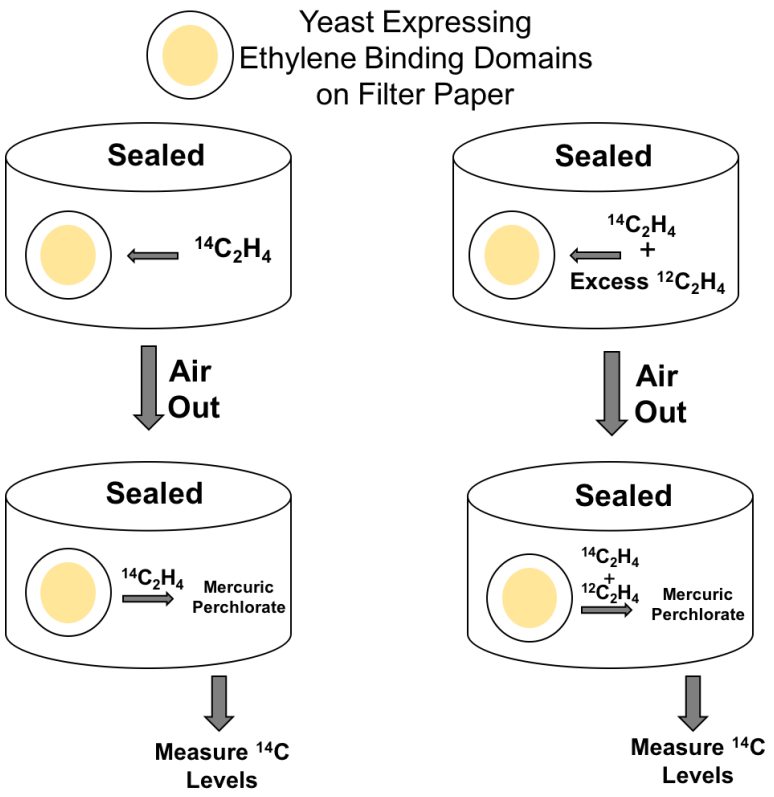

Figure 2.2: Ligand Competition Ethylene Binding Assay Diagram

Diagram of the general steps involved in ethylene binding assays. Ethylene binding proteins are initially expressed yeast. Yeast cell are harvested and spread on filter paper. The yeast cells are then exposed to ^{14}C ethylene or ^{14}C ethylene with excess ^{12}C ethylene in sealed containers. Following an incubation period, the yeast cells are aired out and transferred to another sealed container with mercuric perchlorate. Bound ethylene is then released and trapped in mercuric perchlorate with subsequent measure of ^{14}C levels in the mercuric perchlorate. Yeast exposed to ^{14}C and excess ^{12}C provide a measure of background ethylene binding.

were obtained from Dr. Roman Sobotka (Linhartová et al., 2014).Following pili isolation or whole cell extraction (described below), 2X SDS loading buffer was added at a 1:1 ratio. Proteins were then separated on 12% SDS-PAGE gels with subsequent transfer to PVDF membranes. Following membrane blocking using 5% (w/v) non-fat dry milk, PilA antibodies were added at 1:10,000 dilution. Following overnight incubation at 4^{O}C, the membrane was washed using 4X for 10 mins in TBST buffer. HRP conjugated secondary antibodies were then added and incubated at room temp for one hour. The membranes were then washed 4x for 10 mins in TBST buffer, with subsequent imaging using a Biorad Chemidoc system.

Synechocystis Phototaxis Assays

All phototaxis assays were performed on .4% (w/v) agar BG-11 agar plates unless otherwise specified. Initially, *Synechocystis* was taken from 1% (w/v) agar BG-11 agar plates and resuspended in fresh liquid BG-11 to a high density. Prior to plating all resuspended strains were normalized to a standard density. Following density normalization, 10 uL of cells were spotted on the .4% (w/v) agar BG-11 plates. The plates were then placed in diffuse light at 30 uM/m^2/s overnight to dry and acclimate. The plates were then wrapped exposing the cells to only light from one direction and placed in sealed containers (Figure 2.3). The containers had either hydrocarbon free air or 1 ppm ethylene in constant circulation. All assays were performed at 28° C with white light at a fluence rate of 30 µmol/m^2/s unless otherwise specified. In some cases, monochromatic light arrays were used. These assays were also at a fluence rate of 30 µmol/m^2/s using LED arrays from Quantum Devices Inc. (Barneveld, WI) For red light (λ_{max} = 672 nm), green light (λ_{max} = 525 nm), and blue light (λ_{max} = 462 nm). The duration of the

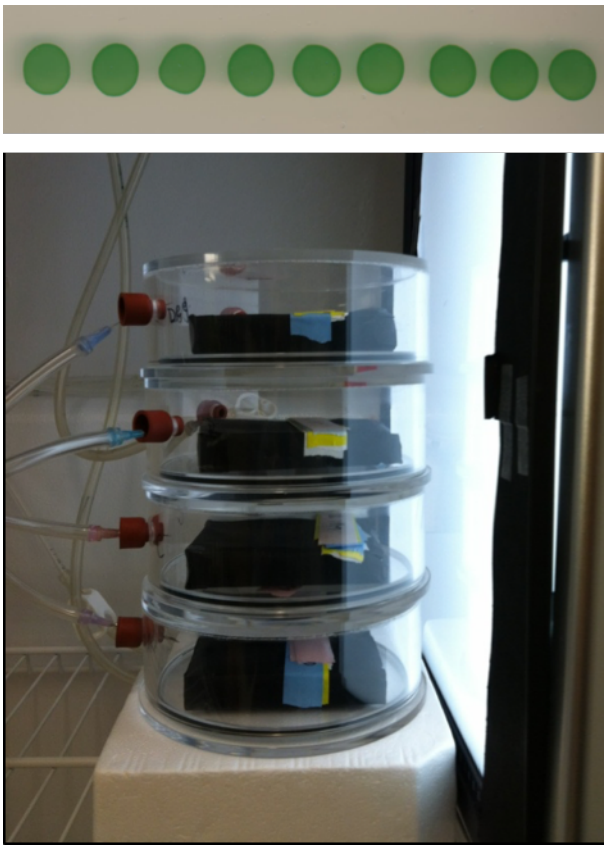

Figure 2.3: Phototaxis Assay Set-up

Cells are removed from 1% (w/v) agar BG-11 plates, resuspended in liquid BG-11 and spotted on .4% (w/v) agar BG-11 plates (Above). The plates are wrapped exposing one side to a light source and placed in sealed chambers allowing for flow through of air or varying concentrations of ethylene gas.

assays varied depending on what was being tested. Following completion of the assay, images of each plate were acquired using a flatbed scanner. Images were then analyzed and measured using ImageJ. Overall, colony movement was measured as total distance moved from the front edge of the colony. Within each assay there were minimum of three colonies and each assay was repeated minimum of three times.

RNA Isolation from *Synechocystis*, DNAse Treatment, and cDNA Synthesis

For RNA extraction, *Synechocystis* cells were initially exposed to directional light for 3 days on 1% (w/v) agar BG-11 plates in the presence of air or 1 ppm ethylene. Following this treatment, cells were removed from the plate and resuspended in 1 mL of fresh BG-11 at equal densities. The cells were then harvested at 10,000 RPMs for 10 mins and resuspended in 1 mL cold Trizol. The cells were next incubated at 95°C for 5 minutes followed by 5 minutes on ice. Next 200 uL chloroform was added and the cells were vortexed for 30 seconds. After 5 min at room temp, the cells were centrifuged for 15 min at 12000 x g at 8°C. The aqueous phase (~450 uL) was then transferred to a new tube and RNA was precipitated by addition of an equal volume (~450 uL) of isopropanol. After 5 mins at room temperature the precipitated RNA was pelleted by centrifugation (12000 x g) for 10 minutes at 8°C. The RNA pellet was then washed twice by in 75% ethanol with subsequent centrifugation (8000 x g) for 5 minutes at 8°C. The washed RNA was then air-dried for 10 mins at room temp and was subsequently resuspended in 50-100 µL DEPC-treated water. The concentration of RNA was then measured using a NanoDrop spectrophotometer. 8 µg of the total RNA was then treated with DNAse for 30 minutes at 37°C using the TURBO DNA free kit from Invitrogen in a 50 uL reaction. Following

inactivation of the DNAse by use of the inactivation reagent supplied by the kit, the RNA was the then further washed using the Spectrum Plant Total RNA Kit from Sigma and eluted in 50µl of DEPC-treated water. For cDNA synthesis, 800 ng of total RNA was reverse transcribed using the TaqMan Reverse Transcription Reagents Kit from Applied Biosystems in a total volume of 40 µl with reagents at concentrations suggested by the manufacturer with random hexamers being used for priming. Samples lacking reverse transcriptase were used as controls testing for DNA contamination. In these samples water was used in place of the reverse transcriptase. Following synthesis, the cDNA was diluted at a ratio of 1:4 for a total final volume of 160 uL.

Quantitative RT-PCR

Primers for qPCR were designed using the qPCR primer design software on the Genscript website. qPCR primers can be found in Appendix A. qPCR was performed using the Bio-Rad iQ5 Real-Time PCR Detection System. Each reaction was 10 µL total with 5 µL of Ssofast EvaGreen Supamix from Biorad, 4 µL of 1:4 diluted cDNA (1:10 final dilution), and 1 µL of a 10 µM forward and reverse primer mix (0.5 µM each final primer concentration). Cycle times were dependent on primers used. Transcript amounts for each cell under each condition were normalized to levels of TrpA as the internal standard using the method of Livak and Schmittgen (Livak and Schmittgen, 2001). Each gene was analyzed with two biological replicates with three technical replicates per biological replicate. The transcript abundance for each biological replicate was then normalized to the levels of that gene in wildtype samples in air and the average ± SEM shown for all experiments.

Pili Isolation and Whole Cell Protein Extraction in *Synechocystis*

Pili were isolated from equal density *Synechocystis* extracted from 1% (w/v) agar BG-11 plates exposed to directional light in the presence of either air or ppm ethylene for 4 days. Pili isolation was performed as described previously (Nakasugi et al., 2006).

Transmission Electron Microscopy of *Synechocystis* Pili

To image the pili, *Synechocystis* cells were extracted at equal densities from 1% (w/v) agar BG-11 plates exposed to directional light for four days in air or 1 uL/L ethylene. They were then stained with 1% (w/v) uranyl acetate for 1 minute with images obtained using a Zeiss Libra 200 MC electron microscope. At least 10 cells were examined from three separate colonies for each condition.

Low Temperature Fluorescence and Quantification of photosystem I: photosystem II ratios in *Synechocystis*

To determine photosystem I: photosystem II ratios, we first extracted *Synechocystis* cells at equal densities from 1% (w/v) agar BG-11 plates exposed to directional light for four days in either air or 1 uL/L ethylene. We then analyzed them with chlorophyll low temperature (77 K) fluorescence at an excitation wavelength of 440nm according to methods previously described (Murakami, 1997; Kiley et al., 2005; Iwuchukwu et al., 2010). For quantification of relative photosystem I: photosystem II ratios, each sample was initially normalized to PSI chlorophyll fluorescence levels. The curves representing chlorophyll fluorescence of either PSI or PSII were then deconvoluted, and the are under the curve was measured. The combined area of both

peaks for PSII were combined and compared to PSI to generate a ratio between the two (Figure 2.4).

Synechocystis Sedimentation Assays

For sedimentation assays, *Synechocystis* cells were initially removed from 1% (w/v) agar BG-11 plates and resuspended at a density of OD_{730} = 1 in fresh BG-11. 2 mL of each sample was then placed in loosely sealed tubes to allow for gas exchange and exposed to ~30 uM/m^2/s white light for varying lengths of time at 24˚C. Images were taken following the incubation period.

Biofilm Assays

Initially, *Synechocystis* was harvested from 1% (w/v) agar BG-11 agar plates and resuspended in liquid BG-11 to a density of OD_{730} = .1. Assays were performed as described previously (Fisher et al., 2013). Each sample was placed in a sealed container with varying circulating ethylene concentrations or air. Modifications to Fisher et al., 2013 include use of .1% crystal violet and exposure to ~30 uM/m^2/s white light at 24˚C.

Statistics

Statistical significance for all experiments outside of RNA-seq was calculated using a two-tailed Student's *t* test. *P* values, which indicate statistical significance, are labelled for each figure.

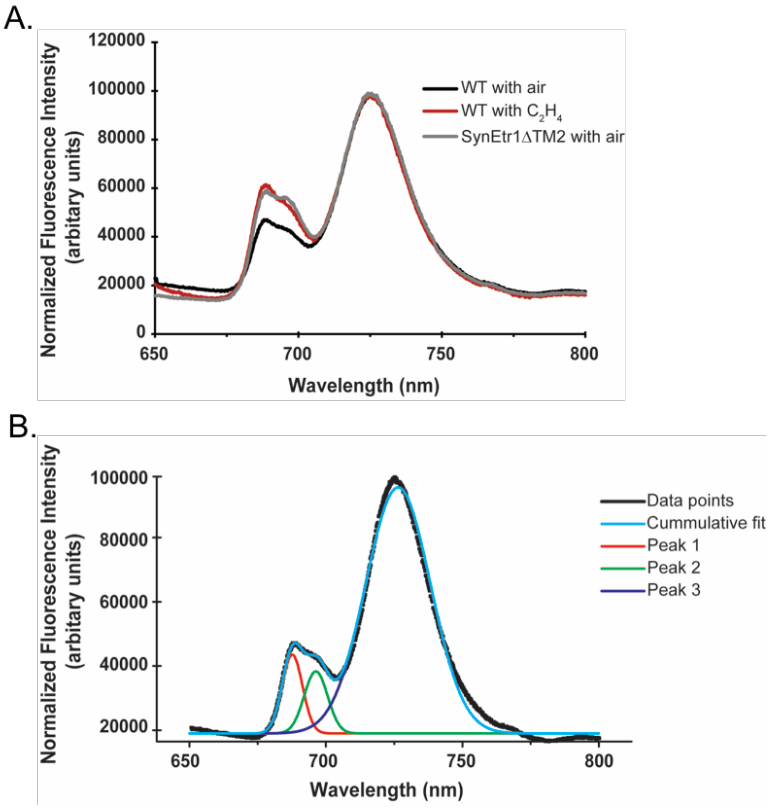

Figure 2.4: Low-Temperature Fluorescence Analysis

Quantification of low-temperature chlorophyll fluorescence. (A) Normalization of samples to PSI levels in WT cells exposed to air. (B) Deconvolution of each of the peaks. Peaks 1 and 2 both represent chlorophyll fluorescence associated with PSII. Peak 3 is PSI chlorophyll fluorescence. The area under each curve was then calculated. Peaks 1 and 2 combined represent total PSII chlorophyll fluorescence.

RNA-seq Analysis

For transcriptome analysis, RNA-seq was performed. Initially, RNA was extracted (previously described) from *Synechocystis* on 1% (w/v) agar BG-11 agar plates exposed to 30uM/m2/s white light for 4 days in either air or 1 ppm ethylene. For each sample, three biological replicates were generated. To generate biological replicates, following each 4 day exposure of *Synechocystis* samples to directional light in air or 1 ppm ethylene, a new plate of cells was streaked out and exposed to the same conditions. This was repeated until RNA was isolated from the same line *Synechocystis* cells three separate times. RNA samples were then sent to Genome Sequencing and Analysis Facility at the University of Texas at Austin. Sequencing was performed using the NextSeq 500 platform producing approximately 20 million single end 75 base pair reads per sample. For all data analysis the Sun Grid engine Newton at UTK was used. All code used for RNA-seq data analysis can be found in Appendix C. The data files containing the raw reads were first uploaded to Newton and the quality was analyzed using FastQC. Additionally, the reference *Synechocystis* genome was downloaded along with the annotated gff genome file. Next, read trimming was performed with a 4:15 sliding window and a minimum read length of 75. The trimmed quality of the trimmed reads was then analyzed once again using FastQC. The trimmed reads were then indexed and mapped to the reference genome using Bowtie2 and Tophat. The BAM files produced from Tophat were first sorted then converted to SAM files, and the reads were then counted using HTSeq. The read counts were loaded into R and differential expression analysis was performed using DESeq2.

Chapter 3

Ethylene Binding to SynEtr1 and Function in Phototaxis

Portions of the research presented here are presented in a recent publication in Plant Physiology under the title “Ethylene Regulates the Physiology of the cyanobacterium Synechocystis sp. PCC 6803 via an Ethylene Receptor” (Lacey and Binder, 2016).

Introduction

An endosymbiotic event approximately 1.5 billion years ago involving an ancient cyanobacterium gave rise to the chloroplast in modern plants (Sanderson et al., 2004; Yoon et al., 2004). Since that time, the cyanobacterial endosymbiont became reduced in function with several of its genes predicted to be transferred to nuclear genome of the host organism. Two gene families present in plants thought to have a plastid origin are the phytochromes and the ethylene receptors (Kehoe and Grossman, 1996; Martin et al., 2002; Schaller et al., 2011). Supporting this, in plants, both phytochromes and ethylene receptors have a domain architecture similar to that of two-component signaling systems found in prokaryotes. While several phytochromes and phytochrome like two-component receptors have been characterized in cyanobacteria (Fiedler et al., 2005), no functional ethylene receptors have been identified.

In plants, ethylene mediates growth and many developmentally related processes (Abeles et al., 1992). The receptors that perceive and elicit ethylene responses are characterized by an N-terminal transmembrane EBD followed by a series of soluble domains

(Lacey and Binder, 2014). In *Arabidopsis* there are five ethylene receptors. The sequence of the EBD domain in these receptors is highly conserved and specific residues with importance in ethylene binding are known (Wang et al., 2006). The sequence conservation of EBDs allows for the identification of possible EBDs in non-plant species. Recently, we scanned for possible EBDs based on sequence similarity to the AtETR1 in all known non-plant genomes (Figure 3.1 and Table A2). 112 different prokaryotic species were identified that encode proteins containing all seven of the known conserved residues required for ethylene binding (Wang et al., 2006). This included many cyanobacterial species as well as non-photosynthetic bacteria. Among the identified genes encoding putative EBDs was the gene locus *slr1212* from *Synechocystis*.

Slr1212 was previously identified as a gene encoding a possible EBD containing protein (Rodriguez et al., 1999). It was reported that *Synechocystis* is able to bind ethylene with high affinity and disruption of the *slr1212* gene locus eliminated ethylene binding. While suggesting that the protein product of *slr1212*, SynEtr1, is involved in ethylene binding in *Synechocystis*, this observation does not prove that SynEtr1 binds ethylene. Similar to the *Arabidopsis* ethylene receptors SynEtr1 contains a predicted N-terminal transmembrane EBD followed by soluble domains including a GAF domain and a histidine kinase domain (Figure 3.2). Previous work has shown that the GAF domain binds a bilin chromophore that allows SynEtr1 function photochemically as blue/green photoreversible CBCR (Ulijasz et al., 2009). CBCRs are phytochrome-like photoreceptors unique to cyanobacteria that have been implicated in several physiological processes including phototaxis (Rockwell et al., 2013). Thus, as I began working on this project we knew that SynEtr1 may be involved in ethylene binding and that it

Figure 3.1: Phylogenetic Tree of Predicted EBDs in Non-Plants

A BLAST search was performed in April of 2014 to find putative EBDs in all non-plant and algal species. AtETR1 (1-130) was used as the query sequence. To be considered, the protein must contain all 7 amino acids required for ethylene binding in AtETR1 and an E value of < 1e-10. Clustal Omega was used for sequence alignment, and Clustal W was used for generating the phylogenic tree. In the tree, the cyan color indicates cyanobacterial species, black indicates other bacteria, and the five *Arabidopsis* receptors are in green.


ETR1|Arabidopsis_thaliana
ERS1|Arabidopsis_thaliana
ERS2|Arabidopsis_thalianas
ETR2|Arabidopsis_thaliana
EIN4|Arabidopsis_thaliana
GI_495567658|Methylophaga_thiooxydans
GI_516343515|Nafulsella_turpanensis
GI_90020309|Saccharophagus_degradans
GI_83649935|Hahella_chejuensis_KCTC_2396
GI_495319814|Reinekea_MED297
GI_494242859|Methylophaga_aminisulfidivorans
GI_348028029|Glaciecola_nitratireducens
GI_491634368|Pseudoalteromonas_luteoviolacea_ATCC_29581
GI_498069774|Pseudoalteromonas_rubra_ATCC_29570
GI_498063176|Pseudoalteromonas_piscicida
GI_498291517|Pseudoalteromonas_flavipulchra
GI_515784614|Pseudoalteromonas_NJ631
GI_516746942|Asticcacaulis_benevestitus
GI_557830516|Asticcacaulis_AC460
GI_493319688|Asticcacaulis_biprosthecum
GI_557820388|Asticcacaulis_AC402
GI_494341607|Hydrocarboniphaga_effusa
GI_551356121|Nevskia_ramosa
GI_521960204|Zavarzinella_formosa
GI_518739914|Methylotenera_mobilis
GI_253996028|Methylotenera_mobilis
GI_167648286|Caulobacter_K31
GI_494942938|Caulobacter_sp._AP07
GI_493945542|Methylobacter_tundripaludum
GI_493946777|Methylobacter_tundripaludum
GI_493947740|Methylobacter_tundripaludum
GI_493947739|Methylobacter_tundripaludum
GI_519004353|Methylobacter_marinus
GI_254000138|Methylovorus_glucosetrophus
GI_495722902|Janthinobacterium_HH01
GI_498131442|Pseudomonas_fuscovaginae
GI_591395722|Pseudomonas_brassicacearum
GI_330812561|Pseudomonas_brassicacearum_subsp_brassicacearum
GI_517434659|Pseudomonas_CFII68
GI_359763627|Pseudomonas_fluorescens
GI_489299342|Pseudomonas_fluorescens
GI_495527462|gamma_proteobacterium_BDW918
GI_333982799|Methylomonas_methanica_MC09
GI_558562971|Methyloglobulus_morosus
GI_521973497|Methylomonas_MK1
GI_521079810|Hahella_ganghwensis
GI_501088421|Marinobacter_lipolyticus
GI_392377229|Azospirillum_brasilense_Sp245
GI_288958265|Azospirillum_B510
GI_374291663|Azospirillum_lipoferum_4B
GI_402770875|Methylocystis_SC2
GI_115523501|Rhodopseudomonas_palustris
GI_90422733|Rhodopseudomonas_palustris
GI_163853566|Methylobacterium|extorquens
GI_254563496|Methylobacterium_extorquens_DM4
GI_188583868|Methylobacterium_populi
GI_489694910|Methylobacterium_extorquens_DSM13060
GI_240140985|Methylobacterium_extorquens_AM1
GI_218532426|Methylobacterium_extorquens_CM4
GI_587643757|Skermanella_stibiiresistens
GI_392373508|Candidatus_Methylomirabilis_oxyfera
GI_517227901|Methyloversatilis_NVD
GI_519009451|Methyloversatilis|universalis
GI_518760078|Rhodocyclaceae_bacterium
GI_497353964|Oxalobacteraceae_bacterium_IMCC9480
GI_494038993|Chthoniobacter_flavus_Ellin428
GI_498153540|Acaryochloris_CCMEE_5410
GI_497242913|Oscillatoriales_cyanobacterium_JSC-12
GI_428219864|Pseudanabaena_PCC_7367
GI_428219681|Pseudanabaena_PCC_7367
GI_427736248|Rivularia_PCC
GI_518333542|Pleurocapsa_PCC_7319
GI_428221455|Synechococcus_PCC_7502
GI_497472233|Lyngbya_PCC_8106
GI_515875979|Spirulina_subsalsa
GI_553729765|Lyngbya_aestuarii
GI_497472989|Lyngbya_PCC_8106
GI_515515874|Anabaena_PCC_7108
GI_493032864|Coleofasciculus_chthonoplastes_PCC_7420
GI_440681237|Anabaena_cylindrica_PCC_7122
GI_434406889|Cylindrospermum_stagnale_PCC_7417
GI_428214479|Oscillatoria_acuminata_PCC_6304
GI_515874234|Spirulina|subsalsa
GI_497239980|Oscillatoriales_cyanobacterium_JSC-12
GI_517210500|filamentous_cyanobacterium_ESFC-1
GI_428223547|Geitlerinema_PCC_7407
GI_553732500|Lyngbya_aestuarii
GI_172039202|Cyanothece_ATCC_51142
GI_495553311|Cyanothece
GI_454396182|Stanieria_cyanosphaera_PCC_7437
GI_516257932|Geitlerinema_PCC_7105
GI_494598248|Oscillatoria_PCC_6506
GI_428318322|Oscillatoria_nigro-viridis_PCC_7112
GI_493720891|Arthrospira_maxima
GI_495326409|Arthrospira_PCC_8005
GI_493674252|Arthrospira_platensis
GI_516257491|Geitlerinema_PCC_7105
GI_517207104|filamentous_cyanobacterium_ESFC-1
GI_427723604|Leptolyngbya_PCC_7376
GI_257057938|Cyanothece_PCC_8802
GI_218441038|Cyanothece_PCC_7424
GI_307154701|Cyanothece_PCC_7822
GI_172036121|Cyanothece_ATCC_51142
str1212|Synechocystis_PCC6803
GI_493574983|Gloeocapsa_PCC_73106
GI_440683654|Anabaena_cylindrica_PCC_7122
GI_493031845|Coleofasciculus_chthonoplastes_PCC_7420
GI_497469251|Lyngbya_PCC_8106
GI_553731020|Lyngbya_aestuarii
GI_493681967|Microcoleus_vaginatus
GI_428320955|Oscillatoria_nigro-viridis_PCC_7112
GI_497312328|Pseudanabaena_biceps_PCC_7429
GI_516325099|Oscillatoria_PCC_10802
GI_427705958|Nostoc_PCC_7107
GI_515346074|Fischerella_muscicola
GI_515879719|Fischerella_PCC_9339
GI_186682032|Nostoc_punctiforme_PCC_73102
GI_515357413|Fischerella_muscicola
GI_497067904|Fischerella
GI_515382644|Chlorogloeopsis_fritschii
GI_428307974|Crinalium_epipsammum_PCC_9333
GI_516352979|Scytonema_hofmanni
GI_518321959|Calothrix_PCC_7103
GI_515377348|Chlorogloeopsis_fritschii
GI_515344627|Fischerella_muscicola
GI_515878322|Fischerella_PCC_9339
GI_515356103|Fischerella_muscicola
GI_497067119|Fischerella_JSC-11
GI_434404121|Cylindrospermum_stagnale_PCC_7417
GI_427739075|Rivularia_PCC_7116
GI_428318321|Oscillatoria_nigro-viridis_PCC_7112
GI_493684362|Microcoleus_vaginatus_FGP-2
GI_494598249|Oscillatoria_PCC_6506
GI_516350230|Scytonema_hofmanni
GI_516324086|Oscillatoria_PCC_10802
GI_516324208|Oscillatoria_PCC_10802
GI_494597484|Oscillatoria_PCC_6506
GI_493560916|Leptolyngbya_PCC_7375
GI_172036793|Cyanothece_ATCC_51142
GI_493040130|Coleofasciculus_chthonoplastes_PCC_7420
GI_428200632|Pleurocapsa_PCC_7327
GI_494597992|Oscillatoria_PCC_6506
GI_428210107|Chroococcidiopsis_thermalis_PCC_7203
GI_494598892|Oscillatoria_PCC_6506
GI_428310796|Microcoleus_PCC_7113
GI_428226797|Geitlerinema_PCC_7407
GI_428319206|Oscillatoria_nigro-viridis_PCC_7112
GI_516351696|Scytonema_hofmanni
GI_427708578|Nostoc_PCC_7107
GI_186685521|Nostoc_punctiforme_PCC_73102
GI_516353908|Scytonema_hofmanni
GI_515363488|Fischerella_muscicola
GI_516358044|Scytonema_hofmanni
GI_428310447|Microcoleus_PCC_7113
GI_516359343|Scytonema_hofmanni
GI_428314292|Microcoleus_PCC_7113
GI_493031910|Coleofasciculus_chthonoplastes_PCC_7420
GI_428311029|Microcoleus_PCC_7113
GI_516354477|Scytonema|hofmanni||ref|WP_017744510.1|
GI_434393773|Gloeocapsa_sp._PCC_7428
GI_428311548|Microcoleus_PCC_7113
GI_434388786|Chamaesiphon_minutus_PCC_6605
GI_218883241|Cyanothece_PCC_7425
GI_220907505|Cyanothece_PCC_7425
GI_218441969|Cyanothece_PCC_7424
GI_307150158|Cyanothece_PCC_7822
GI_427730879|Nostoc_PCC_7524
GI_172276781Nostoc_PCC_7120
GI_75908887|Anabaena_variabilis_ATCC_29413
GI_434406815|Cylindrospermum_stagnale_PCC_7417
GI_186682272|Nostoc|punctiforme|PCC73102
GI_516249982|Microchaete_PCC_7126
GI_440882283|Anabaena_cylindrica_PCC_7122
GI_494594981|Oscillatoria_PCC_6506
GI_493036837|Coleofasciculus_chthonoplastes_PCC_7420
GI_428310395|Microcoleus_PCC_7113
GI_493684409|Microcoleus_vaginatus_FGP-2
GI_428315437|Oscillatoria_nigro-viridis_PCC_7112
GI_427716966|Calothrix_PCC_7507
GI_516247349|Microchaete_PCC_7126
GI_427728766|Nostoc_PCC_7524
GI_172322081Nostoc_PCC_7120
GI_75908175|Anabaena_variabilis_ATCC_29413
0.05

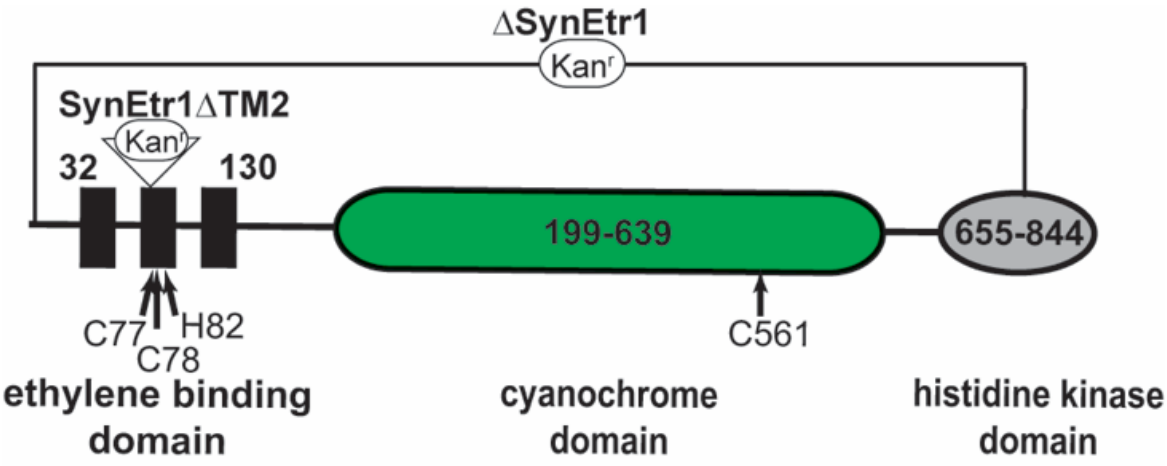

Figure 3.2: Domain Architecture of SynEtr1, Important Residues, and Mutational Constructs

Predicted domain architecture of SynEtr1. The numbers indicate the range of amino acid residues that constitute the domain. The black bars are predicted transmembrane alpha helices. Residues that are mutated are indicated by arrows. The location of the slr1212 gene disruption (SynEtr1ΔTM2) is indicated by the triangle in the second alpha helix of the EBD. The region that is deleted in ΔSynEtr1 is outlined above. Both constructs use Kanamycin resistance genes for either disruption or deletion.

belongs to a class of photoreceptors that have a role in mediating phototaxis. From this we hypothesized that ethylene affects phototaxis through SynEtr1.

The work presented in this chapter will focus on characterizing SynEtr1 as an ethylene binding protein and determining a role for ethylene in phototaxis. As we explored the role of ethylene and SynEtr1 in phototaxis, two papers were published that confirmed that SynEtr1 regulates phototaxis (Narikawa et al., 2011; Song et al., 2011). The methods and results from these papers were conflicting and neither addressed the function of the EBD (Table 1.2). Here, I will attempt to help clarify the reported discrepancies by reproducing methods from both studies, while also showing that SynEtr1 functions as an ethylene receptor.

Results

SynEtr1 Directly Binds Ethylene

Previous studies have utilized various strains of yeast as exogenous expression systems for ethylene receptors in plants (Schaller and Bleecker, 1995; McDaniel and Binder, 2012). Expressing individual ethylene receptors in yeast allows for the direct measurement of binding to the receptor as yeast express no EBPs. Additionally, it allows for more direct biochemical analysis of ethylene binding via site directed mutagenesis. Here, we expressed a truncated SynEtr1 in *Pichia pastoris* (*Pichia*) expressing only the first 130 amino acids (SynEtr1:1-130) that corresponds to the predicted EBD. SynEtr1:1-130 was fused to glutathione S-transferase (GST) to allow for detection of protein expression by western blot. We performed ethylene binding assays on whole cell *Pichia* expressing SynEtr1:1-130 and found that it bound ethylene with

high affinity (Figure 3.3). Control experiments involving *Pichia* transformed with an empty vector and with only GST expressing *Pichia* indicated that there was no internal ethylene binding in Pichia or to GST under our conditions. Expression of the proteins can be seen in isolated *Pichia* membranes via western blots using anti-GST antibodies (Figure 3.3).

We next examined whether or not conserved residues required for ethylene binding in plant ethylene receptors were also required for ethylene binding in SynEtr1. We examined three residues: cysteine 77 (Cys77), cysteine 78 (Cys78), and histidine 82 (His82) (Figure 3.2). Cys78 and His82 are conserved residues. Cys77 is not conserved but its proximity to Cys78 was intriguing. Previous studies suggest that residues corresponding to Cys78 and His82 in plants are involved in forming the ethylene binding pocket in the EBD (Rodriguez et al., 1999). Copper is also a required cofactor for ethylene binding in plant receptors and it is thought that the cysteine that corresponds to Cys78 in plants is involved in copper coordination. Point mutations including Cys77Ala, Cys78Ala, Cys78Ser, and His82Ala all generated a SynEtr1:1-130 that was incapable of binding ethylene (Figure 3.3), indicating that the role of these residues in ethylene binding is conserved from SynEtr1 to higher plants. Collectively, this shows that SynEtr1 is directly involved in ethylene binding in *Synechocystis*.

Ethylene and SynEtr1 Regulate Phototaxis

With the observation that SynEtr1 is capable of directly binding ethylene, we next wanted to explore the capacity for SynEtr1 to elicit physiological responses in the presence of ethylene. As mentioned above, SynEtr1 had been reported to function in regulating phototaxis (Narikawa et al., 2011; Song et al., 2011). Thus, we examined whether or not ethylene altered

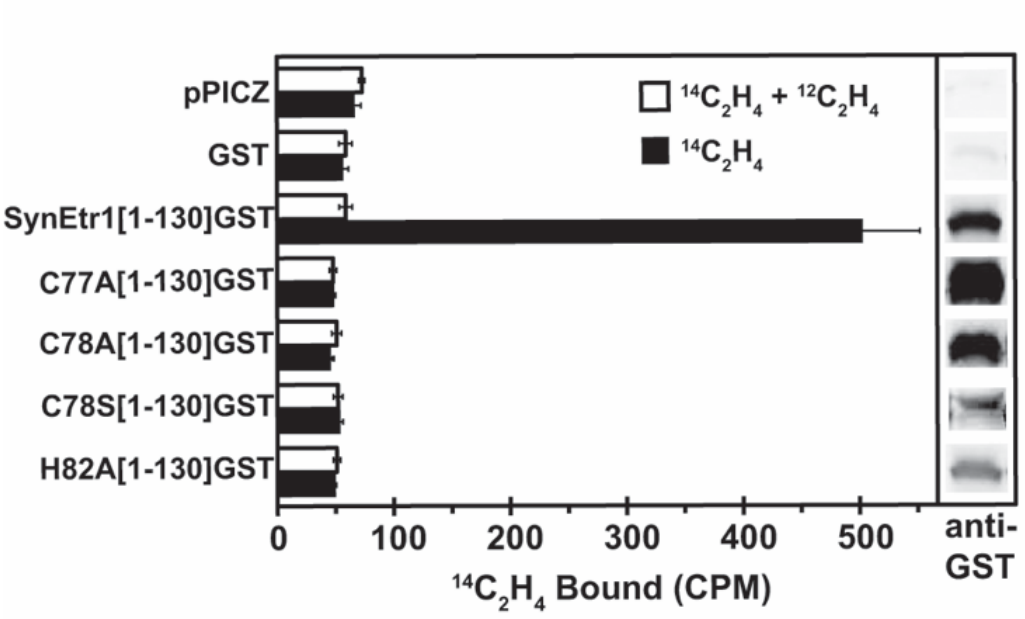

Figure 3.3: Ethylene Binding Assay for Pichia Expressed SynEtr1-EBD

Ethylene binding activity measured in equal amounts of yeast expressing the indicated construct fused to GST, GST alone, or empty vector. Black bars indicate samples exposed to only ^{14}C ethylene. White bars are samples exposed to ^{14}C ethylene and excess ^{12}C ethylene. The data shown represents average counts per minute. Membranes from yeast expressing each of the indicated constructs were isolated. Proteins were isolated by SDS-PAGE and probed by Western Blot using anti-GST antibodies. Western blots are shown on the right panel.

phototaxis. To do this we first optimized the phototaxis assay. The assay, which is described in the materials and methods, incorporated aspects of techniques from several publications (Bhaya et al., 1999; Bhaya et al., 2001; Savakis et al., 2012; Ursell et al., 2013). The general set-up of the assay (Figure 2.3) involves removal of indicated *Synechocystis* cultures from 1% (w/v) agar BG-11 plates, resuspension in fresh liquid BG-11 at a high density (OD_{730} > 20), and placing the cultures on 0.4 % (w/v) agar with BG-11. The plates are then wrapped and exposed to directional light in sealed containers that allow for the application of air or varying concentrations of ethylene. We found 0.4% (w/v) agar allowed for the greatest rate of phototaxis while maintaining a semi-solid state (Figure 3.4A). We also used several different light sources, and ultimately found that LEDs at 30µM/m^2/s of light elicited the strongest phototactic response. All phototaxis assays seen here are at 30µM/m^2/s unless otherwise stated. Another factor we found to play a significant role in affecting phototaxis was the length of time in which the culture had been maintained on 1% (w/v) agar with BG-11. For WT *Synechocystis*, the longer the culture had been maintained on a plate the less it was able to move in response to light (Figure 2.1). Overall, we have optimized and controlled for as many variables as possible, however due to the complexity and sensitivity of the phototactic response minor variations still exist from assay to assay (Figure 3.4B).

To test the effect of ethylene on WT phototaxis, under the conditions described above, we exposed the cells to air or 1 ppm ethylene for 4 days in white light. Phototaxis assays were quantified by measuring overall distance moved from the front edge of the colony. We observed a slight but significant increase in positive phototaxis in cells exposed to ethylene (Figure 3.5B,C). To determine if this effect was caused by signaling through SynEtr1, we

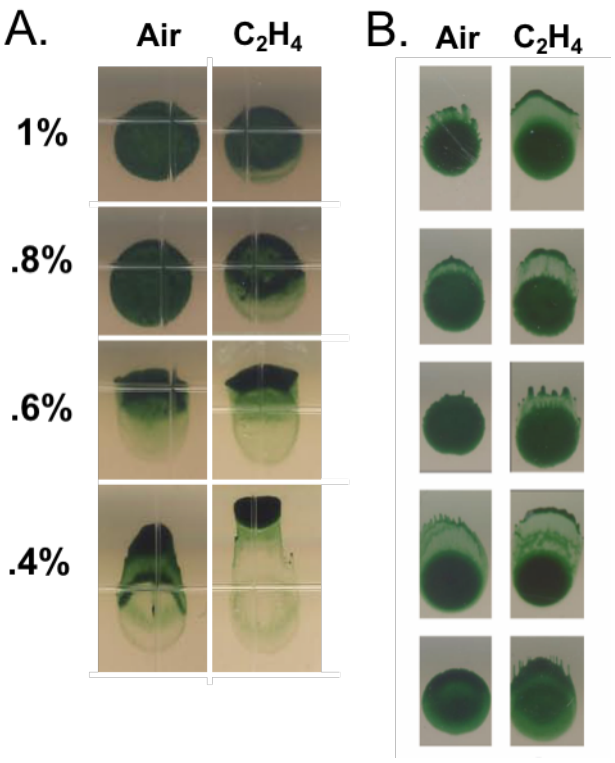

Figure 3.4: Phototaxis Assay Agar Concentration Dependency and Assay Variation

(A) WT *Synechocystis* cultures exposed to air and 1 ppm ethylene in directional white light at varying concentrations of agar. Percentages indicate (w/v) of agar in BG-11. (B) Comparison of WT phototaxis assays. Each of these assays were performed under the same conditions including 30µMs/m^2/s of white light for four days in air or 1 ppm ethylene on .4% (w/v) agar BG-11 plates.

disrupted *slr1212* with a kanamycin resistance gene inserted in region of the gene corresponding to the second transmembrane helix of the EBD (SynEtr1ΔTM2) and examined the effect of ethylene (Figure 3.2). Disruption of *slr1212* was confirmed by colony PCR (Figure 3.5A). The SynEtr1ΔTM2 cells moved much farther towards light in air and ethylene enhanced phototaxis was eliminated (Figure 3.5B,C). These observations suggest that SynEtr1 is functioning to inhibit movement toward white light and ethylene is inhibiting the function of SynEtr1.

To further confirm the role of ethylene signaling through SynEtr1 in phototaxis, we next reconstituted *slr1212* in the SynEtr1ΔTM2 background (WT/SynEtr1ΔTM2). This was done by expressing *slr1212* and *slr1213* in a plasmid with an origin of replication specific to *Synechocystis*. *Slr1213* was also expressed as the nature of the *slr1212* disruption possibly affects *slr1213*. This plasmid in SynEtr1ΔTM2 was confirmed by colony PCR (Figure 3.5A). WT/SynEtr1ΔTM2 displayed a slight but significant increase in positive phototaxis in the presence of 1 ppm ethylene, similar to WT (Figure 3.5B,C). There was an overall increase in phototaxis in air compared to WT, indicating that this is only a partial rescue. However, qualitatively the cells appear much more similar to WT than to SynEtr1ΔTM2 (Figure 3.5B). In the same expression system, we next examined what effect an ethylene insensitive SynEtr1 would have on phototaxis. We reconstituted Cys78SerSynEtr1 in the SynEtr1ΔTM2 background (C78S/SynEtr1ΔTM2), and observed a similar pattern to what we see in SynEtr1ΔTM2. There was a large increase in positive phototaxis in air and no response to ethylene (Figure 3.5B,C). This suggests that Cys78 in SynEtr1 may be required for producing a functional protein. These results confirm the role of SynEtr1 as an ethylene receptor involved in mediating phototaxis.

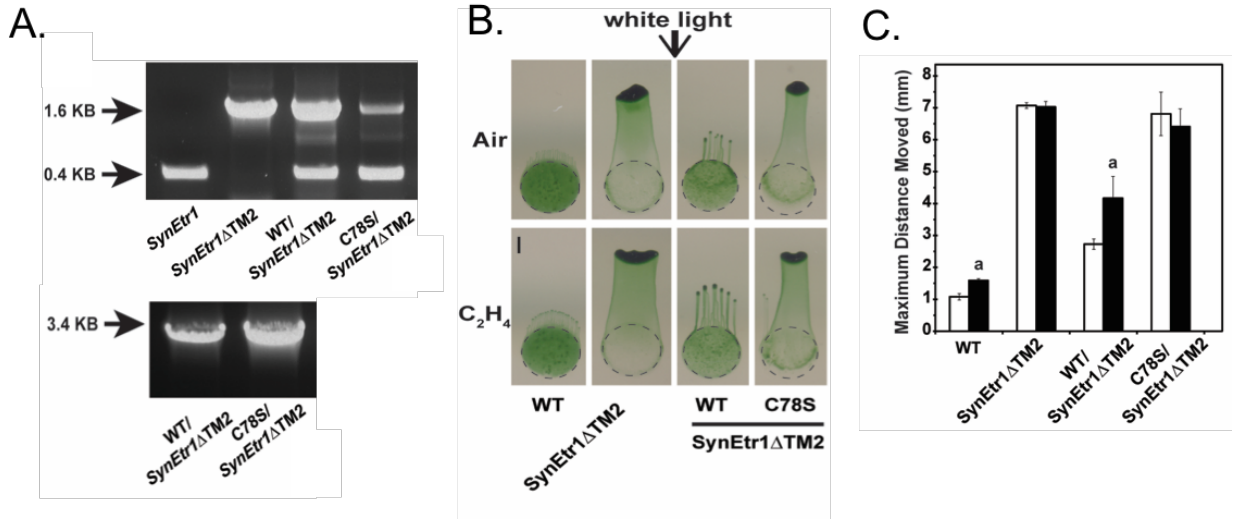

Figure 3.5: Phototaxis Assay of WT, SynEtr1ΔTM2, Reconstitution of SynEtr1 Lines with Colony PCR Confirmation

(A) Colony PCR confirmation of WT and transgenic *Synechocystis* lines. The primers used the top panel are slr1212F180 and slr1212R480. In WT this produces a 400 bp fragment. In SynEtr1ΔTM2 this produces a 1.6 kb fragment due to the presence of the 1.2 kb Kan^r gene located in the region corresponding to the EBD. Two bands appear in the reconstitution lines as they have the disrupted *slr1212* gene in the genome and *slr1212-1213* reconstituted on a plasmid. The bottom panel is confirmation of the plasmid harboring reconstituted *slr1212-1213* with primers pPetJF and slr1213R1. PCR conditions are described in material and methods. (B) Colonies of *Synechocystis* strains exposed to phototaxis conditions described in materials and methods. Dashed circles indicate starting colony position. The black bar = 2 mm. (C) Quantification of assay in B. The data are averages ± SD. **a** indicates significant difference caused by ethylene ($P < 0.05$).

Ethylene Enhances Phototaxis Across Several Wavelengths of Light

As previously mentioned, SynEtr1 has been photochemically characterized to sense UV, violet, and blue light (Ulijasz et al., 2009; Narikawa et al., 2011; Song et al., 2011). In all three cases it was shown to be photoreversible with green light. Song et al. showed that deletion of *slr1212* had no effect on phototaxis toward visible monochromatic light. In contrast, we observed a major enhancement of phototaxis in white light. Because of this discrepancy, we sought to determine if phototaxis toward monochromatic light is altered by ethylene or disruption of SynEtr1. UV-A (365nm), Blue (462nm), Green (525nm), and Red (672nm) LEDs were used to assess phototaxis in WT and SynEtr1ΔTM2 *Synechocystis* in both air and 1 ppm ethylene. Aside from UV-A, ethylene lead to an increase in phototaxis in all tested wavelengths of light (Figure 3.6). Typically, WT *Synechocystis* does not move toward blue light. Our observation of phototaxis toward blue light suggests that SynEtr1 is possibly playing a role in inhibiting blue light phototaxis. In SynEtr1ΔTM2 a large increase in phototaxis compared to WT was observed at all wavelengths of light tested. This result is similar to what has been previously observed in UV-A, but it contrasts with what was seen in visible monochromatic light. The large increase in movement toward blue light in SynEtr1ΔTM2 further supports the idea that SynEtr1 is inhibiting movement toward blue light.

It is possible that ethylene is affecting sensitivity to light. To test this, we examined WT phototaxis at intensities of white light ranging from 3.5μM/m^2/s up to 30μM/m^2/s in the presence of air and 1 ppm ethylene. Quantitatively, it was observed that ethylene caused enhanced movement toward light at relatively similar levels across the light intensities tested (Figure 3.7), suggesting that ethylene is not likely to be affecting sensitivity to light.

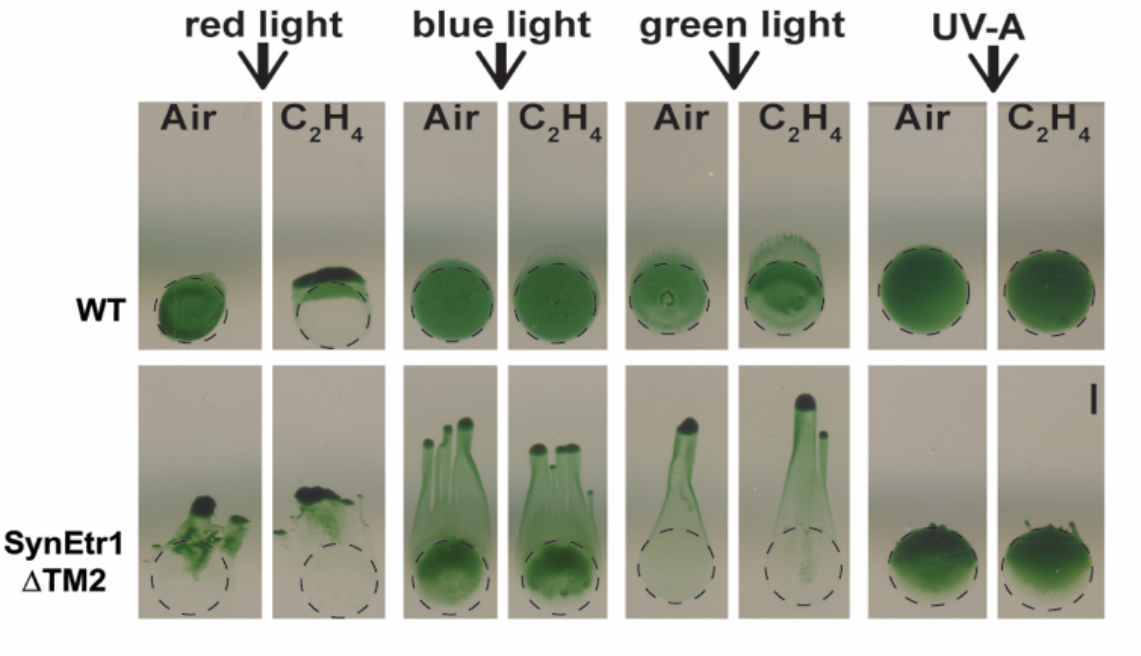

Figure 3.6: Monochromatic Light Phototaxis

Colonies of WT and SynEtr1ΔTM2 strains were exposed to 30µM/m^2/s directional monochromatic red light (672nm) for 4 days, green light (525nm) for 4 days, blue light (462nm) for 7 days, or 60µM/m^2/s UV-A light (365nm) for 7 days in the absence or presence of 1 ppm ethylene.

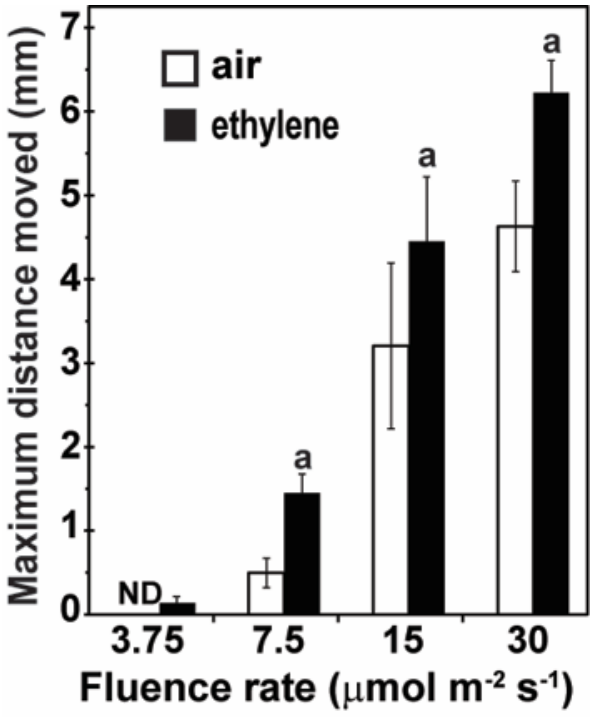

Figure 3.7: Effect of Ethylene on Light Sensitivity

Quantification of WT *Synechocystis* colonies exposed to varying fluence rates of white light for 14 days in either air or 1 ppm ethylene. The data are averages ± SD. **a** indicates significant difference caused by ethylene ($P < 0.05$). ND indicates no movement was detected.

Ethylene Signaling via SynEtr1 is Independent of Light Signaling in Phototaxis

The results thus far suggest the SynEtr1 is functioning as dual input receptor with one input for light and one input for ethylene. To gain further insight into the relationship between these two inputs, we sought to disrupt the ability of SynEtr1 to perceive light and examined how it responds to ethylene. To do this, we made a site directed mutant of Cys561 of SynEtr1. Cys561 is conserved in CBCRs and plays a role in coordination of the bilin chromophore (Ulijasz et al., 2009; Rockwell and Lagarias, 2010). Mutation of this residue in other CBCRs has been reported to eliminate their ability to perceive and respond to light (Ulijasz et al., 2009; Song et al., 2011). Using the self-replicating plasmid system described above we reconstituted SynEtr1 with a Cys561Ala point mutation in the SynEtr1ΔTM2 background (C561A/SynEtr1ΔTM2) (Figure 3.2). Positive transformants were confirmed by colony PCR (Figure 3.8A). We then exposed these cells to directional light in air or 1 ppm ethylene as described above. Interestingly, C561A/SynEtr1ΔTM2 responded to ethylene by showing an increase in phototaxis toward white light (Figure 3.8B,C). In air however, C561A/SynEtr1ΔTM2 phototaxis appeared qualitatively intermediate between WT and SynEtr1ΔTM2. Thus, ethylene signaling in phototaxis appears to occur independently of light signaling.

Disruption and Deletion of slr1212 Have Different Phenotypes in Phototaxis

Song et al., 2011 and Narikawa et al., 2011 both generated *Synechocystis* cell lines that were SynEtr1 deficient. Both found phototaxis to be altered (Narikawa et al., 2011; Song et al., 2011). In both cases, however, there were major qualitative differences in how phototaxis was affected. Several factors possibly contributed to these differences. First, different sub-strains of

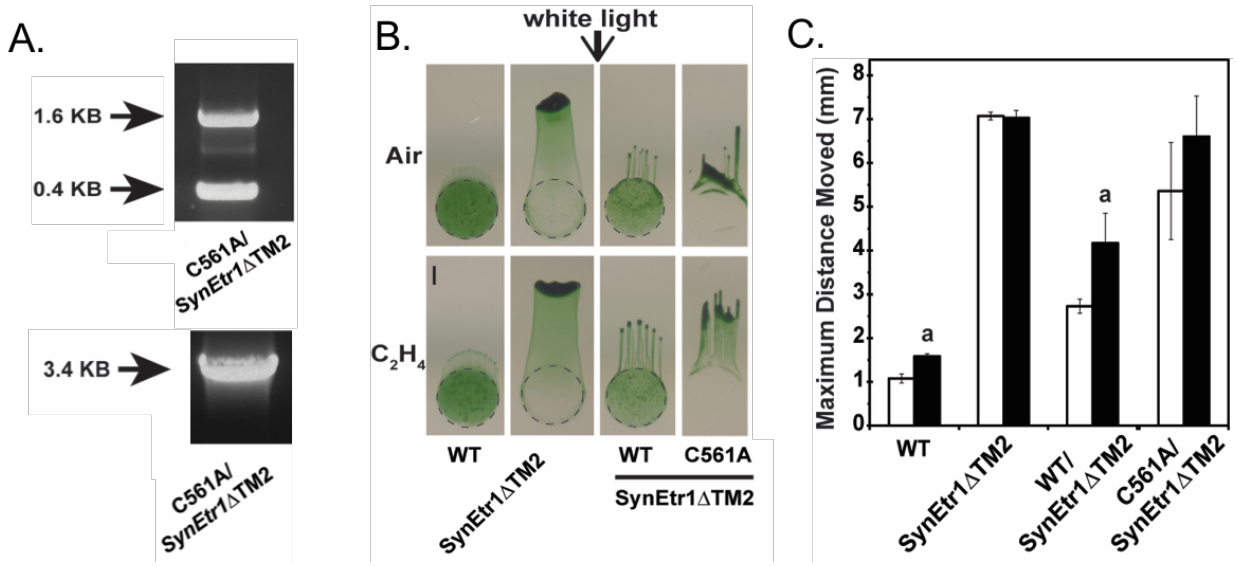

Figure 3.8: C561A Phototaxis and Colony PCR Confirmation

(A) Colony PCR confirmation of transgenic C561A/SynEtr1ΔTM2 *Synechocystis* line. The primers used the top panel are slr1212F180 and slr1212R480. In WT this produces a 400 bp fragment. In SynEtr1ΔTM2 this produces a 1.6 kb fragment due to the presence of the 1.2 kb Kan^r gene located in the region corresponding to the EBD. Two bands appear as C561A/SynEtr1TM2 has the disrupted *slr1212* gene in the genome and *slr1212-1213* reconstituted on a plasmid. The bottom panel is confirmation of the plasmid harboring reconstituted *slr1212-1213* with primers pPetJF and slr1213R1. PCR conditions are described in material and methods. (B) Colonies of *Synechocystis* strains exposed to phototaxis conditions described in materials and methods. Dashed circles indicate starting colony position. The black bar = 2 mm. (C) Quantification of assay in B. The data are averages ± SD. **a** indicates significant difference caused by ethylene ($P < 0.05$).

Synechocystis were used in each study. Recently, all known sub-strains of *Synechocystis* were sequenced with genetic variations defined (Table 1.1) (Trautmann et al., 2012). Song et al., (2011) used the original motile strain from the Pasteur Institute, whereas Narikawa et al., (2011) used newly discovered lab strains termed PCC-P and PCC-N for positive and negative phototaxis respectively. Secondly, they each performed assays under varying conditions. Most notably Song et al., (2011) used monochromatic light and Narikawa et al., (2011) used white light. For this study, we used the original Pasteur Institute *Synechocystis* strain to generate SynEtr1ΔTM2 and observed similar phenotypes in white light compared to the SynEtr1 deficient PCC-P strain used by Narikawa et al. We also found monochromatic responses of SynEtr1ΔTM2 (Figure 3.6) to differ from the SynEtr1 deficient *Synechocystis* generated by Song et al. From this we hypothesized that the nature in which SynEtr1 function is knocked-out accounts for the differences in phenotype.

As mentioned above, SynEtr1ΔTM2 is a disruption of *slr1212* generated by inserting a kanamycin resistance gene in the region of *slr1212* corresponding the EBD. Narikawa et al., (2011) also generated an *slr1212* disruption in the ethylene binding region, whereas Song et al., (2011) generated a full gene deletion of *slr1212*. To determine if these differences accounted for the differences in phototaxis, we generated an *slr1212* gene deletion (ΔSynEtr1) (Figure 3.2) using the methods described in Song et al., (2011) and performed phototaxis assays. The deletion construct was confirmed by colony PCR (Figure 3.9A). We observed similar phenotypes as Song et al., (2011) that involved enhanced motility towards light, but a smaller enhancement of motility compared with SynEtr1ΔTM2 (Figure 3.9B). Not surprisingly, ΔSynEtr1 was unable to respond to ethylene. We next reconstituted WT, C78S, and C561A SynEtr1 in the ΔSynEtr1

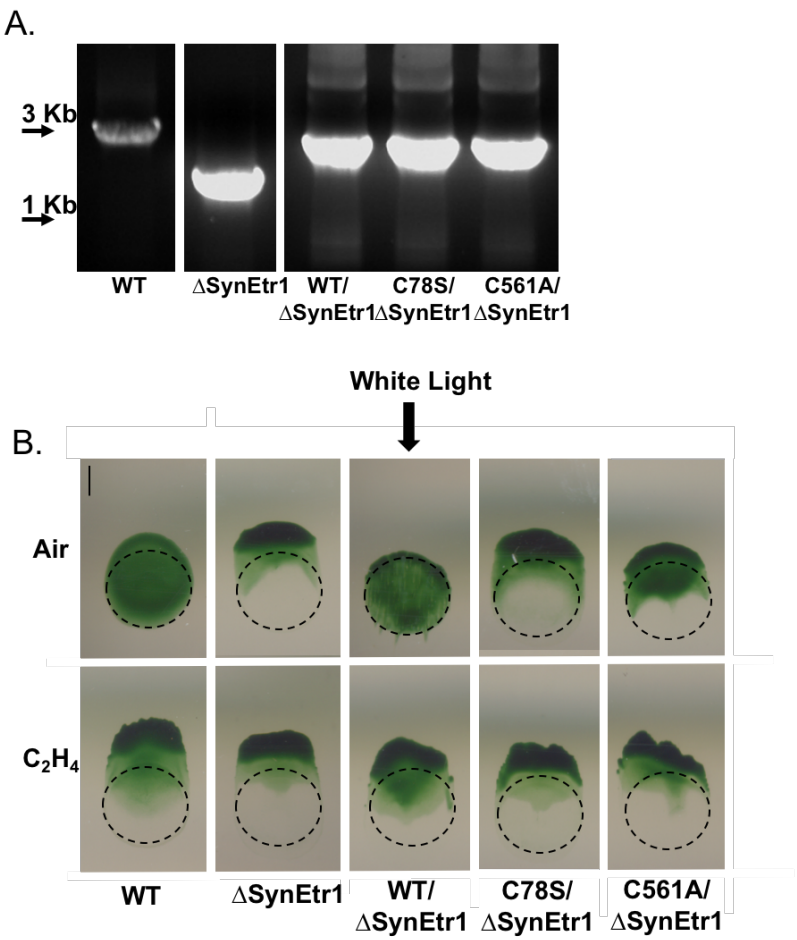

Figure 3.9: Phototaxis Assay of WT, ΔSynEtr1, and Reconstitution Lines with Colony PCR Confirmation

(A) Colony PCR confirmation of WT and transgenic ΔSynEtr1 and *slr1212* reconstitution lines in ΔSynEtr1. Primers used in the first two panels are slr1212upF and slr1212downR. In WT this produces a 3KB band and in ΔSynEtr1 this a 2KB band. This confirms *slr1212* gene deletion. To confirm reconstitution of slr1212 WT and point mutants, the forward primer is pPetJF and slr1212R1. This band should be 2.5KB. (B) Colonies of *Synechocystis* strains exposed to phototaxis conditions described in materials and methods. Dashed circles indicate starting colony position. The black bar = 2 mm.

background. In each case the phototactic responses were similar in trend to what was observed in the SynEtr1ΔTM2 rescue lines (Figure 3.9A). WT/ΔSynEtr1 rescued ethylene enhanced phototaxis, but only showed a partial rescue of WT phototaxis in air. C78S/ΔSynEtr1 was ethylene insensitive and lack any major phenotypic changes compared to ΔSynEtr1 further supporting the idea the Cys78 is essential for the function of SynEtr1. C561A/ΔSynEtr1 responded to ethylene by increasing phototaxis toward white light. Overall, the observed phenotypic differences in phototaxis among SynEtr1 deficient *Synechocystis* cell lines seem to at least be partially a result of whether *slr1212* is disrupted or deleted.

Slr1214 is Necessary for Ethylene Signaling in Phototaxis

Both Song et al., (2011) and Narikawa et al., (2011) examined the role of slr1214 in phototaxis (Narikawa et al., 2011; Song et al., 2011). Song et al., (2011) reported that slr1213 was activated by SynEtr1 via phosphorelay. Activated slr1213 is then able to transcriptionally activate *slr1214*. Interestingly, slr1214 has been shown to directly interact with SynEtr1 (Sato et al., 2007), suggesting that it possibly functions as an alternative response regulator to slr1213. Because of the dual input nature of SynEtr1 it is possible that the output of ethylene signaling through SynEtr1 differs from that of light signaling. We explored the role of slr1214 by deleting the gene (Δslr1214) and performing phototaxis assays in the white light in the presence of air and 1 ppm ethylene. We found slr1214 to be required for ethylene enhanced phototaxis (Figure 3.10). In air Δslr1214 *Synechocystis* phototaxis was similar to what is observed in ΔSynEtr1 under the same conditions. These results suggest that slr1214 is required for the ethylene signaling and light signaling output of SynEtr1 in phototaxis.

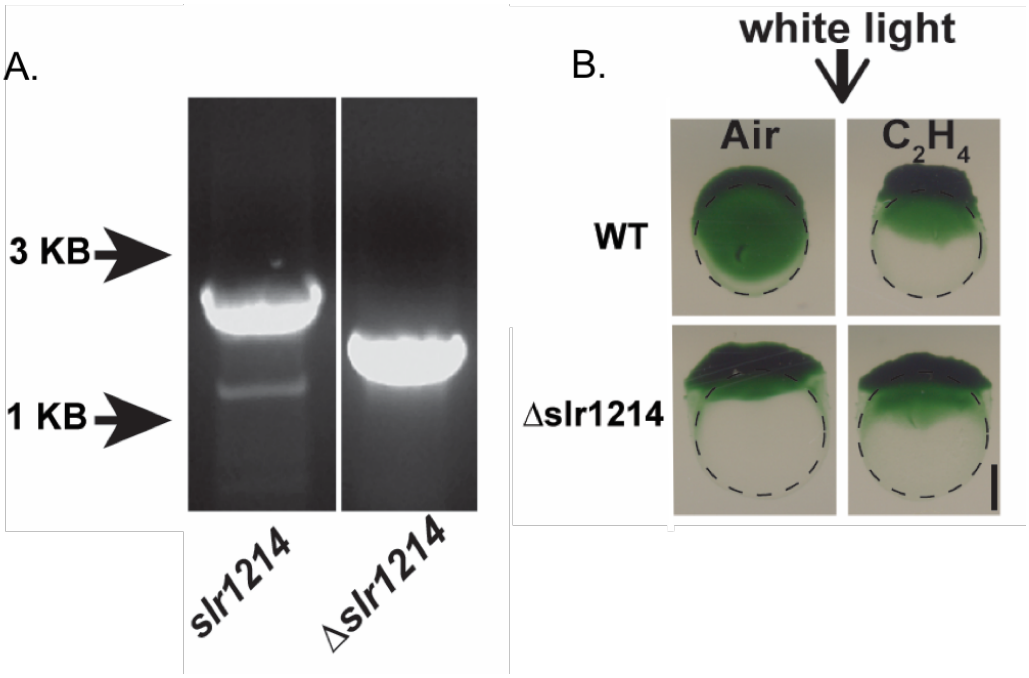

Figure 3.10: Phototaxis Assay of WT and Δslr1214 with Colony PCR Confirmation

(A) Colony PCR confirmation of WT and transgenic Δslr1214. Primers used in both panels are slr1214UpF and slr1214DownR. In WT this produces a 2KB fragment and in Δslr1214 this produces a 1.5KB fragment. (B) Colonies of *Synechocystis* strains exposed to phototaxis conditions described in materials and methods. Dashed circles indicate starting colony position. The black bar = 2 mm.

Discussion

The EBDs of ethylene receptors in plants are highly conserved in sequence with several residues known to be required for ethylene binding (Rodriguez et al., 1999; Wang et al., 2006). Previously it was discovered that sequences similar to the ethylene binding domains of plant receptors exist in cyanobacterial species as well (Wang et al., 2006). In this study, from newly sequenced genomes we identified 112 species that contain putative EBDs in non-plant species including many cyanobacterial species as well as non-phototrophic bacteria. To gain insight into the possible role of ethylene as a signaling molecule in non-plant species, we sought to characterize the ethylene receptor SynEtr1 from *Synechocystis*. We found SynEtr1 to directly bind ethylene with high affinity and residues conserved in plants that are required for ethylene binding are also required for ethylene binding in SynEtr1. Previous reports implicated SynEtr1 as a regulator of phototaxis. We confirmed this, and further showed that ethylene altered phototaxis via SynEtr1. Additionally, the putative response regulator slr1214 appears to be necessary for ethylene responses in phototaxis.

In an attempt to resolve conflicting prior reports regarding the role of SynEtr1 in phototaxis, we replicated experiments performed by Song et al. (2011) and Narikawa et al. (2011) by either deleting or disrupting *slr1212* respectively. In deleting *slr1212*, we observed phototaxis similar to what Song et al. (2011) reported with an overall slight increase in positive phototaxis. In disrupting *slr1212*, we observed a larger increase in positive phototaxis similar to what Narikawa et al. (2011) reported. Thus, the nature of how *slr1212* is altered is likely a contributor to the phenotypic differences in phototaxis from the previous reports. It is unclear as to why this is the case. It is possible the disruptions are having either downstream or

upstream effects on nearby genes that do not occur with the deletion. It is also possible that because *slr1212* is only being disrupted, other parts of the gene are expressed and produce a protein product that remains semi-functional. Further investigation is needed; however, it is evident from this work that differences in how SynEtr1 function is eliminated can lead to significant differences in phenotype.

Our observations clearly show that ethylene affects phototaxis via SynEtr1 in *Synechocystis*. However, whether ethylene plays a physiological role in *Synechocystis* in nature remains an open question. Unlike plants and other organisms *Synechocystis* is unable to endogenously produce ethylene (Guerrero et al., 2012; Ungerer et al., 2012). Thus, *Synechocystis* must encounter ethylene from outside sources. These sources could be either biotic or abiotic. Because cyanobacteria often live in heterogeneous communities (Rai, 1990), it is possible that ethylene production from nearby organisms influences *Synechocystis* behavior. Ethylene has also been shown to be produced abiotically when light interacts with hydrocarbons in the water column (Swinnerton and Linnenborn, 1967; Wilson et al., 1970; Swinnerton and Lamontagne, 1974; Ratte et al., 1998). The dual input nature of SynEtr1 would allow for simultaneous regulation of phototaxis by both light and ethylene in these conditions. As we have shown, ethylene enhances movement toward light. Because ethylene diffuses in the water column this may lead to stimulation of *Synechocystis* movement toward more optimal lighting.

Here, we have characterized the first non-plant, cyanobacterial ethylene receptor. This shows that ethylene evolved as a signaling molecule prior to the evolution of higher plants. Interestingly, all of the known downstream ethylene signaling components of plants are not

found in *Synechocystis* or other cyanobacteria, suggesting that the signaling pathway in plants evolved later (Ju et al., 2015). While we have shown that ethylene functions as a signaling molecule in *Synechocystis*, the presence of ethylene binding proteins in many other species of both phototrophic and non-phototrophic prokaryotes suggests that ethylene is more wide spread in function that previously thought.

Chapter 4

Signaling and Physiological Output of Ethylene in SynEtr1

Portions of the research presented here are presented in a recent publication in Plant Physiology under the title “Ethylene Regulates the Physiology of the cyanobacterium Synechocystis sp. PCC 6803 via an Ethylene Receptor” (Lacey and Binder, 2016).

Introduction

Cyanobacteria navigate their environment to optimal lighting conditions in a process known as phototaxis. Phototaxis is complex and involves the coordination of photoreceptors that perceive light cues, machinery involved in the mechanical process of moving, and energetic signals that indicate optimal environmental conditions (Bhaya, 2004). Previously, we have shown that the ethylene receptor SynEtr1 perceives ethylene and responds to it by altering rates of phototaxis. Here, we will explore ethylene signaling output of SynEtr1 and the underlying aspects of phototaxis that are affected by both ethylene and SynEtr1.

It has been proposed that SynEtr1 is activated by light and signals to the response regulator slr1213 via phosphorelay (Song et al., 2011; Ramakrishnan and Tabor, 2016). Slr1213 then binds to a region of the genome upstream of *slr1214*. It was initially thought to activate transcription of this *slr1214* (Song et al., 2011). More recently it was discovered that the likely transcriptional target of slr1213 is both *slr1214* and the ncRNA *csiR1*, which lies in the intergenic region between *slr1213* and *slr1214* (Ramakrishnan and Tabor, 2016). Slr1214, a predicted AraC response regulator, is required for the function of SynEtr1 in phototaxis as

demonstrated in Chapter 3 and in previous reports; however, the exact function of slr1214 remains unknown. The role of ethylene in SynEtr1 signal transduction remains an open question (Figure 4.1).

SynEtr1 is one of several photoreceptors that mediate phototaxis in *Synechocystis* (Fiedler et al., 2005). Movement in *Synechocystis* is directly controlled by type IV pili and EPS. Type IV pili are large protein complexes found in many microbes that function by extending from the cell, attaching to a surface, and retracting, thus propelling the cells in a particular direction (Shi and Sun, 2002; Schuergers and Wilde, 2015). As the cells move along surfaces, they secrete and leave behind EPS (Ursell et al., 2013; Wilde and Mullineaux, 2015). The EPS is thought to function by modifying the surface cells are moving allowing other cells to more efficiently follow behind leading cells. Additionally, a major purpose of phototaxis is to position cells in conditions of optimal lighting for photosynthesis (Jekely, 2009). Therefore, alterations in photosynthetic capacity may contribute to altered phototaxis. SynEtr1 and ethylene alter phototaxis, but the underlying physiological nature in which this occurs is unknown.

In this chapter we further explore the ethylene signaling and physiological output of SynEtr1 in *Synechocystis*. We examine transcript levels of *slr1212*, *slr1213*, and *slr1214* in varying conditions. In addition, we will both directly and indirectly look at the components of phototaxis mentioned above including type IV pili, EPS, and photosynthetic capacity. Collectively, this will provide a clearer picture of the function of ethylene and SynEtr1 in *Synechocystis*.

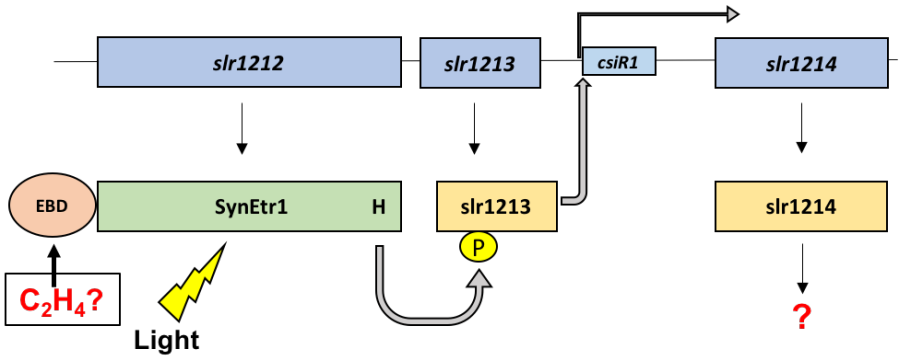

Figure 4.1: SynEtr1 Two-Component Signaling

Diagram of two-component signaling in SynEtr1. The blue boxes are the genes involved with arrows indicating the proteins they encode. Light is thought to stimulate phosphate transfer from SynEtr1 to slr1213. Activated slr1213 then binds to the promoter of *csiR1*, a ncRNA, and is thought to transcriptionally activate it and *slr1214*. The downstream targets/functions of slr1214 are unknown. It also unknown what role ethylene plays in mediating signaling/phosphorelay.

Results

SynEtr1 Two-Component Signaling

To address the effect of ethylene on signal output of SynEtr1 we examined transcript levels of *slr1212*, *slr1213*, and *slr1214*. Initially, we hypothesized that ethylene would alter *slr1214* expression levels by altering SynEtr1-slr1213 signaling. To test this, we extracted RNA from WT and SynEtr1ΔTM2 *Synechocystis* cells exposed to directional light for 4 days in either air or 1 ppm ethylene, matching the conditions described in chapter 3. This will be referred to as phototaxis conditions throughout this chapter. qRT-PCR was then performed on the each of the samples to determine levels of gene expression relative to the house keeping gene *trpA* (Alfonso et al., 2000). No significant difference was observed in *slr1212* or *slr1213* expression levels when exposed to 1 ppm ethylene (Figure 4.2A). Interestingly, *slr1214* showed a significant decrease in transcript abundance when exposed to 1 ppm ethylene. Additionally, *slr1214* transcript levels were very low in SynEtr1ΔTM2 as well. This presented a clear picture that mimicked what was observed in phototaxis. *Slr1214* transcription, the predicted output of SynEtr1-slr1213 two-component signaling, was reduced in the presence of ethylene and nearly eliminated when SynEtr1 is disrupted. In phototaxis, ethylene increased motility slightly in WT and disruption of SynEtr1 lead to a large increase in motility. From this we concluded that slr1214 inhibits motility, and ethylene inhibits *slr1214* expression through SynEtr1.

The WT cultures used for expression analysis were cultivated on BG-11 agar plates for long periods of time. Over time they gradually became diminished in motility as described in Materials and Methods (Figure 2.1). Thus, frozen stocks of WT *Synechocystis* were revived. The freshly revived cultures responded to ethylene by enhanced phototaxis, similar to what was

observed prior to the decline in motility (Figure 3.5B). Surprisingly, a different trend was observed in examining expression levels of *slr1212*, *slr1213*, and *slr1214*. *Slr1212* and *slr1213* transcript levels were unaffected by application of ethylene, however *slr1214* levels showed a significant increase in expression (Figure 4.2B). This is the opposite of what was observed in cultures with reduced motility. It is unclear why this discrepancy exists. It is possible that the reduction in motility initiates a feedback mechanism that affects *slr1214* expression levels. Overall, because we observed no difference on the effect of ethylene on phototaxis regardless of cell age, the results here suggest that ethylene signaling among SynEtr1, slr1213, and slr1214 is likely occurring on a post-translational level.

SynEtr1 and Ethylene Regulate Pili Form and Function

To more closely examine the underlying aspects of phototaxis affected by SynEtr1 and ethylene, we first looked at the motility apparatus: type IV pili (Figure 1.3). The size and complexity of type IV pili allow for several means of investigation. Initially, we examined transcript levels of the pili related genes *PilA1*, *PilB1*, and *PilC* in WT and SynEtr1ΔTM2 under phototaxis conditions (Figure 4.3) (Bhaya et al., 2000). *PilA1*, the main structural component of type IV pili, did not have altered expression in ethylene in WT. SynEtr1ΔTM2 showed a significant increase in expression of *PilA1* in air. *PilB1* and *PilC*, both of which are involved in formation and function of the pili, were significantly increased in expression in the presence of ethylene in WT. Both also showed increased expressed in SynEtr1ΔTM2 in air, with *PilC*

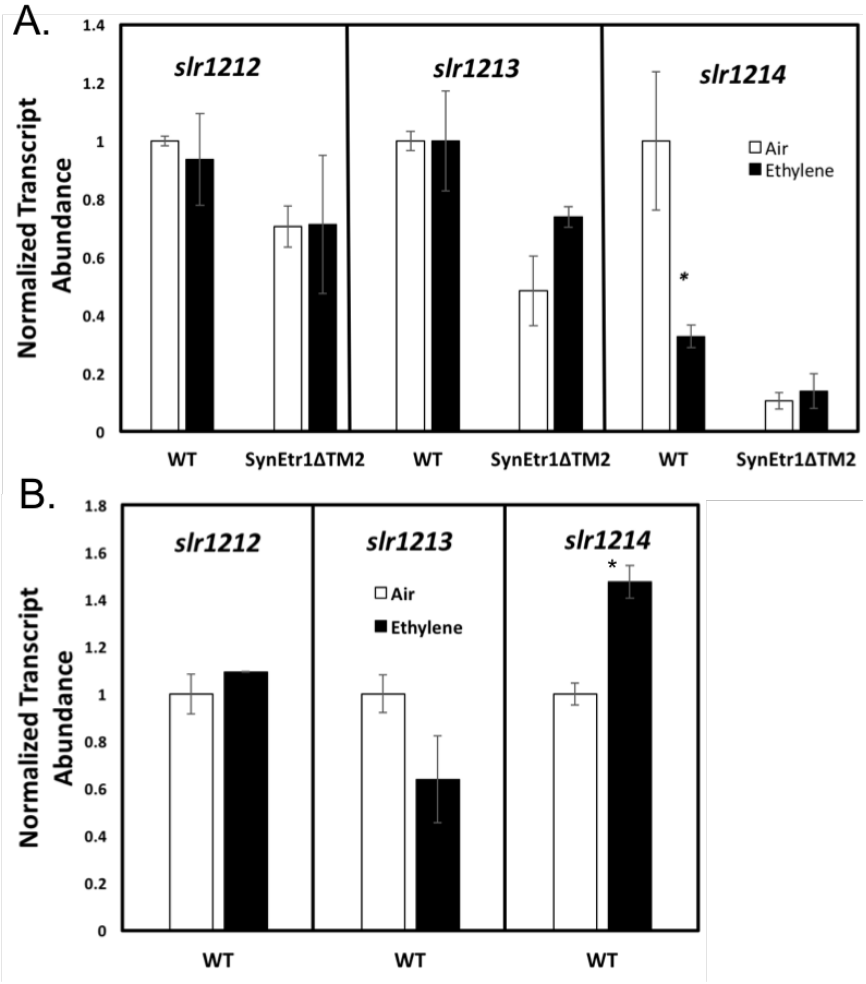

Figure 4.2: qPCR Analysis of *slr1212*, *slr1213*, and *slr1214* in WT and SynEtr1ΔTM2

qRT-PCR analysis of *slr1212*, *slr1213*, and *slr1214* in phototaxis conditions in various *Synechocystis* strains. Cells were harvested, RNA was extracted and reverse transcribed, and qPCR was performed. Expression levels were first normalized to a house keeping gene, then each gene was normalized to WT in air. Data are averages ± SD. * indicate statistical difference of expression in WT exposed to ethylene compared to air ($P < 0.05$). (A) Comparing WT cell cultures that had been maintained for many generations on 1% (w/v) agar BG-11 plates to SynEtr1ΔTM2. (B) Comparing WT expression levels from cells that have recently been revived from frozen stock.

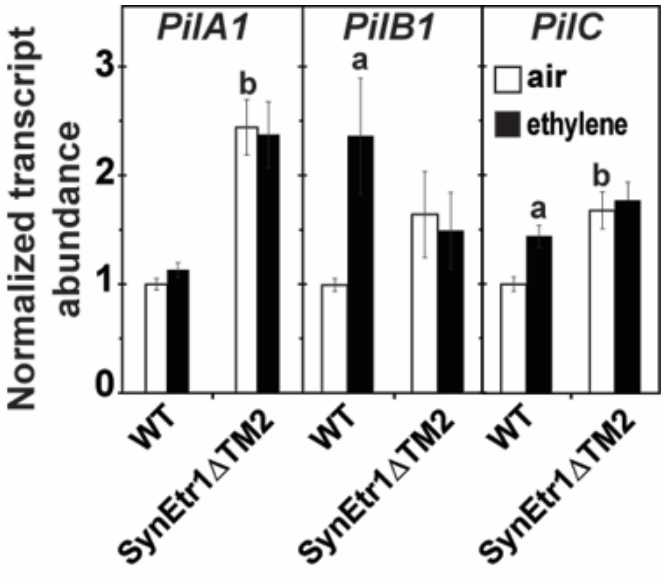

Figure 4.3: qPCR Analysis of Pili related genes in WT and SynEtr1ΔTM2

qRT-PCR analysis of *PilA1*, *PilB1*, and *PilC* in phototaxis conditions in various *Synechocystis* strains. Cells were harvested, RNA was extracted and reverse transcribed, and qPCR was performed. Expression levels were first normalized to a house keeping gene, then each gene was normalized to WT in air. Data are averages ± SD. a indicate statistical difference of expression in WT exposed to ethylene compared to WT in air ($P < 0.05$). b indicates statistical difference of expression in WT in air compared to SynEtr1ΔTM2 in air ($P < 0.05$).

expression increased to a greater degree. Overall, ethylene and SynEtr1 appear to alter expression of several genes associated with type IV pili.

To follow up the expression analysis, immunoblotting was performed using PilA1 antibodies to directly look at protein levels. PilA1 protein levels were measured from both isolated pili and whole cells in WT and SynEtr1ΔTM2 *Synechocystis* under phototaxis conditions (Figure 4.4A). Coomassie-blue staining was used to confirm equal loading of whole cell samples. Consistent with *PilA1* expression levels, no difference in protein levels were observed in ethylene treated WT samples. As indicated by a stronger intensity band, SynEtr1ΔTM2 showed higher PilA1 levels compared to WT. A shift in molecular weight was also observed for PilA1 in SynEtr1ΔTM2. This shift corresponds to the previously reported molecular weight of a non-glycosylated pre-PilA1 (Kim et al., 2009; Linhartová et al., 2014). Pre-PilA1 is processed by the peptidase PilD to its final functional PilA1 form. Mature PilA1 is often glycosylated. Disruption of PilD function leads to an accumulation of non-glycosylated pre-PilA1 (Linhartová et al., 2014). Because SynEtr1ΔTM2 is likely accumulating a non-glycosylated form of pre-PilA1, we examined *PilD* expression levels. SynEtr1ΔTM2 showed decreased PilD expression levels compared to WT, supporting the idea that SynEtr1 accumulates non-glycosylated pre-PilA1 (Figure 4.4B).

The size and extracellular nature of type IV pili make them easily visible using transmission electron microscopy (Bhaya et al., 2000). WT and SynEtr1ΔTM2 *Synechocystis* exposed to phototaxis conditions were negative stained and examined for differences in type IV pili (Figure 4.5). Consistent with previous reports, two pilus morphotypes were observed: thick and thin (Bhaya et al., 2000; Yoshihara et al., 2001). Thick pili represent type IV pili and are

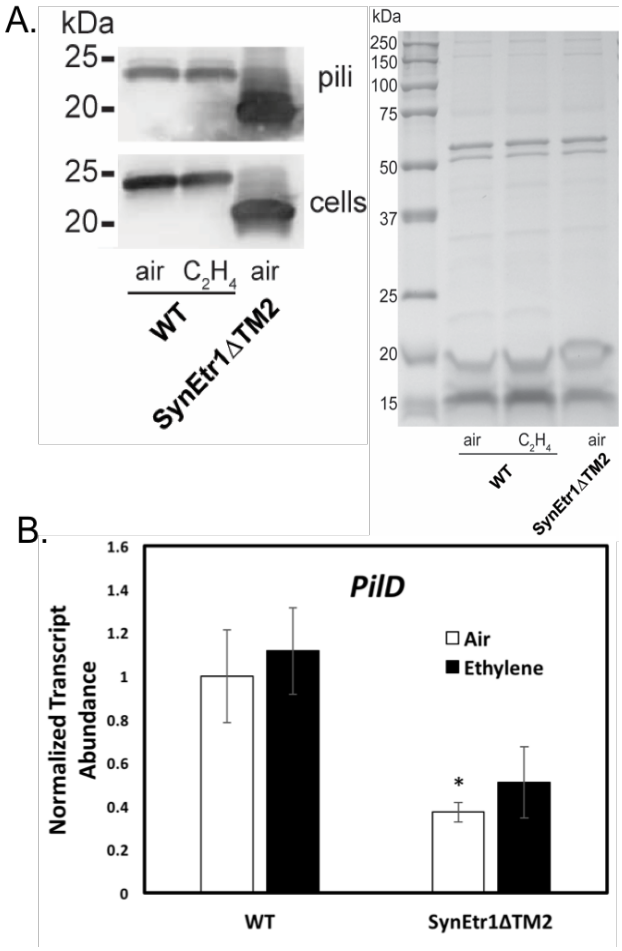

Figure 4.4: PilA1 Protein Analysis and qPCR Analysis of *PilD*

(A) *Synechocystis* exposed to phototaxis conditions were harvested and pili were extracted (pili). Pili proteins were precipitated and solubilized. The proteins were then separated by SDS-PAGE. In parallel, total protein was extracted analyzed (cells). Western blotting was performed with anti-PilA1 antibodies. Equal protein loading for whole cell extracts was confirmed by Coomassie-Blue staining (left panel). (B) qRT-PCR analysis of *PilD* expression levels. Cells were harvested, RNA was extracted and reverse transcribed and qPCR was performed. Expression levels were first normalized to a house keeping gene, with subsequent normalization to WT in air. Data are averages ± SD. * indicate statistical difference of expression in SynEtr1ΔTM2 compared to WT in air ($P < 0.05$).

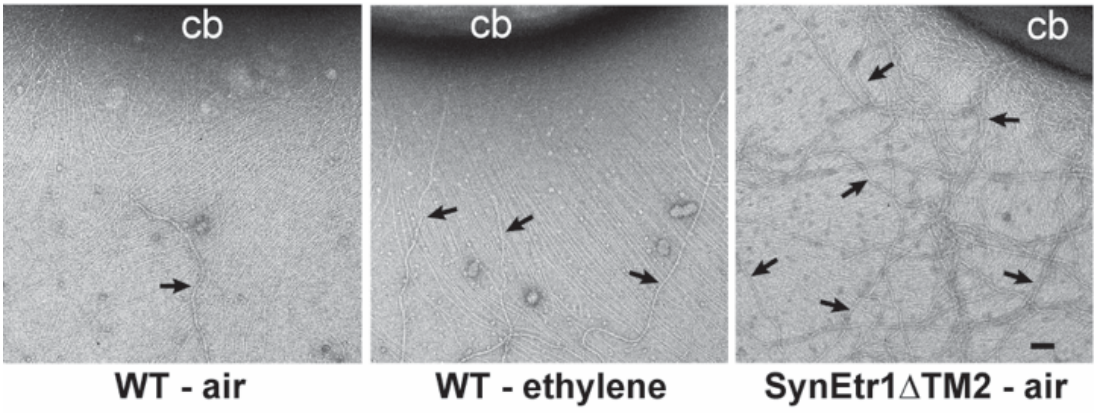

Figure 4.5: TEM Images of Pili from WT and SynEtr1ΔTM2

Electron micrographs from the leading edge of *Synechocystis* cells exposed to phototaxis conditions. CB indicates cell body. Black arrows indicate selected type IV pili. Black bars = 100nm. Magnification = 20,000x.

required for motility. PilA1 encodes the thick pili subunits. The function of thin pili is unknown. We observed a slight but consistent increase in the number of thick pili in WT cells exposed to ethylene (Table 4.1). SynEtr1ΔTM2 showed a very large increase in thick pili compared to WT, corresponding to PilA1 expression and protein levels. Collectively, SynEtr1 and ethylene appear to be affecting the form and function of type IV pili.

SynEtr1 and Ethylene Regulate EPS Related Gene Expression and Cell Sedimentation

The role of EPS in *Synechocystis* phototaxis is less-established than the role of type IV pili. No known genes involved in EPS production have been directly linked to phototaxis. However, secreted substances left behind moving *Synechocystis* cells have been shown to alter motility of cells that follow behind these cells (Ursell et al., 2013; Chau et al., 2015). Additionally, in other organisms that move in a surface dependent manner, polysaccharide production and secretion has been shown to be essential for motility (Lu et al., 2005). To determine if alterations in phototaxis in ethylene or SynEtr1ΔTM2 occur as a result of alterations in EPS production, we examined the expression levels of EPS related genes under phototaxis conditions (Figure 4.6A). *Slr1875*, *sll1581*, *sll5052*, and *sll0923* were previously identified as *Synechocystis* genes with sequence homology to genes associated with EPS production in heterotrophic bacteria (Jittawuttipoka et al., 2013). All four genes were reported to play varying roles in EPS production in *Synechocystis*. We observed *slr1875* transcript levels to be significantly increased and *sll5052* to be significantly decreased in SynEtr1ΔTM2 compared to WT in air (Figure 4.6A). There was no significant difference between *sll1581* and

Table 4.1: Effect of Ethylene on Number Type IV Pili in WT *Synechocystis*

	Average Number of Type IV Pili per Cell Observed in Field of View	Number of Cells Observed
Air	1.8 ± 1.1	13
Ethylene	4.1 ± 2.8*	15

Number of type IV pili in WT cells treated with ethylene in phototaxis conditions with a magnification at 20,000x. The number of type IV pili in the field of view of each cell was determined and the average ± SD was calculated. * indicates significance at $P < 0.003$.

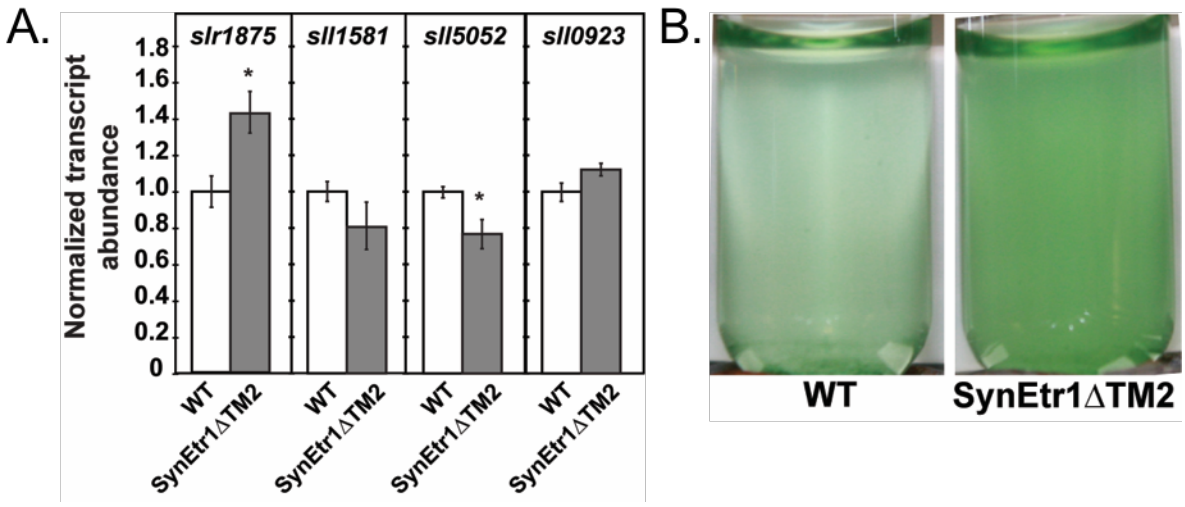

Figure 4.6: qPCR Analysis of EPS related genes in WT and SynEtr1ΔTM2 and Sedimentation of WT and SynEtr1ΔTM2

(A) qRT-PCR analysis of *slr1875*, *sll1581*, *sll5052*, and *sll0923* in WT and SynEtr1ΔTM2 *Synechocystis* in phototaxis conditions only in air. Cells were harvested, RNA was extracted and reverse transcribed and qPCR was performed. Expression levels were first normalized to a house keeping gene, then each gene was normalized to WT in air. Data are averages ± SD. * indicate statistical difference of expression in WT compared to SynEtr1ΔTM2 ($P < 0.05$). (B) Sedimentation assay. Photographs of WT and SynEtr1ΔTM2 cultures that were kept static for four days in diffuse light in air.

sll0923 transcript levels, however *sll1581* expression was slightly reduced in SynEtr1ΔTM2 compared to WT.

In the study that identified and characterized these EPS related genes, it was reported that disruption of these genes caused the cells to sediment, or settle, at varying rates (Jittawuttipoka et al., 2013). Deletion of either *sll1581* and *sll5052* enhanced the rate of sedimentation, whereas deletion of either *slr1875* and *sll0923* had little effect. *Slr1875* was increased in expression, and *sll1581* was slightly reduced in expression in SynEtr1ΔTM2. SynEtr1ΔTM2 cells showed a decreased rate of sedimentation relative to WT (Figure 4.6B). It is possible that overexpression of *slr1875* contributes to increased cell buoyancy, as this was not previously examined. Collectively, these results suggest that SynEtr1 plays a role in regulating EPS production and in turn sedimentation in *Synechocystis*.

Ethylene Enhances Biofilm Formation

Both type IV pili and EPS production have been linked to biofilm formation in several heterotrophic microbes. Similar to phototaxis, in biofilm formation type IV pili function to allow cells to adhere to a surface and to other cells (O'Toole and Kolter, 1998; Shi and Sun, 2002). EPS is produced to help stabilize cell-to-cell interactions, while also serving as a functional barrier from stress inducing substances (Flemming and Wingender, 2010). With the observation that ethylene and SynEtr1 both play a role in regulating type IV pili and EPS, we hypothesized that they also affect biofilm formation in *Synechocystis*. Initially, WT and SynEtr1ΔTM2 liquid cultures were exposed to .3 ppm ethylene for four days in diffuse light. Using crystal violet staining, we found ethylene to quantifiably increase the number of adhered cells, while fewer

SynEtr1ΔTM2 cells adhered in air compared to WT in air (Figure 4.7A). However, qualitatively, it appeared that SynEtr1ΔTM2 caused an increase in cell adherence. It is likely that cells were lost during the crystal violet staining assay. Thus, SynEtr1ΔTM2 may cause an increase in number of adhered cells, but the strength of adherence may be reduced. We next looked at WT biofilm formation at a range of ethylene concentrations. A gradual increase in biofilm formation was seen up to .3 ppm ethylene (Figure 4.7B). At .7 ppm ethylene cell adherence was reduced back to levels similar to air. Like SynEtr1ΔTM2, this quantitative reduction in adherence is possibly due to loss of weakly adhered cells in the crystal violet staining assay. The ability to respond to very low levels of ethylene also occurs in ethylene receptors in higher plants (Binder et al., 2004).

Photosynthesis is Altered by Ethylene

One of the functions of phototaxis is to allow organisms to move conditions most optimal for photosynthesis. Too much light can be harmful and too little light can lead to energy deficiencies (Bhaya, 2004). When phototaxis is altered, it is possible that the cause is from alterations in sensitivity of the photosynthetic machinery. To test whether ethylene treated WT or disruption of SynEtr1 affects the photosynthetic capacity of *Synechocystis* we performed low-temperature fluorescence on WT and SynEtr1ΔTM2 under phototaxis conditions. Low temperature fluorescence allows for measurement of the relative amounts of PSI and PSII in the cells. Ethylene caused a slight increase in PSII levels in WT as indicated by a decrease in ratio of PSI:PSII (Figure 4.8). Compared to WT in air, SynEtr1ΔTM2 in air had a greater increase in PSII levels. Ethylene had minimal effect on PSII levels in SynEtr1ΔTM2 (data not shown). These

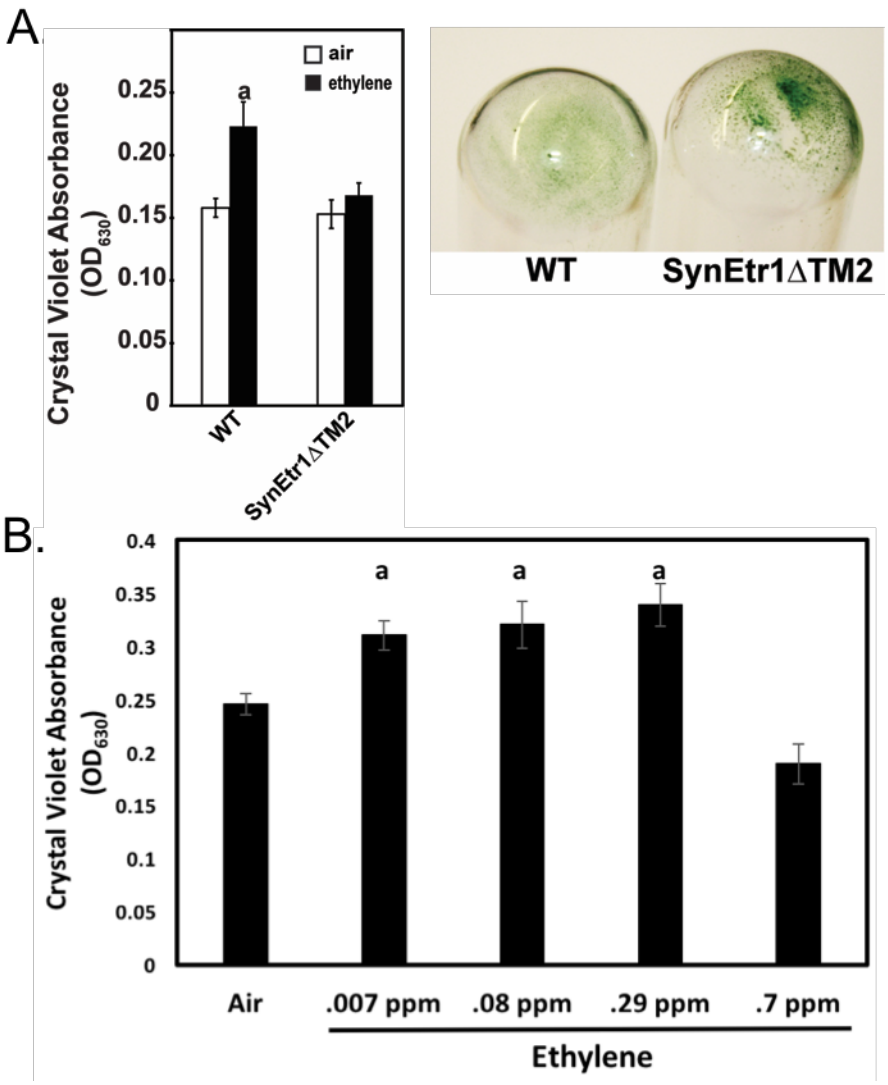

Figure 4.7: Biofilm Assays for WT and SynEtr1ΔTM2

(A) Biofilm assay for WT and SynEtr1ΔTM2 cultures exposed to air or .3 ppm ethylene for four days in diffuse light. Quantification of the biofilm formation was performed by crystal violet staining of attached cells. Optical density was measured at OD_{630}. Data are averages ± SD. a indicate statistical difference caused by addition of ethylene ($P < 0.05$). (Left Panel) Images of adhered cells prior to crystal violet staining. (B) Dose response biofilm assay for WT exposed to air or concentrations of ethylene indicated below the chart. a indicates statistical difference caused by addition of ethylene ($P < 0.05$).

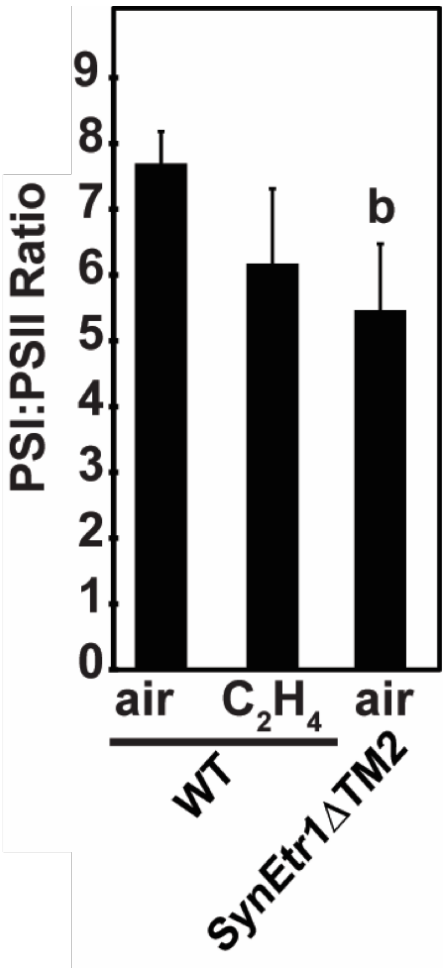

Figure 4.8: Low-Temperature Chlorophyll Fluorescence of WT and SynEtr1ΔTM2

Relative ratio of of PSI:PSII of WT and SynEtr1 exposed to phototaxis conditions. b indicates statistical difference of SynEtr1ΔTM2 compared to WT in air.

results suggest that ethylene and SynEtr1 may affect phototaxis by altering the photosynthetic capacity of the cells.

Ethylene and SynEtr1 Have Extracellular Effects

At this point the results suggest that both extracellular (type IV pili, EPS) and intracellular (photosynthesis) components of *Synechocystis* are possibly contributing to ethylene and SynEtr1ΔTM2 phenotypes in phototaxis. To better understand whether extracellular or intracellular components were affecting phototaxis we performed phototaxis assays with mixed populations of WT and SynEtr1ΔTM2. If extracellular components are causing altered phototaxis in SynEtr1ΔTM2 it is possible that a mixed culture of WT and SynEtr1ΔTM2 will move as a single population. Two populations of moving cells are expected if the contributing components are intracellular. We mixed cells at WT:SynEtr1ΔTM2 ratios including 10:1, 1:1, and 1:10 and performed phototaxis assays in air. A single population of moving cells was observed in both 1:1 and 1:10 ratios (Figure 4.9A). This indicates that disrupting SynEtr1 leads to an extracellular phenotype that affects other cells in the population. To further confirm this, we expressed green fluorescent protein (GFP) in WT cells and performed the same mixed cell phototaxis assay. GFP fluorescence at the leading edge of mixed cultures would indicate that WT cells are moving at a faster rate when mixed with SynEtr1ΔTM2 cells. GFP fluorescence was overall fairly low. This was likely caused by the large amounts of chlorophyll present. Chlorophyll is known to cause reduced GFP fluorescence (Zhou et al., 2005). The higher intensity GFP fluorescence in areas of lower chlorophyll fluorescence support this claim. Nonetheless, GFP fluorescence was present at the leading edge of moving populations of

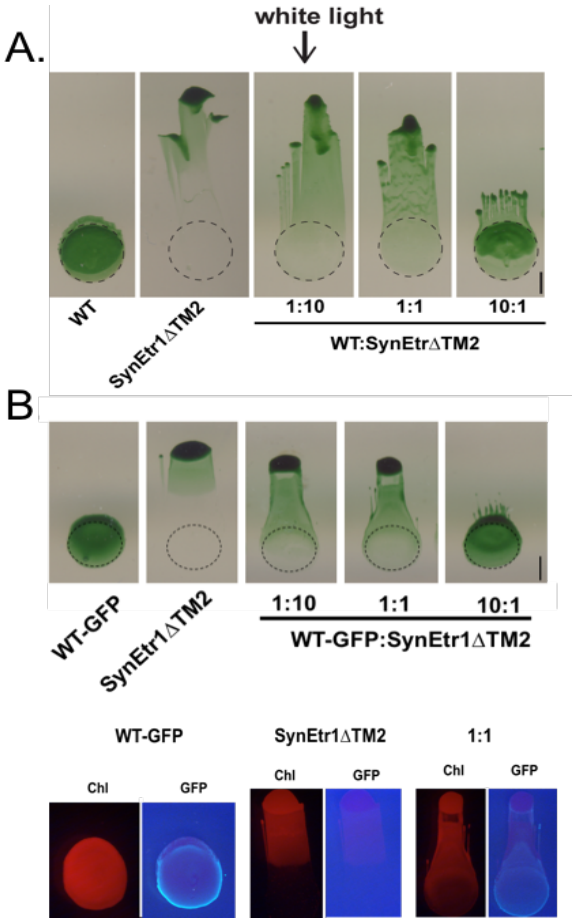

Figure 4.9: Mixed Population Phototaxis Assay of WT and SynEtr1ΔTM2

(A) Phototaxis assays of mixed populations of WT and SynEtr1ΔTM2 in air. WT and SynEtr1 were harvested from plates and resuspended to the same density. The cultures were then mixed at the ratios indicated below each panel. (B) Phototaxis assays of mixed populations of WT expressing GFP and SynEtr1ΔTM2. Assays were performed under normal phototaxis conditions with the exception of $CuSO_4$ being removed from the BG-11. This was to increase GFP expression in the pUR plasmid. The bottom panel shows chlorophyll fluorescence (chl) and GFP fluorescence (GFP) in individual select colonies from the assay above. Dashed lines indicated the starting position of colonies. Black bar = 2 mm.

cells at both 1:1 and 1:10 ratios indicating that WT motility is influence by extracellular components of SynEtr1ΔTM2 (Figure 4.9B).

Discussion

The presence of predicted EBDs in many species of both phototrophic and autotrophic prokaryotes (Figure 3.1) suggests that ethylene may function as a wide spread signaling molecule in bacteria. We have previously shown that ethylene regulates phototaxis in *Synechocystis* through the ethylene receptor SynEtr1. Phototaxis is complex and involves the coordination of several major physiological processes. Here, we sought to gain insight into the underlying aspects of phototaxis that SynEtr1 and ethylene mediate. Not all of the organisms that contain predicted EBDs use phototaxis; however, many are known to utilize type IV pili and EPS in some capacity. Thus, the findings presented in this chapter may provide insights into the function of ethylene as a signaling molecule in other prokaryotes.

Our results show that ethylene and SynEtr1 play a role in regulating type IV pili and EPS in *Synechocystis*. We found type IV pili to be affected on a transcriptional, protein, and complete structural level. Transcription of EPS related genes were also affected. These genes have been reported to be associated with cell sedimentation in *Synechocystis*. Consistent with this observation, SynEtr1ΔTM2 showed altered rates of sedimentation compared to WT. Additionally, biofilm production, a process that involves both type IV pili and EPS, was affected by both ethylene and disruption of SynEtr1. We confirmed that these extracellular factors, type IV pili and EPS, were affected by disrupting SynEtr1 by showing that mixed cultures of WT and SynEtr1ΔTM2 moved as a single population in phototaxis. Interestingly, we also observed that

photosynthesis was affected by ethylene and SynEtr1. It is possibly that this is a feedback mechanism from alterations in type IV pili. Accumulation of prepilins, which was observed in SynEtr1ΔTM2, has been shown to affect PSII assembly (He and Vermaas, 1999; Linhartová et al., 2014). It is also possible that because both ethylene treated WT and SynEtr1ΔTM2 show increased motility, there is greater need for energy production.

In chapter 3 we speculated on the ecophysiological role of ethylene in *Synechocystis*. SynEtr1 functions as receptor for both light and ethylene. Light is known to stimulate production of diffusible ethylene in the water column through interactions with hydrocarbons (Swinnerton and Linnenborn, 1967; Wilson et al., 1970; Swinnerton and Lamontagne, 1974; Ratte et al., 1998). Thus, the combination of both light and photochemically produced ethylene likely alters the activity and output of SynEtr1. We previously showed that phototaxis is affected by both ethylene and SynEtr1. The physiological responses observed in this chapter, including sedimentation and biofilm formation, provide a more complete picture of the potential environmental role for ethylene in *Synechocystis*. The combination of light and ethylene cues may allow *Synechocystis* cells to adjust their buoyancy based on the most efficient photosynthetic conditions in the water column. Additionally, interaction of cells through increased production or activity of type IV pili may be influenced by ethylene and SynEtr1 as well. Interestingly, many of the organisms predicted to contain EBDs are soil bacteria. It is possible that ethylene produced from roots stimulates root colonization of these bacteria by alterations in type IV pili activity and EPS production.

The physiological output of ethylene signaling in *Synechocystis* is more clear, but the biochemical output remains unknown. Both slr1213 and slr1214 are predicted response

regulators and are required for the function of SynEtr1 in phototaxis. Slr1213 is known to function as transcription factor for *CsiR1*, but the function of slr1214 is unknown. It is possible that ethylene alters activity and phosphorelay among these proteins, however more direct biochemical analysis is required.

Chapter 5

Analysis of the Global Transcriptional Effects of Ethylene and SynEtr1 on *Synechocystis*

Introduction

In the previous chapters, understanding the role of ethylene and SynEtr1 in *Synechocystis* was approached using predictions of function based off of the domain architecture of SynEtr1. From this it was discovered that, physiologically, ethylene and SynEtr1 regulate phototaxis by altering EPS production and type IV pili. Using qRT-PCR expression analysis, specific genes affected by ethylene and SynEtr1 were identified that are associated with both EPS production and type IV pili. To develop a more complete picture of the role of ethylene and SynEtr1 in *Synechocystis*, we performed RNA-seq analysis on WT and SynEtr1ΔTM2 exposed to air and 1 ppm ethylene in directional light. This will allow for more directed approaches in understanding the physiological and transcriptional effects of SynEtr1 ethylene signaling.

Traditionally, the method of choice for transcriptome analysis has been DNA microarray (Zhao et al., 2014; Zhang et al., 2015). More recently, RNA-seq has supplanted DNA microarray as an effective alternative for assessing the global transcriptional state of an organism. RNA-seq provides several advantages including higher resolution and reproducibility as well more sensitive detection of novel transcripts (Zhao et al., 2014). Using RNA-seq we hope to develop a more comprehensive view of how ethylene affects *Synechocystis* by identifying genes that are altered by ethylene or in SynEtr1ΔTM2. This is important for our work, but it is also important

from a biotechnological aspect as *Synechocystis* has been developed as an organism for ethylene production (Guerrero et al., 2012; Ungerer et al., 2012; Zavrel et al., 2016). Additionally, the RNA-seq analysis pipeline developed here can be applied to future RNA-seq studies in the lab.

Results

General Characteristics of the RNA-seq Data Set

Initially, RNA was extracted from both WT and SynEtr1ΔTM2 in either 1 ppm ethylene or air in directional light for four days. This was done in triplicate for each condition. The RNA was DNAse treated and shipped to the Genome Sequencing and Analysis Facility (GSAF) at the University of Texas – Austin. mRNA was isolated by ribosomal removal. NextSeq 500 Illumina technology was used for sequencing, producing 75 base pair single end reads. For each sample, approximately 20 million sequence reads were obtained (Table 5.1). All initial processing of the reads was performed using the Newton high performance compute cluster at the University of Tennessee – Knoxville. All code used for read processing and differential expression analysis can be found Appendix C. FastQC analysis showed relatively high overall per base quality of the reads obtained from GSAF (Figure 5.1). The reads were first processed using the trimming software Trimmomatic to remove any low quality reads. This removed less than 10% of the overall reads per sample (Table 5.1). Trimmed reads were next mapped to the *Synechocystis* genome using the programs Bowtie2 and Tophat. Over 80% of the total reads were successfully mapped to the genome for every sample, with most samples having a map rate in the mid 90s (Table 5.1). The mapped reads were then sorted and counted using SamTools and HTSeq.

Table 5.1: Overview of Initial Processing of RNA-seq Sequence Reads

	Total Reads	Total Reads Post Trim	Total Reads Mapped to Genome
WT air 1	21166775	19430869	18406942 (94.7%)
WT air 2	23114903	21249638	20433516 (96.2%)
WT air 3	20021383	18462723	18024492 (97.6%)
WT eth 1	22169239	20479820	19973910 (97.5%)
WT eth 2	19823928	18266276	17848404 (97.7%)
WT eth 3	20682221	19095355	18702469 (97.9%)
SynEtr1ΔTM2 air 1	19064769	17259312	15009954 (87.0%)
SynEtr1ΔTM2 air 2	20444476	18391707	14992132 (81.5%)
SynEtr1ΔTM2 air 3	19546244	17572355	14768202 (84.0%)
SynEtr1ΔTM2 eth 1	22683584	20654707	19518150 (94.5%)
SynEtr1ΔTM2 eth 2	20940843	19120611	18383548 (96.1%)
SynEtr1ΔTM2 eth 3	22816192	20793106	19954631 (96.0%)

Total numbers of initial sequence reads, number of reads after trimming, and total number of reads mapped to the *Synechocystis* genome with the mapping percentage.

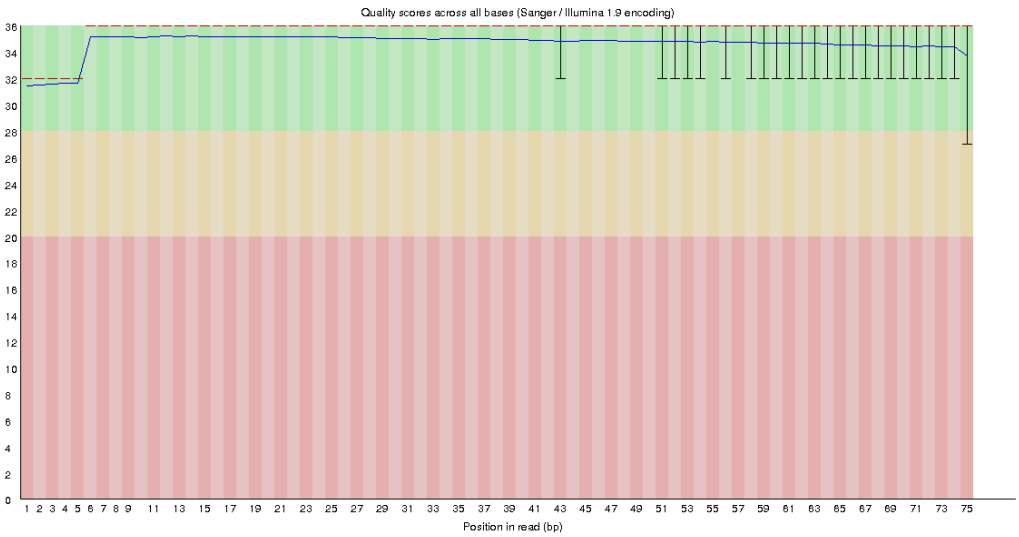

Figure 5.1: Representative Example of FastQC Analysis

A representative example of the average per base quality of RNA-seq reads as generated by FastQC. This is from WT sample example exposed to Air. The horizontal axis represents the base pair position in the set of reads. The vertical axis is the quality score as indicated by the confidence of the base call. A higher score (green) indicates high confidence in the base call.

HTSeq produces a count file that displays the total number of reads mapped to each gene. This file is used directly for differential expression analysis.

Differential Expression Analysis

The overall goal of this experiment is to determine what genes are differentially expressed by ethylene in a SynEtr1 dependent manner. To do this, the count files generated from HTSeq were first loaded into the statistical analysis software R. In R, the package DESeq2 was specifically developed to provide methods for analyzing high-throughput sequencing data. DESeq allows for effective normalization of data across different conditions, with subsequent differential expression analysis. Initially, using DESeq2, we sought to determine expression variance among our samples. Determining sample variance allows for the detection of outliers in biological or technical replicates that may affect identification of significance in differential expression. We examined variance using a principle component analysis (PCA) plot (Figure 5.2). Biological replicates for each condition cluster together well, which indicates that there is minimal variance among the replicates.

From this RNA-seq dataset we were particularly interested in identifying two sets of differentially expressed genes. First, we wanted to examine genes that are differentially expressed in WT vs SynEtr1ΔTM2 exposed to air. This will allow for identification of genes that are potentially upregulated by SynEtr1 in directional light. All *P* values shown here are adjusted for false postives (*Padj*) using the Benjamini-Hochberg method in DESeq2. At *Padj < 0.05* 954 genes were observed to be significantly differential expressed (Figure 5.3). At *Padj < 0.01* this value was reduced to 628. *Synechocystis* has 3,725 known genes. This indicates that disruption

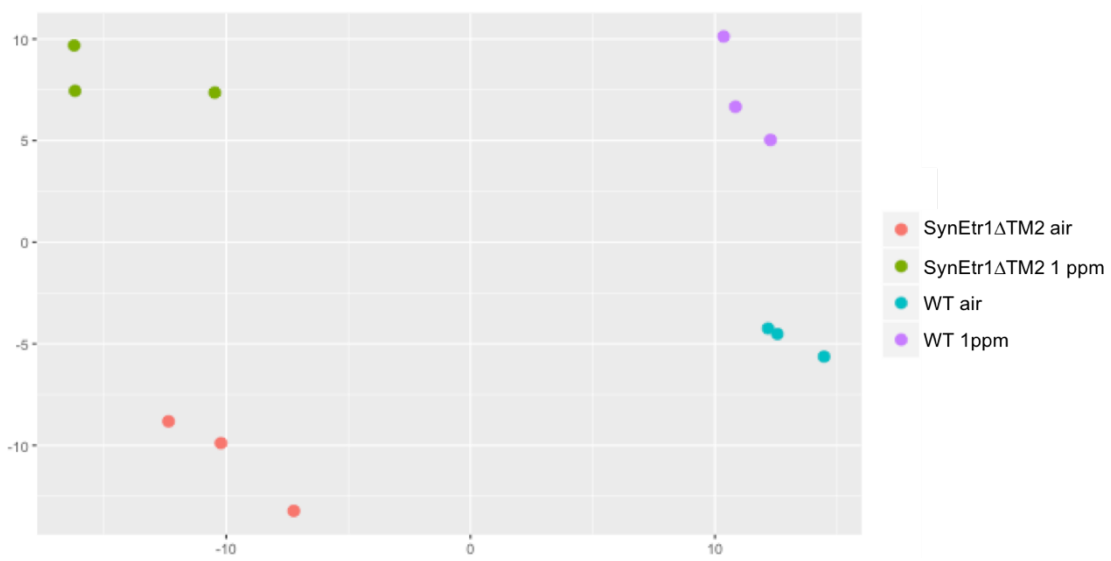

Figure 5.2: PCA Plot of RNA-seq Samples

A principle coordinate analysis (PCA) plot generated from each sample submitted for RNA-seq. For each condition, WT or SynEtr1ΔTM2 exposed to air or ethylene, three biological replicates were analyzed, as indicated by the three data points for each condition in the plot. The normalized read counts are transformed and subjected to PCA using DESeq in R. The results of the PCA are the plot you see above.

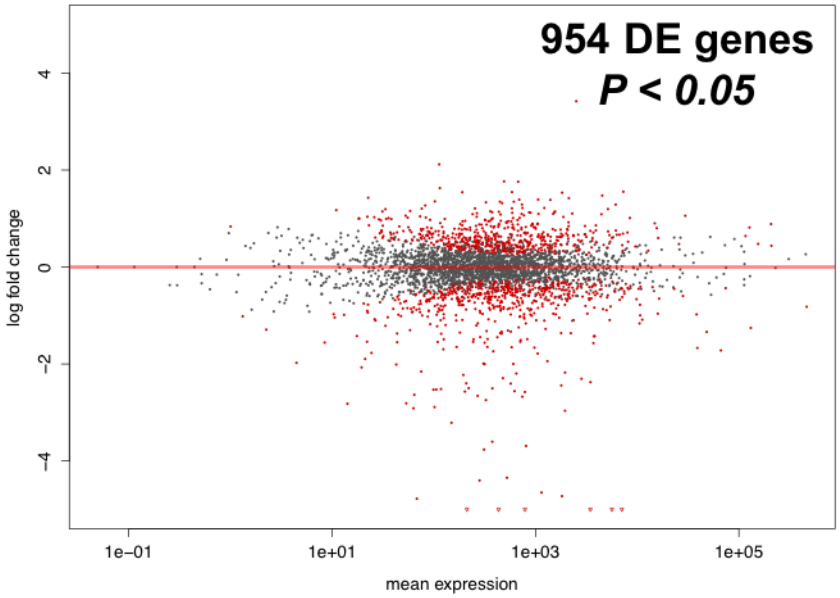

Figure 5.3: Differential Expression Comparison of WT vs SynEtr1ΔTM2 in Air

Identification of differentially expressed (DE) genes in SynEtr1ΔTM2 in air compared to WT in air as shown using an MA plot. 954 genes were identified as differentially expressed with at *Padj < 0.05*. Each dot represents a single gene. The horizontal axis is the mean expression level of each gene. The vertical axis is the log fold change of gene expression in SynEtr1ΔTM2 compared to WT. Red dots indicate significance at *Padj < 0.05*.

of SynEtr1, leads to a high level of differential expression in directional light. It is unlikely that all of these genes are directly transcriptionally regulated by SynEtr1. It is more likely that many of the genes are differentially expressed in response to the significant changes in motility that we have previously observed. *Slr1214* was shown to be down regulated 3.5 fold in SynEtr1ΔTM2, a result that is consistent with what was previously shown using qRT-PCR. This confirms that SynEtr1 affects expression of *slr1214* in UV and white light.

We next wanted to focus on identifying transcriptional changes that are specific to ethylene signaling via SynEtr1. To do this we first examined differential expression in WT in air vs. WT in ethylene. This produced 530 genes that are differentially expressed at *Padj < 0.05* (Figure 5.4A). Next we examined differential expression in SynEtr1ΔTM2 in air vs. SynEtr1ΔTM2 in ethylene. This condition produced 1085 differentially expressed genes at *Padj < 0.05* (figure 5.4A). This observation suggests that 1 ppm ethylene has significant effects on the transcriptome of *Synechocystis* independent of SynEtr1. To determine transcriptional changes associated with ethylene signaling in SynEtr1, we identified genes that were differentially expressed in WT in ethylene that were not differentially expressed in SynEtr1ΔTM2 in ethylene at *Padj < 0.05*. 160 genes were found to be specifically differentially expressed when SynEtr1 was functional in the presence of ethylene (Figure 5.4B). *Slr1214* was not among the 160 genes, suggesting that ethylene signaling in SynEtr1 does not effect *slr1214* expression. Again, many of these 160 genes are likely indirectly affected. However, this smaller number of differential expressed genes, compared to WT vs SynEtr1ΔTM2 in air, provides an easier sample size to work with in identifying direct transcriptional targets affected by SynEtr1 ethylene signaling.

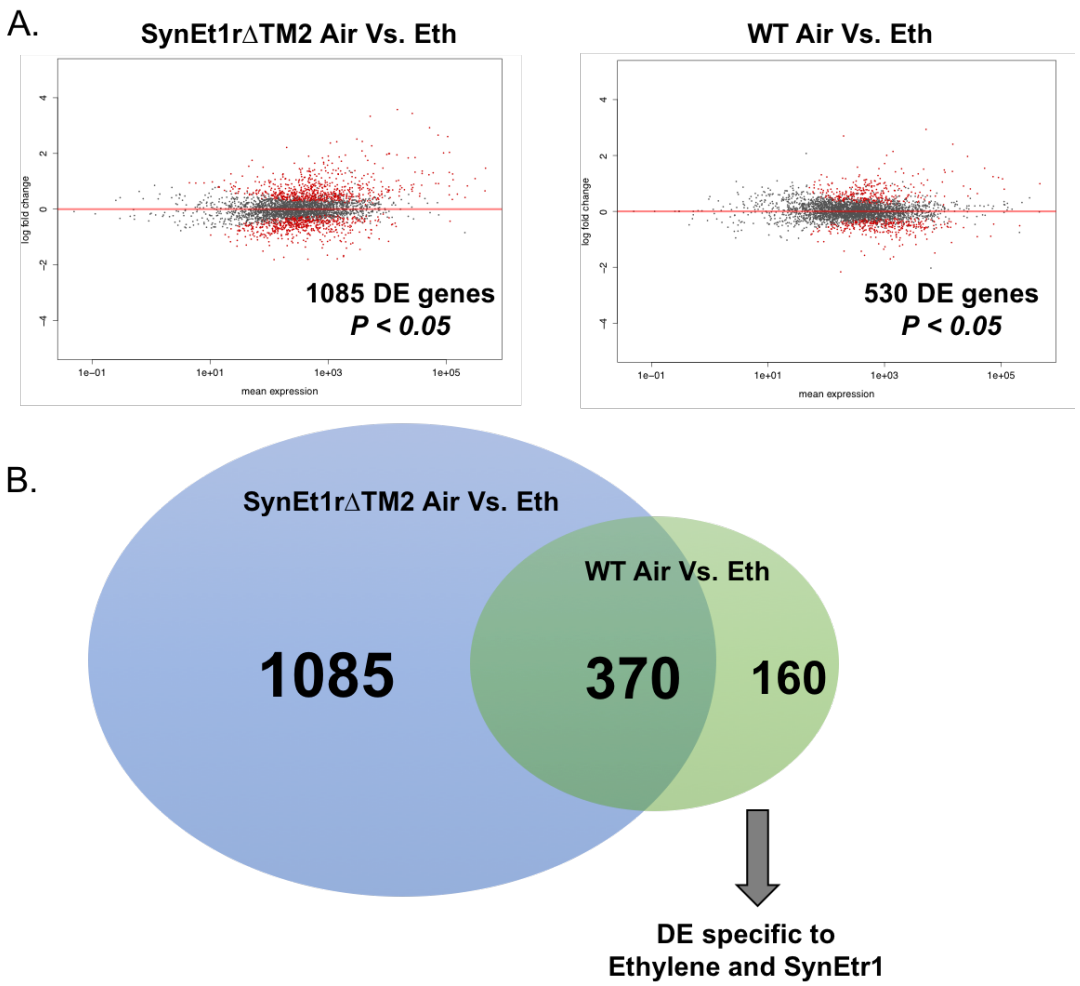

Figure 5.4: Identification of SynEtr1 specific Ethylene induced Differential Expression

(A) MA plots showing the number of differential expressed (DE) genes between ethylene treated SynEtr1ΔTM2 (left) and WT (right)compared to air at *Padj < 0.05*. (B) Diagram showing the number of genes that are DE by ethylene in WT that overlap with genes that are DE by ethylene in SynEtr1ΔTM2. Blue indicates SynEtr1ΔTM2 DE genes in ethylene and green indicates WT DE genes in ethylene. 370 DE genes in WT overlap with SynEtr1ΔTM2. 160 were identified as specifically upregulate in ethylene when SynEtr1 is present.

Discussion

Several studies have performed RNA-seq analysis on *Synechocystis* (Anfelt et al., 2013; Kopf et al., 2014; Lau et al., 2014; Kizawa et al., 2016). Consistent with our results, it has been reported that pharmacological and genetic manipulation of *Synechocystis* can cause large percentages of the genome to be differentially expressed. Because we have observed that ethylene and SynEtr1 regulate phototaxis, a complicated process involving the coordination of many cellular components, it is not surprising that we too observe major transcriptomic effects caused by application of ethylene or disruption of SynEtr1. It does however, complicate the process of identifying specific cellular processes that are affected. Initially, we searched for genes that we have previously observed by qRT-PCR to be transcriptionally affected by ethylene or disruption of SynEtr1. As mentioned above, *slr1214* expression was confirmed to be highly downregulated in SynEtr1ΔTM2 and unaffected by ethylene in WT in this RNA-seq dataset. The type IV pili related gene *PilC* was shown to be significantly upregulated by ethylene in WT and by disruption of SynEtr1. It was among the 160 genes that appear to be specifically affected by ethylene signaling through SynEtr1. Other pili and EPS related genes did not show a similar expression pattern to what was observed by previously by qRT-PCR. Interestingly, RNA-seq revealed that transcription of other EPS and motility related genes were observed to be affected by ethylene and SynEtr1. Thus, multiple points of regulation likely exist in these processes.

We will continue to explore this data set in order to identify either specific genes or groups of genes that are affected by ethylene signaling in SynEtr1. This will allow for refinement of our knowledge of ethylene signaling in *Synechocystis* and hopefully provide insights into the

function of ethylene as a signaling molecule in other prokaryotes. Additionally, as mentioned above, *Synechocystis* has previously been engineered to produce ethylene (Guerrero et al., 2012; Ungerer et al., 2012). Determining the global transcriptional affects of ethylene on *Synechocystis* could provide a useful resource for synthetic biologists seeking to optimize ethylene production in *Synechocystis*.

Chapter 6

Conclusions and Future Directions

Prior to this work, ethylene was only known to function as a signaling molecule in green plants. Several species of cyanobacteria, however, had been reported to encode proteins with predicted EBDs and possess the capacity to bind ethylene with high affinity (Rodriguez et al., 1999; Mount and Chang, 2002; Wang et al., 2006). Whether ethylene affected the physiology of these organisms specifically through predicted EBDs was unclear. Here, we report that SynEtr1 in *Synechocystis* functions to sense and respond to ethylene, making this the first characterization of an ethylene receptor outside of green plants.

SynEtr1, a dual ethylene and light receptor, was previously established as a photoreceptor involved in mediating phototaxis (Narikawa et al., 2011; Song et al., 2011). A precise role for SynEtr1 in phototaxis was inexact, due to conflicting reports likely resulting from variations in experimental methods. In this report, we establish that SynEtr1 functions to inhibit movement toward white light and monochromatic wavelengths of light ranging from UV to red. Ethylene was found to increase phototaxis toward all wavelengths of visible light tested. Ethylene enhanced phototaxis in *Synechocystis* is dependent on the presence of functional SynEtr1. Interestingly, ethylene enhanced phototaxis was observed in a light-insensitive C561A-SynEtr1, suggesting that ethylene signaling may function independently of light signaling.

Because of the complexity of phototaxis, we sought to address the underlying aspects of this process in hopes of determining a more specific physiological output of ethylene signaling in SynEtr1. Three main components affect phototaxis: type IV pili, extracellular polymeric

substances (EPS), and photosynthesis. Alterations in aspects of each of these three components were observed in *Synechocystis* by application of ethylene or removal of SynEtr1. Both type IV pili and EPS affect phototaxis extracellularly, whereas photosynthesis takes places internally. We found that by mixing WT and SynEtr1 deficient *Synechocystis* cultures and performing phototaxis assays, the cells moved largely as a single population. Movement was similar to what was observed in SynEtr1ΔTM2 alone. This suggests that both type IV pili and EPS are likely the main components affected by SynEtr1 disruption, as these external phototaxis components can affect motility of nearby WT cells. If an internal component were altered, two populations of moving cells would be expected. Thus, ethylene and SynEtr1 likely function by altering both type IV pili and EPS production with altered photosynthesis being an indirect effect.

The findings reported here suggest a model in which ethylene affects the physiology of *Synechocystis* through SynEtr1 (Figure 6.1). SynEtr1 inhibits movement toward light and ethylene inhibits SynEtr1. From our observations, SynrEtr1 is altering phototaxis by modulation of an extracellular component such as type IV pili or EPS. Overall, the function of ethylene and SynEtr1 in *Synechocystis* is more clear; however, many questions remain regarding the biochemical mechanisms of ethylene signaling in SynEtr1, the general physiological effects of ethylene in *Synechocystis*, and the possible function of ethylene as a signaling molecule in other prokaryotes.

SynEtr1 has been shown to phosphorylate slr1213 after UV light stimulation. Slr1213 is able to function as a transcription factor for *csiR1* and likely *slr1214* (Ramakrishnan and Tabor, 2016). Thus, the likely scenario for light stimulated two-component signaling in this system is

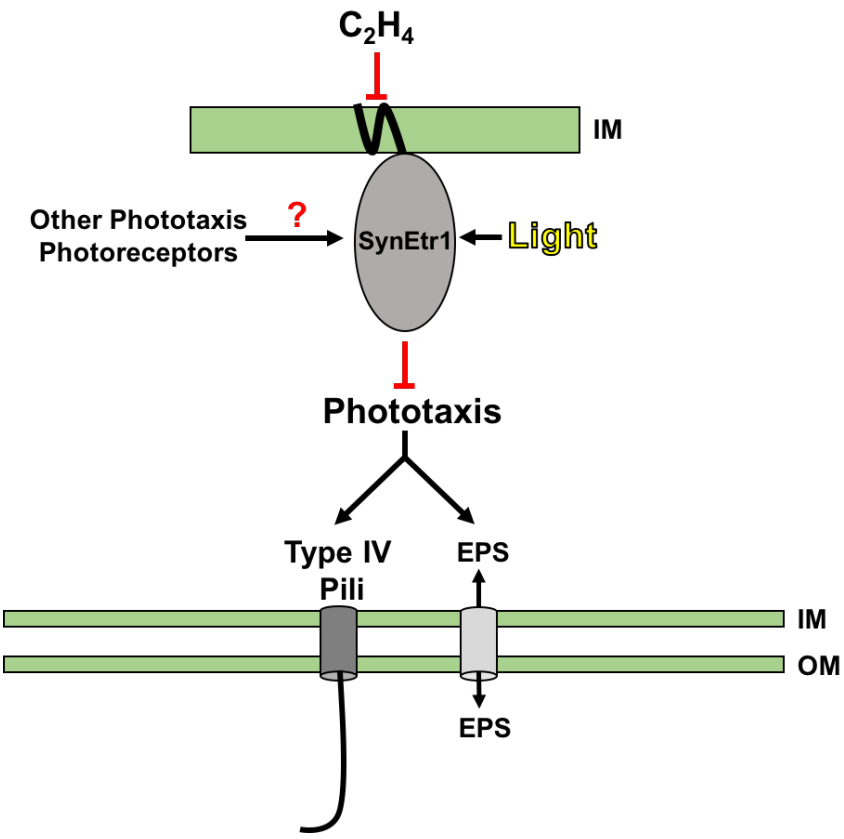

Figure 6.1: A Model for the Function of Ethylene in *Synechocystis*

A basic model depicting the physiological function of ethylene in *Synechocystis*. Membrane bound SynEtr1 is stimulated by light and functions to inhibit inhibit phototaxis toward light. Ethylene inhibits SynEtr1, thus enhancing positive phototaxis. Ethylene enhanced phototaxis is likely occurring through alterations in type IV pili and EPS production. IM and OM indicate inner and outer membranes respectively. It is unknown how SynEtr1 coordinates phototaxis responses with other receptors that are known to be involved in mediating phototaxis.

one in which light activates SynEtr1 causing histidine autophosphorylation. This histidine is transferred to an aspartate on the response regulator slr1213. Slr1213 then activates transcription of *csiR1* and *slr1214*. Where ethylene fits in this picture is unclear (Figure 6.2). Our results from both qRT-PCR and RNA-seq indicate that ethylene has no effect on *slr1214* transcript levels. Slr1214 is also a predicted response regulator and has been shown to directly interact with SynEtr1 (Sato et al., 2007). Song et al. (2011) reported that mutation of a predicted phospho-accepting aspartate on slr1214 eliminated UV avoidance in *Synechocystis*. Thus, slr1214 likely functions in phosphorelay associated with SynEtr1 signal transduction. Whether slr1214 accepts phosphates from SynEtr1 or slr1213 is unknown. It is possible that ethylene signaling in SynEtr1 modulate the transfer of phosphates from SynEtr1 to either slr1213 or slr1214 (Figure 6.2). We plan to explore this by adding slr1214 to the SynEtr1-slr1213 *E. coli* expression system described in Ramakrishnan and Tabor (2016). Using this system, slr1214 can be expressed alone with SynEtr1 or with both SynEtr1 and slr1213. By monitoring the phosphorylation state of slr1213 and slr1214 in cells exposed to UV or visible light in the presence of air or ethylene, we will develop a clearer picture of the relationship between signal input and the biochemical signal output in SynEtr1.

A more complete understanding of the biochemical output of SynEtr1 ethylene signaling combined with the RNA-seq analysis will be essential to understanding the physiological effects of ethylene in *Synechocystis*. It has been reported that high CO_2 levels reduce transcription of *csiR1* and *slr1214* by slr1213 (Kopf et al., 2014). CO_2 functions as an indirect competitor of ethylene binding in ethylene receptors in plants (Sisler, 1979). It is possible that, similar to CO_2, ethylene signaling may function to simply inhibit output of slr1213 leading to

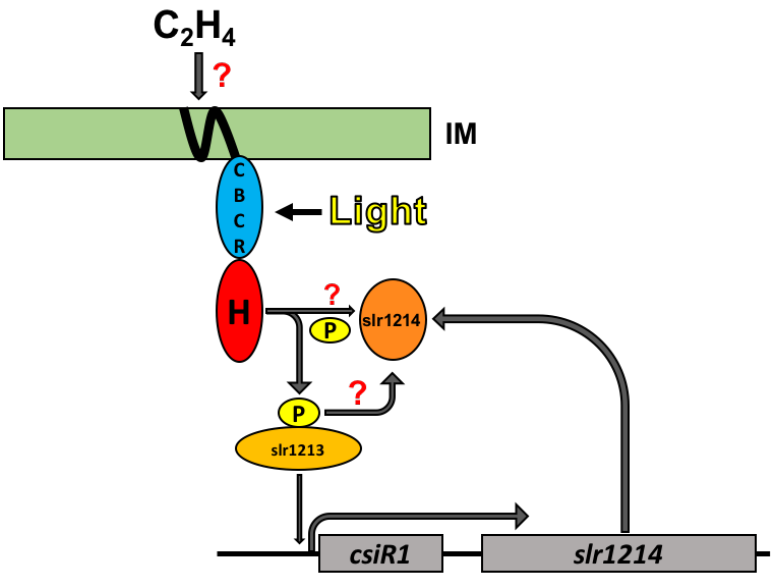

Figure 6.2: Questions Regarding Phosphorelay from SynEtr1 and the Role Ethylene

Several open questions remain regarding signal transduction via phosphorelay in SynEtr1 and how ethylene affects this. It is known that light perception by the CBCR domain of SynEtr1 initiates phosphotransfer from the histidine kinase domain (red) to slr1213. Slr1213 then activates transcription of *csiR1* and *slr1214*. As indicated by the red question marks it is unknown whether slr1214 is involved in phosphotransfer from SynEtr1, slr1213, or neither. Additionally, it is unknown how ethylene affects signal transduction.

reduction of *csiR1* transcripts. Our results thus far indicate that *slr1214* transcript levels are not affected by ethylene. Further analysis is needed to determine if *csiR1* transcription is affected; however, preliminary results suggest ethylene reduces *csiR1* transcription. Because *csiR1* is a ncRNA with potential transcriptional and posttranscriptional regulatory effects, ethylene altered *csiR1* transcription may result in overlap of observed transcriptome changes caused by application of either high CO_2 or ethylene. This overlap of transcriptionally altered genes in previous studies (Kopf et al., 2014) compared to our RNA-seq results could provide insights into direct regulatory targets of *csiR1* and in turn SynEtr1.

Slr1214, similar to slr1213, is a predicted response regulator and transcription factor. Unlike slr1213, transcriptional targets of slr1214 are unknown. For RNA-seq analysis, in addition to WT and SynEtr1ΔTM2 *Synechocystis*, RNA from Δslr1214 exposed to air and ethylene in directional white light was sent for transcriptome sequencing. Differential expression analysis for these samples is currently being performed. We expect this data set to provide valuable information in multiple ways. Comparison of differentially expressed genes between the two data sets, WT air and ethylene and Δslr1214 air and ethylene, will help to identify ethylene induced differentially expressed genes specific to slr1214. These genes will subsequently be compared to the 160 genes that were identified to be transcriptionally altered by ethylene in a SynEtr1 specific manner discussed in chapter 5. Genes that are differentially expressed by ethylene specific to SynEtr1 and not slr1214 could indicate an ethylene signaling output of SynEtr1 that is independent of slr1214. This type of regulation may be caused by *csiR1* or other possible transcriptional targets of slr1213.

Collectively, this will help to further our understanding of how ethylene and SynEtr1 affect *Synechocystis*. Additionally, it may also provide insights into the function of ethylene as a signaling molecule in other prokaryotes. Most of the 112 bacterial species identified that contain predicted ethylene binding proteins are either cyanobacteria or soil-dwelling proteobacteria known to form non-pathogenic associations with plant roots. It is possible that in many of these species ethylene is a motility based cue. In cyanobacteria, ethylene likely affects phototaxis, whereas in the soil, ethylene produced from plants may affect bacterial root colonization. Current work has begun to explore the role of ethylene in the soil bacterium *Azospirillum brasilense*. All of the identified proteins contain predicted ethylene binding domains at the N-terminus. The C-terminal components vary significantly. Thus, there is unlikely to be a universal biochemical ethylene signaling output among these proteins. It is possible, however, that the physiological output of ethylene signaling is similar among many of these organisms.

List of References

Abeles F, Morgan P, Saltveit MJ (1992) Ethylene in Plant Biology, Ed 2nd. Academic Press, San Diego, CA

Alfonso M, Perewoska I, Kirilovsky D (2000) Redox control of psbA gene expression in the cyanobacterium Synechocystis PCC 6803. Involvement of the cytochrome b(6)/f complex. Plant Physiol **122:** 505-516

Anfelt J, Hallstrom B, Nielsen J, Uhlen M, Hudson EP (2013) Using transcriptomics to improve butanol tolerance of Synechocystis sp. strain PCC 6803. Appl Environ Microbiol **79:** 7419-7427

Bhaya D (2004) Light matters: phototaxis and signal transduction in unicellular cyanobacteria. Molecular Microbiology **53:** 745-754

Bhaya D, Bianco NR, Bryant D, Grossman A (2000) Type IV pilus biogenesis and motility in the cyanobacterium Synechocystis sp. PCC6803. Molecular Microbiology **37:** 941-951

Bhaya D, Takahashi A, Shahi P, Grossman AR (2001) Novel Motility Mutants of Synechocystis Strain PCC 6803 Generated by In Vitro Transposon Mutagenesis. Journal of Bacteriology **183:** 6140-6143

Bhaya D, Watanabe N, Ogawa T, Grossman AR (1999) The role of an alternative sigma factor in motility and pilus formation in the cyanobacterium *Synechocystis* sp. strain PCC6803. Proceedings of the National Academy of Science USA **96:** 3188-3193

Binder BM, Chang C, Schaller GE (2012) Perception of Ethylene by Plants - Ethylene Receptors. *In* MT McManus, ed, Annual Plant Reviews, The Plant Hormone Ethylene, Vol 44. Wiley-Blackwell, Hoboken, NJ, pp 117-145

Binder BM, Mortimore LA, Stepanova AN, Ecker JR, Bleecker AB (2004) Short-term growth responses to ethylene in Arabidopsis seedlings are EIN3/EIL1 independent. Plant Physiology **136:** 2921-2927

Bleecker AB, Kende H (2000) Ethylene: A gaseous signal molecule in plants. Annual Review of Cell and Developmental Biology **16**

Burriesci M, Bhaya D (2008) Tracking phototactic responses and modeling motility of Synechocystis sp. strain PCC6803. Journal of Photochemistry and Photobiology B: Biology **91:** 77-86

Chang C, Kwok SF, Bleecker AB, Meyerowitz EM (1993) *Arabidopsis* ethylene-response gene ETR1: similarity of product to two-component regulators Science **262:** 539-544

Chang C, Meyerowitz EM (1995) The ethylene hormone response in arabidopsis - a eukaryotic two-component signaling system. Proceedings of the National Academy of Sciences of the United States of America **92:** 4129-4133

Chau RM, Ursell T, Wang S, Huang KC, Bhaya D (2015) Maintenance of motility bias during cyanobacterial phototaxis. Biophys J **108:** 1623-1632

Chen Y-F, Randlett MD, Findell JL, Schaller GE (2002) Localization of the ethylene receptor ETR1 to the endoplasmic reticulum of *Arabidopsis*. Journal of Biological Chemistry **277:** 19861-19866

Cho YH, Yoo SD (2014) Novel connections and gaps in ethylene signaling from the ER membrane to the nucleus. Front Plant Sci **5:** 733

Costerton JW, Lewandowski Z, Caldwell DE, Korber DR, Lappin-Scott HM (1995) Microbial biofilms. Annu Rev Microbiol **49:** 711-745

Ehling-Schulz M, Bilger W, Scherer S (1997) UV-B-induced synthesis of photoprotective pigments and extracellular polysaccharides in the terrestrial cyanobacterium Nostoc commune. J Bacteriol **179:** 1940-1945

Enomoto G, Ni Ni W, Narikawa R, Ikeuchi M (2015) Three cyanobacteriochromes work together to form a light color-sensitive input system for c-di-GMP signaling of cell aggregation. Proc Natl Acad Sci U S A **112:** 8082-8087

Essen LO, Mailliet J, Hughes J (2008) The structure of a complete phytochrome sensory module in the Pr ground state. Proc Natl Acad Sci U S A **105:** 14709-14714

Fiedler B, Börner T, Wilde A (2005) Phototaxis in the Cyanobacterium *Synechocystis* sp. PCC 6803: Role of Different Photoreceptors. Photochemistry and Photobiology **81:** 1481-1488

Fisher ML, Allen R, Luo Y, Curtiss R, III (2013) Export of extracellular polysaccharides modulates ddherence of the cyanobacterium *Synechocystis*. PLoS ONE **8:** e74514

Flemming HC, Wingender J (2010) The biofilm matrix. Nat Rev Microbiol **8:** 623-633

Gallie D (2015) Appearance and elaboration of the ethylene receptor family during land plant evolution. Plant Molecular Biology **87:** 521-539

Gao R, Mack TR, Stock AM (2007) Bacterial response regulators: versatile regulatory strategies from common domains. Trends Biochem Sci **32:** 225-234

Georg J, Voss B, Scholz I, Mitschke J, Wilde A, Hess WR (2009) Evidence for a major role of antisense RNAs in cyanobacterial gene regulation. Mol Syst Biol **5:** 305

Gomez-Suarez C, Pasma J, van der Borden AJ, Wingender J, Flemming HC, Busscher HJ, van der Mei HC (2002) Influence of extracellular polymeric substances on deposition and redeposition of Pseudomonas aeruginosa to surfaces. Microbiology **148:** 1161-1169

Grefen C, Stadele K, Ruzicka K, Obrdlik P, Harter K, Horak J (2007) Subcellular localization and in vivo interactions of the *Arabidopsis thaliana* ethylene receptor family members. Moleclular Plant **1:** 308-320

Guerrero F, Carbonell V, Cossu M, Correddu D, Jones PR (2012) Ethylene synthesis and regulated expression of recombinant protein in *Synechocystis* sp. PCC 6803. PLoS ONE **7:** e50470

Hall AE, Chen QHG, Findell JL, Schaller GE, Bleecker AB (1999) The relationship between ethylene binding and dominant insensitivity conferred by mutant forms of the ETR1 ethylene receptor. Plant Physiology **121:** 291-299

He Q, Vermaas W (1999) Genetic deletion of proteins resembling Type IV pilins in Synechocystis sp. PCC 6803: their role in binding or transfer of newly synthesized chlorophyll. Plant Mol Biol **39:** 1175-1188

Hernandez-Prieto MA, Schon V, Georg J, Barreira L, Varela J, Hess WR, Futschik ME (2012) Iron deprivation in Synechocystis: inference of pathways, non-coding RNAs, and regulatory elements from comprehensive expression profiling. G3 (Bethesda) **2:** 1475-1495

Hirose Y, Rockwell NC, Nishiyama K, Narikawa R, Ukaji Y, Inomata K, Lagarias JC, Ikeuchi M (2013) Green/red cyanobacteriochromes regulate complementary chromatic acclimation via a protochromic photocycle. Proc Natl Acad Sci U S A **110:** 4974-4979

Hoiczyk E (2000) Gliding motility in cyanobacterial: observations and possible explanations. Arch Microbiol **174:** 11-17

Hua J, Meyerowitz EM (1998) Ethylene responses are negatively regulated by a receptor gene family in *Arabidopsis thaliana*. Cell **94:** 261-271

Ikeuchi M, Ishizuka T (2008) Cyanobacteriochromes: a new superfamily of tetrapyrrole-binding photoreceptors in cyanobacteria. Photochemical & Photobilogical Sciences **7:** 1159-1167

Iwuchukwu IJ, Vaughn M, Myers N, O'Neill H, Frymier P, Bruce BD (2010) Self-organized photosynthetic nanoparticle for cell-free hydrogen production. Nature Nanotechnology **5:** 73-79

Jakovljevic V, Leonardy S, Hoppert M, Sogaard-Andersen L (2008) PilB and PilT are ATPases acting antagonistically in type IV pilus function in Myxococcus xanthus. J Bacteriol **190:** 2411-2421

Jekely G (2009) Evolution of phototaxis. Philos Trans R Soc Lond B Biol Sci **364:** 2795-2808

Jittawuttipoka T, Planchon M, Spalla O, Benzerara K, Guyot F, Cassier-Chauvat C, Chauvat F (2013) Multidisciplinary evidences that Synechocystis PCC6803 exopolysaccharides operate in cell sedimentation and protection against salt and metal stresses. PLoS One **8:** e55564

Ju C, Chang C (2015) Mechanistic Insights in Ethylene Perception and Signal Transduction. Plant Physiol **169:** 85-95

Ju C, Van de Poel B, Cooper ED, Thierer JH, Gibbons TR, Delwiche CF, Chang C (2015) Conservation of ethylene as a plant hormone over 450 million years of evolution. Nature Plants **DOI: 10.1038/nplants.2014.4:** 1-7

Kaneko T, Sato S, Kotani H, Tanaka A, Asamizu E, Nakamura Y, Miyajima N, Hirosawa M, Sugiura M, Sasamoto S, Kimura T, Hosouchi T, Matsuno A, Muraki A, Nakazaki N, Naruo K, Okumura S, Shimpo S, Takeuchi C, Wada T, Watanabe A, Yamada M, Yasuda M, Tabata S (1996) Sequence analysis of the genome of the unicellular cyanobacterium Synechocystis sp. strain PCC6803. II. Sequence determination of the entire genome and assignment of potential protein-coding regions. DNA Research **3:** 109-136

Kanesaki Y, Shiwa Y, Tajima N, Suzuki M, Watanabe S, Sato N, Ikeuchi M, Yoshikawa H (2012) Identification of substrain-specific mutations by massively parallel whole-genome resequencing of Synechocystis sp. PCC 6803. DNA Res **19:** 67-79

Kehoe DM, Grossman AR (1996) Similarity of a chromatic adaptation sensor to phytochrome and ethylene receptors. Science **273:** 1409-1412

Kendrick MD, Chang C (2008) Ethylene signaling: new levels of complexity and regulation. Curr Opin Plant Biol **11:** 479-485

Khayatan B, Meeks JC, Risser DD (2015) Evidence that a modified type IV pilus-like system powers gliding motility and polysaccharide secretion in filamentous cyanobacteria. Mol Microbiol **98:** 1021-1036

Kiley P, Zhao X, Vaughn M, Baldo MA, Bruce BD, Zhang S (2005) Self-assembling peptide detergents stabilize isolated photosystem ion a dry surface for an extended time. PLoS Biology **3:** e230

Kim D, Forst S (2001) Genomic analysis of the histidine kinase family in bacteria and archaea. Microbiology **147:** 1197-1212

Kim YH, Kim JY, Kim S-Y, Lee JH, Lee JS, Chung Y-H, Yoo JS, Park YM (2009) Alteration in the glycan pattern of pilin in a nonmotile mutant of Synechocystis sp. PCC 6803. Proteomics **9:** 1075-1086

Kizawa A, Kawahara A, Takimura Y, Nishiyama Y, Hihara Y (2016) RNA-seq Profiling Reveals Novel Target Genes of LexA in the Cyanobacterium Synechocystis sp. PCC 6803. Front Microbiol **7:** 193

Klahn S, Orf I, Schwarz D, Matthiessen JK, Kopka J, Hess WR, Hagemann M (2015) Integrated Transcriptomic and Metabolomic Characterization of the Low-Carbon Response Using an ndhR Mutant of Synechocystis sp. PCC 6803. Plant Physiol **169:** 1540-1556

Kooß S, Lamparter T (2016) Cyanobacterial origin of plant phytochromes. Protoplasma**:** 1-5

Kopf M, Klahn S, Scholz I, Matthiessen JK, Hess WR, Voss B (2014) Comparative analysis of the primary transcriptome of Synechocystis sp. PCC 6803. DNA Res **21:** 527-539

Kopf M, Klähn S, Scholz I, Matthiessen JKF, Hess WR, Voß B (2014) Comparative Analysis of the Primary Transcriptome of Synechocystis sp. PCC 6803. DNA Research **21:** 527-539

Kozlovskaya IB, Aslanova IF, Grigorieva LS, Kreidich Yu V (1982) Experimental analysis of motor effects of weightlessness. Physiologist **25:** S49-52

Kwon J, Oh J, Park C, Cho K, Kim SI, Kim S, Lee S, Bhak J, Norling B, Choi J-S (2010) Systematic cyanobacterial membrane proteome analysis by combining acid hydrolysis and digestive enzymes with nano-liquid chromatography–Fourier transform mass spectrometry. Journal of Chromatography A **1217:** 285-293

Lacey RF, Binder BM (2014) How plants sense ethylene gas — The ethylene receptors. Journal of Inorganic Biochemistry **133** 58–62

Lacey RF, Binder BM (2016) Ethylene Regulates the Physiology of the Cyanobacterium Synechocystis sp. PCC 6803 via an Ethylene Receptor. Plant Physiology **In Press:** DOI:10.1104/pp.1116.00602

Lamparter T (2004) Evolution of cyanobacterial and plant phytochromes. FEBS Lett **573:** 1-5

Lau NS, Foong CP, Kurihara Y, Sudesh K, Matsui M (2014) RNA-Seq analysis provides insights for understanding photoautotrophic polyhydroxyalkanoate production in recombinant Synechocystis Sp. PLoS One **9:** e86368

Linhartová M, Bučinská L, Halada P, Ječmen T, Šetlík J, Komenda J, Sobotka R (2014) Accumulation of the Type IV prepilin triggers degradation of SecY and YidC and inhibits synthesis of Photosystem II proteins in the cyanobacterium Synechocystis PCC 6803. Molecular Microbiology **93:** 1207-1223

Livak KJ, Schmittgen TD (2001) Analysis of relative gene expression data using real-time quantitative PCR and the 2−ΔΔCT method. Methods **25:** 402-408

Lowe BA, Miller JD, Neely MN (2007) Analysis of the polysaccharide capsule of the systemic pathogen Streptococcus iniae and its implications in virulence. Infect Immun **75:** 1255-1264

Lu A, Cho K, Black WP, Duan XY, Lux R, Yang Z, Kaplan HB, Zusman DR, Shi W (2005) Exopolysaccharide biosynthesis genes required for social motility in Myxococcus xanthus. Mol Microbiol **55:** 206-220

Martin W, Rujan T, Richly E, Hansen A, Cornelsen S, Lins T, Leister D, Stoebe B, Hasegawa M, Penny D (2002) Evolutionary analysis of *Arabidopsis*, cyanobacterial, and chloroplast genomes reveals plastid phylogeny and thousands of cyanobacterial genes in the nucleus. Proceedings of the National Academy of Science USA **99:** 12246-12251

Mason MG, Schaller GE (2005) Histidine kinase activity and the regulation of ethylene signal transduction. Canadian Journal of Botany-Revue Canadienne de Botanique **83:** 563-570

McDaniel B, Binder BM (2012) ETHYLENE RECEPTOR1 (ETR1) is sufficient and has the predominant role in mediating inhibition of ethylene responses by silver in *Arabidopsis thaliana*. Journal of Biological Chemistry **287:** 26094-26103

Mitrophanov AY, Groisman EA (2008) Signal integration in bacterial two-component regulatory systems. Genes Dev **22:** 2601-2611

Mitschke J, Georg J, Scholz I, Sharma CM, Dienst D, Bantscheff J, Voss B, Steglich C, Wilde A, Vogel J, Hess WR (2011) An experimentally anchored map of transcriptional start sites in the model cyanobacterium Synechocystis sp. PCC6803. Proc Natl Acad Sci U S A **108:** 2124-2129

Moon YJ, Kim SI, Chung YH (2012) Sensing and responding to UV-A in cyanobacteria. Int J Mol Sci **13:** 16303-16332

Moon YJ, Kim SY, Jung KH, Choi JS, Park YM, Chung YH (2011) Cyanobacterial phytochrome Cph2 is a negative regulator in phototaxis toward UV-A. FEBS Lett **585:** 335-340

Mount SM, Chang C (2002) Evidence for a plastid origin of plant ehylene rceptor genes. Plant Physiology **130:** 10-14

Mount SM, Chang C (2002) Evidence for a Plastid Origin of Plant Ethylene Receptor Genes. Plant Physiology **130:** 10-14

Moussatche P, Klee HJ (2004) Autophosphorylation activity of the Arabidopsis ethylene receptor multigene family. Journal of Biological Chemistry **279:** 48734-48741

Murakami A (1997) Quantitative analysis of 77K fluorescence emission spectra in Synechocystis sp. PCC 6714 and Chlamydomonas reinhardtii with variable PS I/PS II stoichiometries. Photosynthesis Research **53:** 141-148

Nakasugi K, Svenson CJ, Neilan BA (2006) The competence gene, *comF*, from *Synechocysitis* sp. strain PCC 6803 is involved in natural transformation, phototactic motility and piliation. Microbiology **152:** 3623-3631

Narikawa R, Ishizuka T, Muraki N, Shiba T, Kurisu G, Ikeuchi M (2013) Structures of cyanobacteriochromes from phototaxis regulators AnPixJ and TePixJ reveal general and specific photoconversion mechanism. Proc Natl Acad Sci U S A **110:** 918-923

Narikawa R, Suzuki F, Yoshihara S, Higashi K, Watanabe A, Ikeuchi M (2011) Novel photosensory two-component system (PixA-NixB-NixC) involved in the regulation of positive and negative phototaxis of cyanobacterium *Synechocystis* sp. PCC 6803. Plant & Cell Physiology **52:** 2114-2224

Neu TR, Marshall KC (1990) Bacterial polymers: physicochemical aspects of their interactions at interfaces. J Biomater Appl **5:** 107-133

Ng W-O, Grossman AR, Bhaya D (2003) Multiple Light Inputs Control Phototaxis in *Synechocystis* sp. Strain PCC6803. Journal of Bacteriology **185:** 1599-1607

O'Malley RC, Rodriguez FI, Esch JJ, Binder BM, O'Donnell P, Klee HJ, Bleecker AB (2005) Ethylene-binding activity, gene expression levels, and receptor system output for ethylene receptor family members from Arabidopsis and tomato. Plant Journal **41:** 651-659

O'Toole GA, Kolter R (1998) Flagellar and twitching motility are necessary for Pseudomonas aeruginosa biofilm development. Mol Microbiol **30:** 295-304

Okamoto S, Ohmori M (2002) The cyanobacterial PilT protein responsible for cell motility and transformation hydrolyzes ATP. Plant Cell Physiol **43:** 1127-1136

Rai AN (1990) Cyanobacteria in Symbiosis. *In* AN Rai, ed, Handbook of Symbiotic Cyanobacteria. CRC Press, Boca Raton, Florida, pp 1-7

Ramakrishnan P, Tabor JJ (2016) Repurposing Synechocystis PCC6803 UirS–UirR as a UV-Violet/Green Photoreversible Transcriptional Regulatory Tool in E. coli. ACS Synthetic Biology

Ratte M, Bujok O, Spitzy A, Rudolph J (1998) Photochemical alkene formation in seawater from dissolved organic carbon: Results from laboratory experiments. Journal of Geophysical Research **103:** 5707-5717

Rendueles O, Kaplan JB, Ghigo JM (2013) Antibiofilm polysaccharides. Environ Microbiol **15:** 334-346

Rockwell NC, Lagarias JC (2010) A Brief History of Phytochromes. ChemPhysChem **11:** 1172-1180

Rockwell NC, Martin SS, Feoktistova K, Lagarias JC (2011) Diverse two-cysteine photocycles in phytochromes and cyanobacteriochromes. Proc Natl Acad Sci U S A **108:** 11854-11859

Rockwell NC, Ohlendorf R, Moglich A (2013) Cyanobacteriochromes in full color and three dimensions. Proc Natl Acad Sci U S A **110:** 806-807

Rodriguez FI, Esch JJ, Hall AE, Binder BM, Schaller GE, Bleecker AB (1999) A copper cofactor for the ethylene receptor ETR1 from *Arabidopsis*. Science **283:** 996-998

Sanderson MJ, Thorne JL, Wikstrom N, Bremer K (2004) Molecular evidence on plant divergence times. Am J Bot **91:** 1656-1665

Sato S, Shimoda Y, Muraki A, Kohara M, Nakamura Y, Tabata S (2007) A Large-scale Protein–protein Interaction Analysis in Synechocystis sp. PCC6803. DNA Research **14:** 207-216

Savakis P, De Causmaecker S, Angerer V, Ruppert U, Anders K, Essen LO, Wilde A (2012) Light-induced alteration of c-di-GMP level controls motility of Synechocystis sp. PCC 6803. Mol Microbiol **85:** 239-251

Schaller GE (2012) Ethylene and the regulation of plant development. BMC Biol **10:** 9

Schaller GE, Bleecker AB (1995) Ethylene-binding sites generated in yeast expressing the *Arabidopsis ETR1* gene. Science **270:** 1809-1811

Schaller GE, Kieber JJ (2002) Ethylene. *In* C Somerville, E Meyerowitz, eds, The Arabidopsis Book, Vol DOI/10.1199/tab.0071. American Society of Plant Biologists, Rockville, MD

Schaller GE, Shiu S-H, Armitage Judith P (2011) Two-component systems and their co-option for eukaryotic signal transduction. Current Biology **21:** R320-R330

Schuergers N, Nurnberg DJ, Wallner T, Mullineaux CW, Wilde A (2015) PilB localization correlates with the direction of twitching motility in the cyanobacterium Synechocystis sp. PCC 6803. Microbiology **161:** 960-966

Schuergers N, Wilde A (2015) Appendages of the cyanobacterial cell. Life (Basel) **5:** 700-715

Shi W, Sun H (2002) Type IV pilus-dependent motility and its possible role in bacterial pathogenesis. Infect Immun **70:** 1-4

Sisler EC (1979) Measurement of Ethylene Binding in Plant Tissue. Plant Physiology **64:** 538-542

Song J-Y, Cho HS, Cho J-I, Jeon J-S, Lagarias JC, Park Y-I (2011) Near-UV cyanobacteriochrome signaling system elicits negative phototaxis in the cyanobacterium Synechocystis sp. PCC 6803. Proceedings of the National Academy of Sciences USA **108:** 10780-10785

Stepanova AN, Alonso JM (2009) Ethylene signaling and response: where different regulatory modules meet. Curr Opin Plant Biol **12:** 548-555

Stock AM, Robinson VL, Goudreau PN (2000) Two-component signal transduction. Annu Rev Biochem **69:** 183-215

Swinnerton JW, Lamontagne RA (1974) Oceanic distribution of low-molecular-weight hydrocarbons. Environmental Science & Technology **8:** 657-663

Swinnerton JW, Linnenborn VJ (1967) Gaseous hydrocarbons in sea water: Determination. Science **156:** 1119-1120

Theologis A (1992) One rotten apple spoils the whole bushel: the role of ethylene in fruit ripening. Cell **70:** 181-184

Timmis JN, Ayliffe MA, Huang CY, Martin W (2004) Endosymbiotic gene transfer: organelle genomes forge eukaryotic chromosomes. Nature Reviews Genetics **5:** 123-135

Trautmann D, Voß B, Wilde A, Al-Babili S, Hess WR (2012) Microevolution in cyanobacteria: Re-sequencing a motile substrain of Synechocystis sp. PCC 6803. DNA Research **19:** 435-448

Ulijasz AT, Cornilescu G, von Stetten D, Cornilescu C, Velazquez Escobar F, Zhang J, Stankey RJ, Rivera M, Hildebrandt P, Vierstra RD (2009) Cyanochromes are blue/green light photoreversible photoreceptors defined by a stable double cysteine linkage to a phycoviolobilin-type chromophore. Journal of Biological Chemistry **284:** 29757-29772

Ungerer J, Tao L, Davis M, Ghirardi M, Maness P-C, Yu J (2012) Sustained photosynthetic conversion of CO_2 to ethylene in recombinant cyanobacterium *Synechocystis* PCC 6803. Energy & Environmental Science **5:** 8998-9006

Ursell T, Chau RMW, Wisen S, Bhaya D, Huang KC (2013) Motility enhancement through surface modification Is sufficient for cyanobacterial community organization during phototaxis. PLoS Compututational Biology **9:** e1003205

Wang HL, Postier BL, Burnap RL (2002) Optimization of fusion PCR for in vitro construction of gene knockout fragments. Biotechniques **33:** 26, 28, 30 passim

Wang HL, Postier BL, Burnap RL (2004) Alterations in global patterns of gene expression in Synechocystis sp. PCC 6803 in response to inorganic carbon limitation and the inactivation of ndhR, a LysR family regulator. J Biol Chem **279:** 5739-5751

Wang W, Esch JE, Shiu SH, Agula H, Binder BM, Chang C, Patterson SE, Bleecker AB (2006) Identification of important regions for ethylene binding and signaling in the transmembrane domain of the ETR1 ethylene receptor of Arabidopsis. The Plant Cell **18:** 3429-3442

Wang W, Hall AE, O'Malley R, Bleecker AB (2003) Canonical histidine kinase activity of the transmitter domain of the ETR1 ethylene receptor from *Arabidopsis* is not required for signal transmission. Proceedings of the National Academy of Sciences of the United States of America **100:** 352-357

West AH, Stock AM (2001) Histidine kinases and response regulator proteins in two-component signaling systems. Trends in Biochemical Sciences **26:** 369-376

Wiegard A, Doorrich AK, Deinzer H-T, Beck C, Wilde A, Holtzendorff J, Axmann IM (2013) Biochemical analysis of three putative KaiC clock proteins from *Synechocystis* sp. PCC 6803 suggests their functional divergence. Microbiology **159:** 948-958

Wilde A, Fiedler B, Borner T (2002) The cyanobacterial phytochrome Cph2 inhibits phototaxis towards blue light. Mol Microbiol **44:** 981-988

Wilde A, Mullineaux CW (2015) Motility in cyanobacteria: polysaccharide tracks and Type IV pilus motors. Mol Microbiol **98:** 998-1001

Williams JGK (1988) Construction of Specific Mutations in Photosystem-Ii Photosynthetic Reaction Center by Genetic-Engineering Methods in Synechocystis-6803. Methods in Enzymology **167:** 766-778

Wilson DF, Swinnerton JW, Lamontagne RA (1970) Production of carbon monoxide and gaseous hydrocarbons in seawater: Relation to dissolved organic carbon. Science **168:** 1577-1579

Wiltbank LB, Kehoe DM (2016) Two Cyanobacterial Photoreceptors Regulate Photosynthetic Light Harvesting by Sensing Teal, Green, Yellow, and Red Light. MBio **7:** e02130-02115

Yang SF, Hoffmann NL (1984) Ethylene biosynthesis and its regulation in higher plants. Annual Review of Plant Physiology **35:** 155-189

Yoon HS, Hackett JD, Ciniglia C, Pinto G, Bhattacharya D (2004) A molecular timeline for the origin of photosynthetic eukaryotes. Molecular Biology and Evolution **21:** 809-818

Yoshihara S, Geng X, Okamoto S, Yura K, Murata T, Go M, Ohmori M, Ikeuchi M (2001) Mutational analysis of genes involved in pilus structure, motility and transformation competency in the unicellular motile cyanobacterium Synechocystis sp. PCC 6803. Plant Cell Physiol **42:** 63-73

Yoshihara S, Ikeuchi M (2004) Phototactic motility in the unicellular cyanobacterium Synechocystis sp. PCC 6803. Photochem Photobiol Sci **3:** 512-518

Yoshihara S, Suzuki F, Fujita H, Geng XX, Ikeuchi M (2000) Novel putative photoreceptor and regulatory genes Required for the positive phototactic movement of the unicellular motile cyanobacterium Synechocystis sp. PCC 6803. Plant Cell Physiol **41:** 1299-1304

Zavrel T, Knoop H, Steuer R, Jones PR, Cerveny J, Trtilek M (2016) A quantitative evaluation of ethylene production in the recombinant cyanobacterium Synechocystis sp. PCC 6803 harboring the ethylene-forming enzyme by membrane inlet mass spectrometry. Bioresour Technol **202:** 142-151

Zhang W, Yu Y, Hertwig F, Thierry-Mieg J, Zhang W, Thierry-Mieg D, Wang J, Furlanello C, Devanarayan V, Cheng J, Deng Y, Hero B, Hong H, Jia M, Li L, Lin SM, Nikolsky Y, Oberthuer A, Qing T, Su Z, Volland R, Wang C, Wang MD, Ai J, Albanese D, Asgharzadeh S, Avigad S, Bao W, Bessarabova M, Brilliant MH, Brors B, Chierici M, Chu TM, Zhang J, Grundy RG, He MM, Hebbring S, Kaufman HL, Lababidi S, Lancashire LJ, Li Y, Lu XX, Luo H, Ma X, Ning B, Noguera R, Peifer M, Phan JH, Roels F, Rosswog C, Shao S, Shen J, Theissen J, Tonini GP, Vandesompele J, Wu PY, Xiao W, Xu J, Xu W, Xuan J, Yang Y, Ye Z, Dong Z, Zhang KK, Yin Y, Zhao C, Zheng Y, Wolfinger RD, Shi T, Malkas LH, Berthold F, Wang J, Tong W, Shi L, Peng Z, Fischer M (2015) Comparison of RNA-seq and microarray-based models for clinical endpoint prediction. Genome Biol **16:** 133

Zhao S, Fung-Leung WP, Bittner A, Ngo K, Liu X (2014) Comparison of RNA-Seq and microarray in transcriptome profiling of activated T cells. PLoS One **9:** e78644

Zhou X, Carranco R, Vitha S, Hall TC (2005) The dark side of green fluorescent protein. New Phytol **168:** 313-322

Appendices

Appendix A

Primers

Primers for Truncated Codon Optimized *slr1212* for Pichia Expression

FWD Codon Optimized slr1212 w/EcoR1
5’ GAATTCATGGCTATTACAGCTTTTAC

REV Codon Optimized slr1212 w/Xho1
5’ CTCGAGCTCGGTAGGGGACTTCAA

Primers for Codon Optimized *slr1212* Point Mutants for Pichia

C77A
Fwd
5’ CTTTTCTCTACTTTTATTTTGGCTTGCGGAACCTCCCACTTTTTCG

Rev
5’ CGAAAAAGTGGGAGGTTCCGCAAGCCAAAATAAAAGTAGAGAAAAG

C78A
Fwd
5’ CTTTTCTCTACTTTTATTTTGTGTGCTGGAACCTCCCACTTTTTCG

Rev
5’ CGAAAAAGTGGGAGGTTCCAGCACACAAAATAAAAGTAGAGAAAAG

C78S
Fwd
5’ CTTTTCTCTACTTTTATTTTGTGTTCCGGAACCTCCCACTTTTCG

Rev
5’ CGAAAAGTGGGAGGTTCCGGAACACAAAATAAAAGTAGAGAAAAG

H82A
Fwd
5’ TGTGTTGCGGAACCTCCGCGTTTTTCGATATTATC

Rev
5’ GATAATATCGAAAAACGCGGAGGTTCCGCAACACA

Primers for Confirmation of SynEtrΔTM2 in *Synechocystis*

Slr1212F180
5’ CTACTTTTTGCGGAAGCGCCA

Slr1212R480
5’ CGGTCTTCCACTCTTTTTTCAAG

Primers for Gene Deletion of *slr1212* and *slr1214* in *Synechocystis*

1212 Up Frag Fwd
5’ CTAATCCTGCCCAACCAAAAGTGAAG

1212 Up Frag Rev with Kan (Bold)
5’ CGAAGGGAAACGCCTATTATCGGGAAAAAATCCCCCAG

1212 Down Frag Fwd with Kan (Bold) Without T4 Terminator
5’ GAGCAAACGCATTCCCTTTTAGCTTCTCCAGCCATCCAGC

1212 Down Frag Rev with Kan (Bold)
5’ CTAAAGTGAAAATTCCAACCCAAATTG

1214 Up Frag Fwd
5’ ATCGATGTCAAAAATCAACTAGTTTG

1214 Up Frag Rev with Kan (Bold)
5’ CGAAGGGAAACGCCTATTATCGATCACAGCAGTC

1214 Down Frag Fwd with Kan (Bold) with T4 Terminator
5’ CACAAAACGGTTTACAAGCATAATGTCCCTGTTCTTTG

1214 Down Frag Rev
5’ CACAGCACCGGATACACAGGCG

Kan Res Fwd
5’ CGATAATAGGCGTTTCCCTTCG

Kan Res Rev Without T4 Terminator
5’ CTAAAAGGGAATGCGTTTGCTCAC

Kan Res Rev with T4 Terminator
5’ TTATGCTTGTAAACCGTTTTGTGAAAA

Primers for Cloning into pUR

FWD slr1212 w/Nde1
5’ CGCATATGATGGCAATCACCGCATTTACC

Rev slr1212 w/BamH1
5’ GAGGATCCCTAAAGTGAAAATTCCAAC

REV slr1213 w/BamH1 (slr1213R1)
5’ GAGGATCCCTAGCGACTACGATATTCTTTC

pPetJ Fwd
5’ CGATCGCCATCGGCACCATGAAAC

Primers for Generating *slr1212* Point Mutants to Express in *Synechocystis*

C78S
Fwd
5’ CCTAATATTATTTTCCTGTTTAGTACTTTTATTTTATGCTCTGGC

Rev
5’ GCCAGAGCATAAAATAAAAGTACTAAACAGGAAAATAATATTAGG

C561A
Fwd
5’ GTCCCATCTTAGGCAAGCACACATTGACTTTCTTGC

Rev
5’ GCAAGAAAGTCAATGTGTGCTTGCCTAAGATGGGAC

qRT-PCR Primers

trpA
Fwd
5’ GCGGATTTAATTGAGTTGGG

Rev
5’ GCACATCATCCAACTGACC

slr1212
Fwd
5’ TACAGGTGTGGGATAACGGA

Rev
5’ CGCCACCGACATATTCATAG

slr1213
Fwd
5’ AGCCAATCATCAACAGCAAC

Rev
5’ ACGGTAATTCCTTGGTCGAG

slr1214
Fwd
5’ AAAGTGGTTTGCATTGACGA

Rev
5’ AAACGGCAAAGCTCATAACC

PilA1
Fwd
5’ CCAACTTGACCCAAGAGGTT

Rev
5’ AATCGAACTGCTGGTTGTTG

PilB1
Fwd
5’ CTCCATCGACATGAATCTGG

Rev
5’ TTCCTTCCTGGAGAGCCTTA

PilC
Fwd
5’ GAAGCCATGAGTCCAGAACA

Rev
5’ TTTCCAGGAATTCGAGGTTT

PilD
Fwd
5’ TGCTTTCCTACTTGCCATTG

Rev
5’ GGGATAAACCTTCTGGCAAA

slr1875
Fwd
5’ CATTTCCATGATGATTCCCA

Rev
5’ TCCCTGCTCCGGTAATTAAG

sll1581
Fwd
5’ GCGAATATCTGCTTGGGATT

Rev
5’ ATCACCGAAGTGAGTGGTGA

sll5052
Fwd
5’ TTATCATGGGCAATTCCTGA

Rev
5’ ACAGCGACCTTAAATTTGGC

sll0923
Fwd
5’ TAATTTCGTTGAGGCGTGAG

Rev
5’ TTAATGACCAGTTGCCCAAA

Appendix B

Domain Predictions of Putative Ethylene Binding Domain Containing Proteins in Bacteria

Table A2. Domain Prediction of Putative Ethylene Binding Domain Containing Proteins*

Genus species	Phylum (class)	GI #	Predicted Domain Structure †
Acaryochloris CCMEE 5410	Cyanobacteria	498153540	
Anabaena cylindrica PCC 7122	Cyanobacteria	440681237	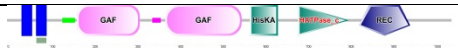
		440683654	
		440682283	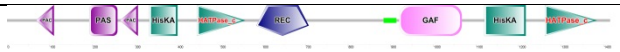
Anabaena PCC 7108	Cyanobacteria	515515874	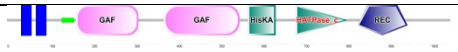
Anabaena variabilis ATCC 29413	Cyanobacteria	75908887	
		75908175	
Arthrospira maxima	Cyanobacteria	493720891	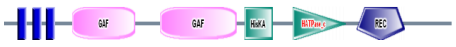
Arthrospira PCC 8005	Cyanobacteria	495326409	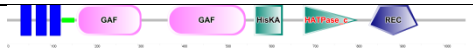
Arthrospira platensis	Cyanobacteria	493674252	
Asticcacaulis AC402	Proteobacteria (α-proteobacteria)	557820388	
Asticcacaulis AC460	Proteobacteria (α-proteobacteria)	557830516	
Asticcacaulis benevestitus	Proteobacteria (α-proteobacteria)	516746942	
Asticcacaulis biprosthecium	Proteobacteria (α-proteobacteria)	493315689	
Azospirillum B510	Proteobacteria (α-proteobacteria)	288958265	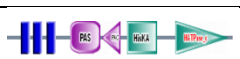

Azospirillum brasilense Sp245	Proteobacteria (α-proteobacteria)	392377229	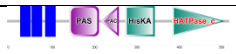
Azospirillum lipoferum 4B	Proteobacteria (α-proteobacteria)	374291663	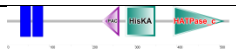
Calothrix PCC 7103	Cyanobacteria	518321959	
Calothrix PCC 7507	Cyanobacteria	427716966	
Candidatus Methylomirabilis oxyfera	unclassified	392373508	
Caulobacter K31	Proteobacteria (α-proteobacteria)	167648286	
Chamaesiphon minutus PCC 6605	Cyanobacteria	434388786	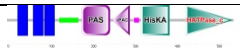
Chlorogloeopsis fritschii	Cyanobacteria	515382644	
		515377348	
Chroococcidiopsis thermalis PCC 7203	Cyanobacteria	428210107	
Chthoniobacter flavus Ellin428	Verrucomicrobia	494038993	
Coleofasciculus chthonoplastes PCC 7420	Cyanobacteria	493032864	
		493031845	
		493040130	
		493031910	
		493036837	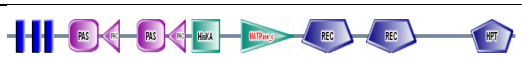
Crinalium epipsammum PCC 9333	Cyanobacteria	428307974	
Cyanothece	Cyanobacteria	495553311	
Cyanothece ATCC 51142	Cyanobacteria	172039202	
		172036121	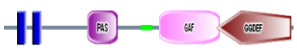
		172036793	

Cyanothece PCC 7424	Cyanobacteria	218441038	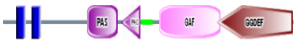
		218441969	
Cyanothece PCC 7425	Cyanobacteria	219883241	
		220907505	
Cyanothece PCC 7822	Cyanobacteria	307154701	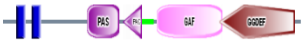
		307150158	
Cyanothece PCC 8802	Cyanobacteria	257057938	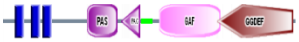
Cylindrospermum stagnale PCC 7417	Cyanobacteria	434406889	
		434404121	
		434406815	
filamentous cyanobacterium ESFC-1	Cyanobacteria	517210500	
		517207104	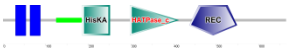
Fischerella	Cyanobacteria	497067904	
Fischerella JSC-11	Cyanobacteria	497067119	
Fischerella muscicola	Cyanobacteria	515346074	
		515357413	
		515344627	
		515356103	
		515363488	

Fischerella PCC 9339	Cyanobacteria	515879719	
		515878322	
gamma proteobacterium BDW918	Proteobacteria (γ-proteobacteria)	495527462	
Geitlerinema PCC 7105	Cyanobacteria	516257932	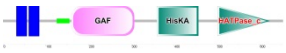
		516257491	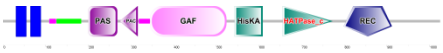
Geitlerinema PCC 7407	Cyanobacteria	428223547	
		428226797	
Glaciecola nitratireducens	Proteobacteria (γ-proteobacteria)	348028029	
Gloeocapsa PCC 73106	Cyanobacteria	493574983	
Gloeocapsa sp. PCC 7428	Cyanobacteria	434393773	
Hahella chejuensis KCTC 2396	Proteobacteria (γ-proteobacteria)	83646935	
Hahella ganghwensis	Proteobacteria (γ-proteobacteria)	521079810	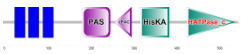
Hydrocarboniphaga effuse	Proteobacteria (γ-proteobacteria)	494341607	
Janthinobacterium HH01	Proteobacteria (β-proteobacteria)	495722902	
Leptolyngbya PCC 7375	Cyanobacteria	493560916	
Leptolyngbya PCC 7376	Cyanobacteria	427723604	
Lyngbya aestuarii	Cyanobacteria	553729765	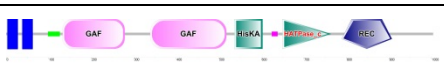
		553732500	
		553731020	

Lyngbya PCC 8106	Cyanobacteria	497472233	
		497472989	
		497469251	
Marinobacter lipolyticus	Proteobacteria (γ-proteobacteria)	501088421	
Methylobacter marinus	Proteobacteria (γ-proteobacteria)	519004353	
Methylobacter tundripaludum	Proteobacteria (γ-proteobacteria)	493945542	
		493946777	
		493947740	
		493947739	
Methylobacterium extorquens	Proteobacteria (α-proteobacteria)	163853566	
Methylobacterium extorquens AM1	Proteobacteria (α-proteobacteria)	240140985	
Methylobacterium extorquens CM4	Proteobacteria (α-proteobacteria)	218532426	
Methylobacterium extorquens DM4	Proteobacteria (α-proteobacteria)	254563496	
Methylobacterium extorquens DSM13060	Proteobacteria (α-proteobacteria)	489694910	
Methylobacterium populi	Proteobacteria (α-proteobacteria)	188583868	
Methylocystis SC2	Proteobacteria (α-proteobacteria)	402770875	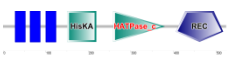
Methyloglobulus morosus	Proteobacteria (γ-proteobacteria)	558562971	
Methylomonas methanica MC09	Proteobacteria (γ-proteobacteria)	333982799	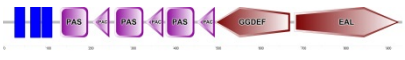
Methylomonas MK1	Proteobacteria (γ-proteobacteria)	521973497	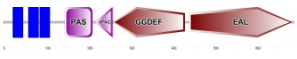

Methylophaga aminisulfidivorans	Proteobacteria (γ-proteobacteria)	494242859	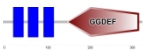
Methylophaga thiooxydans	Proteobacteria (γ-proteobacteria)	495567658	
Methylotenera mobilis	Proteobacteria (β-proteobacteria)	518739914	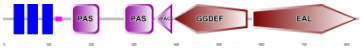
		253996028	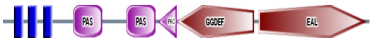
Methyloversatilis NVD	Proteobacteria (β-proteobacteria)	517222790	
Methyloversatilis universalis	Proteobacteria (β-proteobacteria)	519009451	
Methylovorus glucosetrophus	Proteobacteria (β-proteobacteria)	254000138	
Microchaete PCC 7126	Cyanobacteria	516249682	
Microchaete PCC 7126	Cyanobacteria	516247349	
Microcoleus PCC 7113	Cyanobacteria	428310447	
		428314292	
		428311029	
		428311548	
		428310796	
		428310395	
Microcoleus vaginatus	Cyanobacteria	493681967	
Microcoleus vaginatus FGP-2	Cyanobacteria	493684362	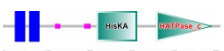
		493684409	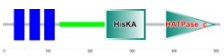
Nafulsella turpanensis	Bacterioides	516343515	

Nevskia ramose	Proteobacteria (γ-proteobacteria)	551356121	
Nostoc PCC 7107	Cyanobacteria	427705958	
		427708579	
Nostoc PCC 7120	Cyanobacteria	17227678	
		17232208	
Nostoc PCC 7524	Cyanobacteria	427730879	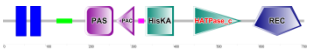
		427728766	
Nostoc punctiforme PCC 73102	Cyanobacteria	186682032	
		186685521	
		186682272	
Oscillatoria acuminata PCC 6304	Cyanobacteria	428214479	
Oscillatoria nigro-viridis PCC 7112	Cyanobacteria	428318322	
		428320955	
		428319206	
		428318321	
		428315437	
Oscillatoria PCC 10802	Cyanobacteria	516325099	
		516324086	
		516324208	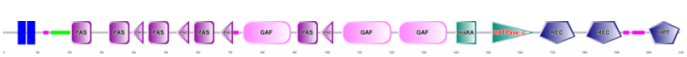

Oscillatoria PCC 6506	Cyanobacteria	494598248	
		494598249	
		494597992	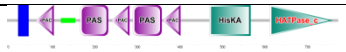
		494598892	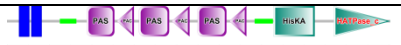
		494597484	
		494594981	
Oscillatoriales cyanobacterium JSC-12	Cyanobacteria	497242913	
		497239980	
Oxalobacteraceae bacterium IMCC9480	Proteobacteria (β-proteobacteria)	497353964	
Pleurocapsa PCC 7319	Cyanobacteria	518333542	
Pleurocapsa PCC 7327	Cyanobacteria	428200632	
Pseudanabaena biceps PCC 7429	Cyanobacteria	497312328	
Pseudanabaena PCC 7367	Cyanobacteria	428219864	
		428219681	
Pseudoalteromonas flavipulchra	proteobacteria (γ-proteobacteria)	498291517	
Pseudoalteromonas luteoviolacea ATCC 29581	Proteobacteria (γ-proteobacteria)	491634368	
Pseudoalteromonas NJ631	Proteobacteria (γ-proteobacteria)	515784614	
Pseudoalteromonas piscicida	Proteobacteria (γ-proteobacteria)	498063176	
Pseudoalteromonas rubra ATCC 29570	Proteobacteria (γ-proteobacteria)	498069774	
Pseudomonas brassicacearum	Proteobacteria (γ-proteobacteria)	591395722	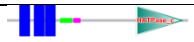
Pseudomonas brassicacearum subsp brassicacearum	Proteobacteria (γ-proteobacteria)	330812561	
Pseudomonas CFII68	Proteobacteria (γ-proteobacteria)	517434659	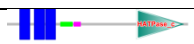

Pseudomonas fluorescens	Proteobacteria (γ-proteobacteria)	359763627	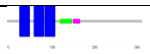
		489299342	
Pseudomonas fuscovaginae	Proteobacteria (γ-proteobacteria)	498131442	
Reinekea MED297	Proteobacteria (γ-proteobacteria)	495319814	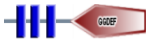
Rhodocyclaceae bacterium	Proteobacteria (β-proteobacteria)	518760078	
Rhodopseudomonas palustris	Proteobacteria (α-proteobacteria)	115523501	
		90422733	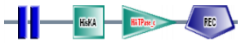
Rivularia PCC 7116	Cyanobacteria	427736248	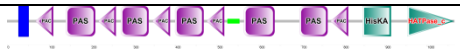
		427739075	
Saccharophagus degradans	Proteobacteria (γ-proteobacteria)	90020309	
Scytonema hofmanni	Cyanobacteria	516352979	
		516351696	
		516353908	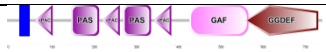
		516358044	
		516359343	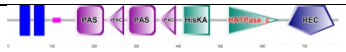
		516350230	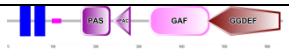
		516354477	
Skermanella stibiiresistens	Proteobacteria (α-proteobacteria)	587643757	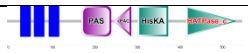
Spirulina subsalsa	Cyanobacteria	515875979	
		515874234	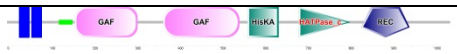
Stanieria cyanosphaera PCC 7437	Cyanobacteria	434399182	
Synechococcus PCC 7502	Cyanobacteria	428221455	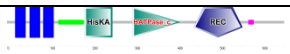
Synechocystis PCC 6803	Cyanobacteria	slr1212	

Zavarzinella formosa	Planctomycetes	521960204	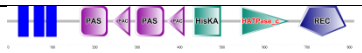

*Putative functional ethylene binding domains were found with a BLAST search that that excluded plants and algae genomes conducted in April 2014 using the ethylene binding domain of ETR1 from *Arabidopsis thaliana* (amino acids 1-130) as bait. Results are limited to hits that had an E value < 1e-10 and that contained the seven amino acid residues required for ethylene binding in ETR1. Domain predictions were generated using the Simple Modular Architecture Research Tool (SMART) http://smart.embl-heidelberg.de/.

Appendix C

Code Used for RNA-seq Analysis

Download data files:

All sample reads were download directly from GSAF to Newton using a temporary access key provided by GSAF.

The files were listed as:

WTair1_S1_R1_001.fastq.gz
WTair2_S2_R1_001.fastq.gz
WTair3_S3_R1_001.fastq.gz
WTeth1_S4_R1_001.fastq.gz
WTeth2_S7_R1_001.fastq.gz
WTeth3_S8_R1_001.fastq.gz
Dis12air1_S5_R1_001.fastq.gz
Dis12air2_S6_R1_001.fastq.gz
Dis12air3_S13_R1_001.fastq.gz
Dis12eth1_S14_R1_001.fastq.gz
Dis12eth2_S15_R1_001.fastq.gz
Dis12eth3_S16_R1_001.fastq.gz

To download the data a script titled gsaf_download.qsh was written containing:

```
#!/bin/bash
wget -O files.html "$1"
for file in `grep '^<!--gsafdata' files.html | grep '.gz' | awk '{print $2}'`
do
   echo $file
   url=`cat files.html | grep -v json | grep -m 1 $file | awk 'BEGIN {FS="\""} {print $2}'`
   echo "Downloading: $url"
   wget -o $file.wget.log -O $file --no-check-certificate "$url"
done
grep '^<!--gsafdata' files.html | grep '.gz' | awk '{print $5"  "$2}' > md5.txt
numfiles=`wc -l md5.txt | awk '{print $1}'`
md5sum -c md5.txt
if [ $? -eq 0 ]
then
   echo "Downloaded $numfiles files successfully."
else
```

```
   echo "Calculated md5sums do not match those provided by the GSAF.  Try requesting a new key and downloading again.  If that fails, contact the GSAF."
fi
```

The script was executed as:

```
bash gsaf_download.qsh “html link to files provided by GSAF”
```

Reference genome:

```
Curl “ftp://ftp.ncbi.nlm.nih.gov/genomes/all/GCF_000009725.1_ASM972v1/GCF_000009725.1_ASM972v1_genomic.fna.gz” > 6803genome.fa.gz
```

GFF File:

```
Curl “ftp://ftp.ncbi.nlm.nih.gov/genomes/all/GCF_000009725.1_ASM972v1/GCF_000009725.1_ASM972v1_genomic.gff.gz” > geneannotation.gff3
```

*both files were unzipped using gunzip

*It is important to note that the reference genome and the GFF file should be downloaded from the same source. If labeling is different between the two files, they will not work for read mapping.

*I will be showing script/code with “filename” or “ouput” in place of where the files would go. It should be assumed that the same script was used for each of these files with only file names and output names changed.

Quality Assessment:

FastQC:

```
Module load fastqc
```

```
Fastqc ../raw_data/filename.fastq.gz –o Output_Folder
```

*This was also performed after trimming.

Trimming Low Quality Reads:

The following script trim.qsh used to trim low quality reads using the software trimmomatic:

```
#$ -N trim
#$ -q medium*
#$ -cwd
#$ -pe threads 8
java -Xmx4G -jar /lustre/projects/rnaseq_ws/apps/Trimmomatic-0.32/trimmomatic-0.32.jar \
SE \
-threads 8 \
-trimlog Filename.log \
-phred33 \
 ../raw_data/Filename.fastq.gz \
 Output_Filename.fastq.trimmed.fq \
ILLUMINACLIP:/lustre/projects/staton/software/Trimmomatic-
0.32/adapters/illuminaClipping.fa:2:30:10 \
SLIDINGWINDOW:4:15 MINLEN:75
>& trim.output
```

Read Mapping with Bowtie and Tophat

Indexing the genome:

Soft links were created for our newly trimmed reads and our gff3 file in a new directory.

```
ln -s /omega/SynEtr1_RNAseq/SynEtr1/2_trimmomatic/filename.trimmed.fastq .
```

```
ln -s / omega/SynEtr1_RNAseq/SynEtr1/raw_data/geneannotations.gff3 .
```

The genome was then copied into the same directory.

```
cp / omega/SynEtr1_RNAseq/SynEtr1/raw_data/6803_genome.fa .
```

The genome was the index with Bowtie2

```
bowtie2-build 6803_genome.fa 6803_genome
```

Mapping the reads to the Synechocystis genome:

The script map.qsh was written to map the reads to the genome:

```
#$ -N Mapping
#$ -cwd
#$ -q medium*
#$ -pe threads 8
module load tophat
module load bowtie2
tophat -p 1 -o Ouput_Folder -G geneannotations.gff3 \
--transcriptome-index ./gene_index/gene \
6803_genome \
Filename.trimmed.fq \
>& Output_Results
```

Counting and Differential Expression Analysis with HTSeq and DESeq2

Counting the reads with HTSeq

First our accepted hits bam files generated from TopHat were copied into a new 5_htseq directory.

```
cp ../../4_tophat/Output_Folder/accepted_hits.bam New_Filename_accepted_hits.bam
```

Next a symbolic link was created for the GFF3 file.

```
ln -s / omega/SynEtr1_RNAseq/SynEtr1/raw_data/geneannotations.gff3 .
```

Following loading of python and htseq the BAM files were then sorted.

```
/lustre/projects/rnaseq_ws/apps/samtools-1.1/samtools sort -n
New_Filename_accepted_hits.bam New_Filename_sorted_byName
```

The BAM files were then converted to SAM Files.

```
/lustre/projects/rnaseq_ws/apps/samtools-1.1/samtools view -o
New_Filename_sorted_byName.sam New_Filename_sorted_byName.bam
```

Then the reads were counted.

```
htseq-count -s no -t gene -i ID New_Filename_sorted_byName.sam geneannotations.gff3 >
New_Filename_counts.txt
```

Differential Expression analysis with DESeq2 in R

First DESeq2 was installed and loaded

```
source("http://bioconductor.org/biocLite.R")
biocLite("DESeq2")

library("DESeq2")
```

The New_Filename_counts.txt files were then transferred from Newton into a folder on the desktop.

In R, the folder in which the New_Filename_counts.txt was set as the working directory with:

```
setwd(“/pathtofolder/”)
```

A DESeqDataSet object was then created using the DESeqDataSetFromHTSeqCount command:

```
sampleFiles <- grep("counts.txt",list.files("."),value=TRUE)
sampleCondition <- sub("(.*)\\d.*","\\1",sampleFiles)
my_sampleTable <- data.frame(sampleName = sampleFiles, fileName = sampleFiles, condition = sampleCondition)
my_data <- DESeqDataSetFromHTSeqCount(sampleTable = my_sampleTable, directory = ".", design= ~ condition)
```

Next, the main DESeq function was performed on the DESeqDataSet object:

```
deseq_results = DESeq(my_data)
```

To compare specific conditions such as WT air vs WT ethylene or WT air vs SynEtr1ΔTM2 air the following command was written:

```
condition1_condition2_results_table = results(deseq_results, contrast = c("condition", "condition1", "condition2"))
```

This data set was then exported as excel spreadsheet with the command:

```
write.csv(as.data.frame(condition1_condition2_results_table),file=(condition1_condition2_results.csv))
```

To produce an MA plot from the specified condition comparison:

```
plotMA(condtion1_condition2_results_table, main="DESeq2", ylim=c(-10,10))
```

To produce a PCA plot the read counts were first transformed by:

```
rld <- rlog(my_data, blind=FALSE)
```

The PCA plot was produced by:

```
plotPCA(rld)
```

Vita

Randy Lacey was born in McKenzie, TN to Frank and Donna Lacey. He is the youngest of three children that includes an older brother, Rory, and an older sister, Ryan. After graduating from McKenzie High School in 2005 he attended Austin Peay State University where he studied biology and chemistry. Following graduation from Austin Peay in 2009, he was admitted to the University of Tennessee, Knoxville Biochemistry & Cellular and Molecular Biology Department. He received his Ph.D. from the University of Tennessee in 2016.